THE DESIGN OF A RATE-GYRO FOR USE ON LAND VEHICLES

MUSA L. AUDU, B.Eng.(Mechanical)

A Thesis Submitted For The Master Of Engineering (Applied Mechanics) Research Programme To The Department Of Mechanical Engineering Of Ahmadu Bello University, Zaria, Nigeria,

April, 1980

TO

Hassana & Zainab

twinkle twinkle

little stars

ACKNOWLEDGEMENT

I will like to express my sincere gratitude to the following people:

- My main Supervisor, Dr. K. P. Zachariah, for his mature and constructive criticisms that help to shape up this work the way it is.
- Dr. S. Y. Aku - Co-Supervisor and Head of Department, for his encouragement both morally and materially.
- Mr. W. K. Neyman, for checking all the Design Drawings, to ensure that they conform.
- Those people in the Air Force and the Civil Aviation Training Centre, for exposing me to the practical aspects of gyroscopy.
- Mr. J. O. Ajayi, for the painstaking care in typing the manuscript.

Thank you all.

M. L. Audu.

February '80.

CONTENTS

		PAGE
NOTATION SUMMARY		v 1
CHAPTER 1:	DEFINITION OF THE PROBLEM	3
CHAPTER 2:	DYNAMICS OF ROAD VEHICLES ON CURVES..	7
2.1.	Vehicle on unbanked track	7
2.2.	Vehicle on superelevated (banked) track	10
2.3.	Factors affecting skidding and over-turning velocities	12
CHAPTER 3:	INTRODUCING THE GYROSCOPE	18
3.1.	Definition	18
3.2.	Classification	21
3.3.	Summary of applications	29
3.4.	Aspects of Gyroscope Design	31
CHAPTER 4:	THE GYRO AS A RATE-OF-TURN SENSOR ..	37
4.1.	Fundamental equation of the rate gyro	37
4.2.	The dynamic response of the rate gyro	39
4.3.	Cross-Coupling Error	41
4.4.	Rate Gyro Design	43
CHAPTER 5:	GYRO DRIVES	44
5.1.	Spiral Spring Drive	44
5.2.	Pneumatic Drive	45

		PAGE
5.3.	The Electric Drive	47
5.4.	Selection of Drive	50
5.5.	Power Supply	50
CHAPTER 6:	THEORY AND DESIGN ASPECTS OF THE HYSTERESIS MOTOR	53
6.1.	Theory of the Hysteresis Motor ..	53
6.2.	Aspects of Hysteresis Motor Design ..	58
CHAPTER 7:	THE ELASTIC RESTRAINT	66
7.1.	Helical Spring Restraint	66
7.2.	Torsion Wire Restraint	68
7.3.	The Elastic Restraint Microsyn ..	68
7.4.	Hairspring or Spiral Spring Restraint	71
CHAPTER 8:	THE DAMPING DEVICE	76
8.1.	Eddy-Current Damping	76
8.2.	Liquid Damping	79
8.3.	Air Damping	80
8.4.	Selection of Damper	83
CHAPTER 9:	THE PICKOFF AND OUTPUT DISPLAY ..	84
9.1.	Introduction	84
9.2.	Gyro Signal Pickoffs	86
9.3.	Selection of Pickoff	97

		PAGE
9.4.	Aspects of Microsyn Design	98
9.5.	The Output Display Unit	102
CHAPTER 10:	MISCELLANEOUS DESIGN ASPECTS ..	103
10.1.	Limit Stops	103
10.2.	Damping Adjustment	110
10.3.	Balance Weights	110
10.4.	Gyro Testing and Calibration ..	111
CHAPTER 11:	THE DESIGN CALCULATIONS	113
11.1.	The Electric Motor Design	113
11.2.	The Spring Design	122
11.3.	The Damper Design	125
11.4.	Design of the Pickoff	132
CONCLUSION		134
APPENDIX		136
REFERENCES		143
DESIGN DRAWINGS		

NOTATION

A	=	pole area of magnet/area of plates of capacitive pickoff/cross-section of conducting path of electrolytic pickoff.
A_m	=	cross-sectional area of permanent magnet.
a	=	half wheel-base (distance between wheel centres when viewed from front or rear/spacing between coils of spiral spring.
B_m	=	peak value of flux density in a magnetic material.
b	=	width of spiral spring.
C	=	capacitance of capacitive pickoff.
e	=	damping coefficient.
D_1	=	inner diameter of cylindrical hysteretic material.
D_2	=	outer diameter of hysteretic material.
D_o	=	outer diameter of spiral spring.
D_i	=	inner diameter of spiral spring.
d	=	distance between plates of capacitive pickoff.
E	=	input voltage of a potentiometer.
E_o	=	output voltage of a microsyn pickoff.
e	=	output voltage of a potentiometer

F_1, F_2 = friction forces between road and wheel of vehicle.

f_m = figure of merit of gyro performance.

g = acceleration due to gravity (9.81 m/s^2).

H = angular momentum.

H_m = peak value of magnetizing force in magnetic material.

h = height of centre of gravity of vehicle above road surface/radial length of microsyn air-gap.

I_x, I_o = inertia of gyro wheel and gimbal assembly about output axis.

I_s, I = moment of inertia of gyro wheel about spin axis/electric current.

I_p = electric current in primary windings.

I_r = inertia of hysteresis ring.

I_t = inertia needed at spin axis of hysteresis motor.

K = torsional constant of elastic restraint (N-m/rad).

k = radius of gyration of rotor wheel assembly.

L = length of conducting path of electrolytic pickoff/axial length of gyro motor rotor and stator.

L_m = total length of permanent magnet.

L_g = length of airgap between poles of magnet.

l = total length of spiral spring restraint.

M = external moments acting on gyro wheel.

N_1, N_2 = road reaction forces at wheel of vehicle.

N_p = number of turns in primary windings.

N_s = number of turns in secondary windings.

n = synchronous spin speed of gyro motor (rpm)/ number of convolutions in a spiral spring.

P = permeance of microsyn air gap.

P_b = power loss due to friction at bearings.

P_w = power loss due to windage

P = pull-out power of hysteresis motor.

p = natural damped frequency of oscillation of gyro system about output axis/number of poles in stator of motor or microsyn pickoff.

R = radius of curvature of road/resultant reaction force on vehicle (due to N_1, N_2, F_1 and F_2)/ resistance ofelectrolyte in electrolytic pickoff/reluctance of microsyn air gap.

r = radius from axis of disc rotation to centre of magnet pole of Eddy-Current damper/radius of microsyn rotor/radius of curvature of road.

S_m = maximum working stress of spiral spring material.

T_d = disturbing torque acting on stablized gyro wheel.

T_R = gyro response torque ($= I\omega\Omega$).

T_e = elastic torque ($= K\theta$)

T = hysteresis torque/friction torque of ball-bearings.

t = thickness of disc of magnetic damper/thickness (width) of microsyn rotor/time taken for electric motor to reach synchronous speed from rest.

V = volume of rotor hysteresis material.

v = velocity of vehicle.

W = weight of vehicle/radial load on ball bearing.

W_h = hysteresis energy loss per cycle of magnetic material.

x = thickness of spiral spring strip.

α = angle which R makes with vertical/angle of lag between B_m and H_m/constant angular acceleration of electric motor.

δ = length of air-gap of hysteresis motor.

μ = coefficient of friction between road and wheel of vehicle/coefficient of friction between balls and races of ball bearings.

μ_o = Permeability of air-gap.

ϵ = dielectric constant of material between plates of capacitive pickoff.

ρ = resistivity of disc material of magnetic damper.

σ = conductivity of electrolyte in electrolytic pickoff.

ϕ = angle for limiting friction conditions/ magnetic flux/pole angle of microsyn pickoff/ maximum angle of spiral spring deflection.

θ = angle of tilt of rate gyro due to angular rate input/road superelevation (or bank) angle/angular deflection of microsyn rotor from null position/angle of rotation of potentiometer wiper.

θ_{max} = maximum possible angle of rotation of potentiometer wiper.

Ω = precessional angular velocity.

Ω_h = input angular velocity about horizontal

spin axis of gyro.

ω = angular velocity of spin of gyro wheel/ frequency of supply to microsyn stator(rad/s).

ω_1 = natural frequency of oscillation of gyro system about its output axis.

ω_s = synchronous spin speed of electric motor (rad/s).

ω_o = initial spin speed of electric motor(rad/s).

η = efficiency of electric motor.

ζ = damping ratio of gyro system about output axis.

S U M M A R Y

The main objective of this work is to design an instrument that could be used on land vehicles to help drivers in the accurate manipulation of their vehicles. The specifications for the design will be deduced after a thorough study of the problem. To this end, Chapter 1 deals with a rigorous definition and evaluation of the problem.

This is followed by Chapter 2 which centres mostly on the dynamics of road vehicles more especially around bends where the greatest hazards are assumed to occur. The last part of the Chapter mentions the selection of an appropriate instrument called the gyroscope (gyro for short) to provide the desired solution.

Chapter 3 introduces the gyro as a vehicle instrument. Its characteristics and classification are discussed. Mention is made of the numerous applications of this instrument. Details of these could be found in the literature. The last part of this Chapter discusses certain aspects that affect gyro design.

Chapter 4 discusses one configuration of the gyro (the rate-of-turn gyro) that has found widespread usage in aero-

nautics; and which could be easily adapted for land vehicles to serve the same function. The various parts of the rate gyro which are critical to the design are also mentioned. These parts include the gyro drive, the elastic restraint, the damping device and the signal pickoff.

Chapters.5 through 9 deal specifically with each of these elements - their characteristics, selection and design.

Chapter 10 deals with miscellaneous aspects of the design. One special feature that distinguishes this design from other designs is the addition of a mechanism that can be used to make the gyro adaptable to all kinds of land vehicles.

Chapter 11 deals with the preliminary design calculations for the main parts of the gyro. The detailed design of some of the components like the stator of the electric motor and the stator of the pickoff are left to experts in those fields.

Finally, a few concluding remarks were made followed by an Appendix and a list of references consulted during the work. The last pages contain the assembly drawing and element drawings of the instrument.

CHAPTER 1

DEFINITION OF THE PROBLEM

The use of instruments to help a person control a vehicle accurately and safely through a desired path can be called Vehicle Instrumentation. Today, instrumentation is almost exclusively associated with marine and air and space travel;(i.e. ships, planes, rockets, etc.). Over the very few years of aeronautical history instrumentation has helped to make aviation not only a safe means of transporting people and goods but also to put it in line costwise with land and marine means of transporting - especially of goods. Thus, despite the apparent hazards associated with air travel, it has become less hazardous than the other means of transport owing to the extensive use of flight instruments. And although the cumulative effect of loss to both lives and property by land vechiles far outweighs that caused by air vehicles, the occurence of air accidents always make headline news. Moreover, accidents with land vehicles are increasing steadily. There is therefore a need for finding means of increasing the safety of land vehicles. Just as the use of instruments has greatly enhanced the safety of air vehicles, it is believed that they could also be used to help the controllers of land vehicles to guide their vehicles properly.

Instruments for either air, marine or land transport serve two basic functions;

1. They help the controller to know as accurately as possible the conditions that affect his vehicle both within and without.
2. They relieve the controller of excess fatigue as he tries to judge the conditions of the road and/or atmosphere.

Basically, most of the instruments used on land vehicles (like hydraulic brake fluid level indicator, oil temperature indicator, battery charging indicator, etc. [1])* only tell the driver the conditions within the vehicle, and with the exception of the speedometer, none tell him the condition of the vehicle relative to the road or rail. And a large number of road accidents could be caused by these 'external' conditions.

Experience has shown that a driver is more strained when he is involved in a maneuver with his vehicle (like negotiating a bend) than when the vehicle is travelling on a straight road. This is because at a bend the driver is forced to control his speed in order to avoid accident through skidding and/or overturning.

---

* Numbers in square brackets [ ] indicate references quoted These are listed on pages 143 - 145.

Most bends on roads and rails are banked (or super-elevated) to counteract the effect of centrifugal force which may cause overturning. Also, the road surface is made rough not only to provide the necessary tractive effort but also to prevent skidding. Both overturning and skidding are functions of the vehicle speed. (Details of this will be discussed in the next chapter). The bankings on the roads are usually built on the basis of a chosen design speed. Also, for any given design speed, a minimum curve radius is imposed. However, the minimum curvature requirement is sometimes difficult to meet due to space restrictions caused by rugged terrain. Thus exceeding the design speed exposes the vehicle to chances of overturning and/or skidding. Since a vehicle driver is often not aware of the actual speed limit for a bend of given superelevation and radius of curvature, he is forced to reduce his speed to a 'low' safe value.

The purpose of this work is to design an instrument which could give the driver a good estimate of the <u>rate</u> at which he is traversing a curve. Since overturning and skidding are functions of this quantity, its measure could be monitored and used to predict the possibility of occurence of any of these effects.

The use of such an instrument on trucks, trailers and trains is expected to be a welcome development because of two reasons:

1. These vehicles are more prone to overturning due to heavy load and consequently a high centre of gravity.
2. There will be need to increase the maximum safe speed limit on trucks so that they could compete effectively with other means of transport like trains and planes.

It could be worth noting also that this same instrument could be used on trains to serve the same function. This is because of a general speculation that derailment of trains often followed by overturning could be caused by centrifugal force acting on one or more of the coaches as the train goes round a bend. Thus if a rate-of-turn indicator is mounted in each carriage, the behaviour of each could be monitored and appropriate action taken by the train driver.

CHAPTER 2

DYNAMICS OF ROAD VEHICLES ON CURVES

2.1. VEHICLE ON UNBANKED TRACK

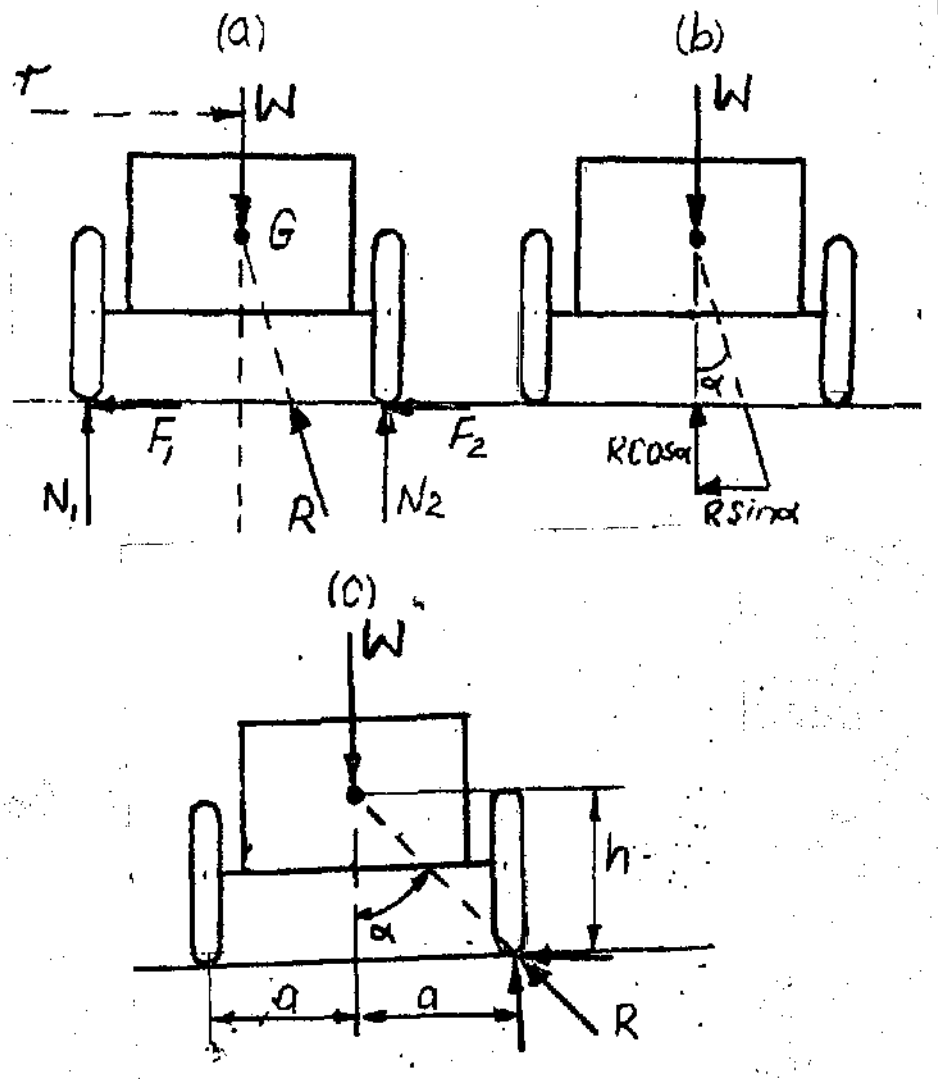


FIG. 1

Fig. 1a shows a vehicle of weight W moving round an unbanked track of radius of curvature r. The velocity of the vehicle is v, the height of its centre of gravity from the road surface is h and the wheel base is 2a as shown. The normal wheel reactions are N_1 and N_2 and the road friction forces F_1 and F_2.

The resultant of the forces N_1, N_2, F_1 and F_2 is R acting at an angle α to the vertical.

For the reaction force R to cause no rotation about the centre of gravity G, its line of action must pass through G.

The only force that tends to counteract the centrifugal force $\frac{W}{g}\frac{v^2}{r}$ is the horizontal component of R. That is

$$R \sin\alpha = \frac{W}{g}\frac{v^2}{r} \quad \text{----------(2.1)}$$

For vertical equilibrium,

$$R \cos\alpha = W \quad \text{----------(2.2)}$$

Dividing (2.1) by (2.2) gives

$$\tan\alpha = \frac{v^2}{gr} \quad \text{----------(2.3)}$$

The maximum permissible value that angle α can have is ϕ, the angle for limiting friction conditions.

If α exceeds this value, the vehicle skids. Thus

when $\alpha = \phi$, then

$$\tan \alpha = \tan \phi = \mu = \frac{v^2}{gr}$$

or $$v = \sqrt{\mu gr} \quad \text{----------(2.4)}$$

This is the maximum velocity for a bend of given radius; and skidding will occur if this value is exceeded.

Depending on the design of the vehicle it is possible for it to overturn about its outer wheels long before the speed is sufficient to cause skidding. For the vehicle to overturn, the reaction N_1 of the inner wheels and hence F_1 will vanish; and the whole load will be transferred to the outer wheels. This condition is depicted in Fig. 10.

From the geometry of this figure, if a is half the wheel base and h the height of the centre of gravity from the road surface then

$$\tan \alpha = \frac{a}{h} \quad \text{----------(2.5)}$$

Substituting $\tan \alpha$ in equation (2.3) gives

$$\frac{v^2}{gr} = \frac{a}{h}$$

or $$v = \sqrt{\frac{gar}{h}} \quad \text{----------(2.6)}$$

If $v > \sqrt{\frac{gar}{h}}$, the vehicle will overturn.

It could be noticed that the tendency to overturn is clearly related to the geometry of the vehicle.

2.2. VEHICLE ON SUPERELEVATED (BANKED) TRACK

Fig. 2a shows a vehicle which is traversing a track banked at an angle θ.

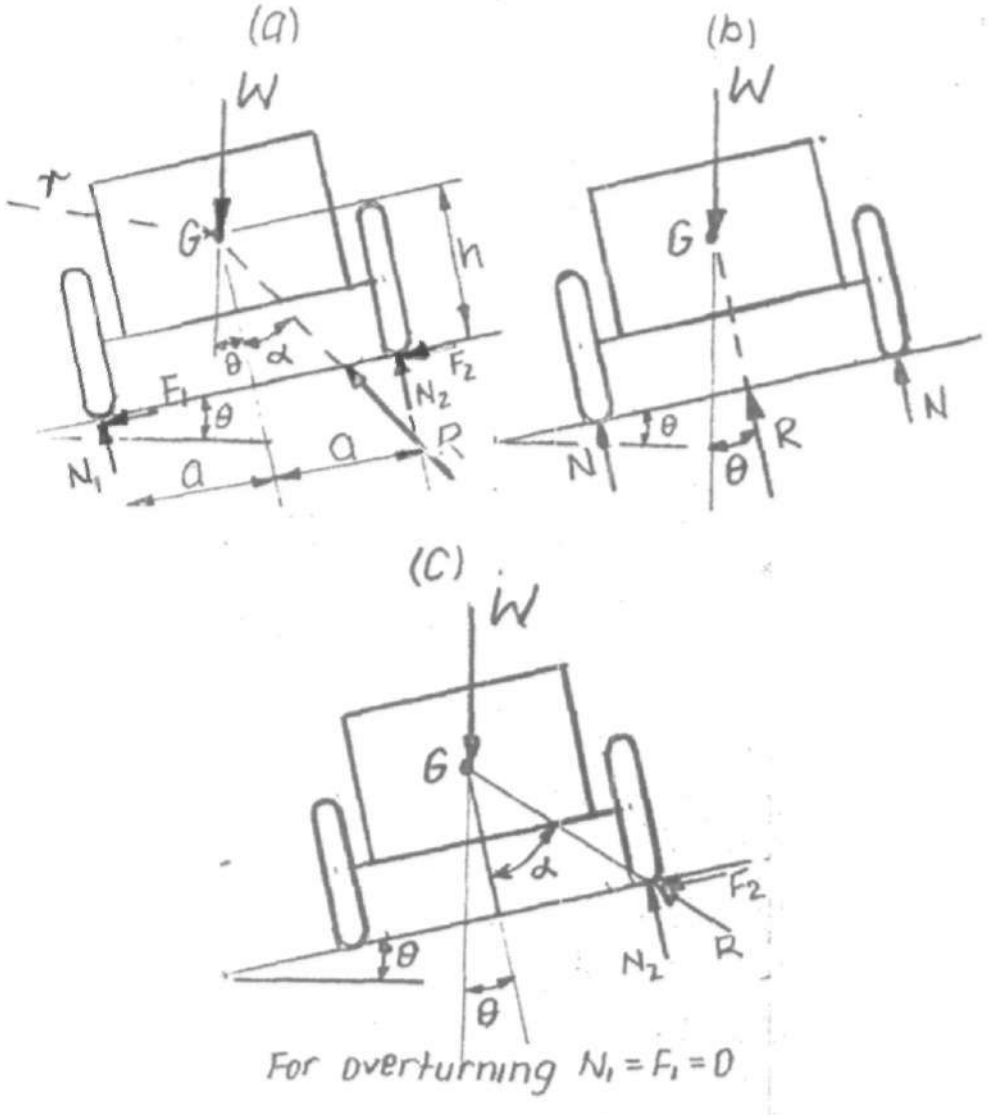


FIG.2

Proceeding as for the horizontal track, we get

$$R \sin(\theta + \alpha) = \frac{Wv^2}{gr}$$

$$R \cos(\theta + \alpha) = W$$

Dividing and rearranging gives

$$v^2 = gr \frac{\tan\theta + \tan\alpha}{1 - \tan\theta \tan\alpha} \quad \text{----------(2.7)}$$

There are two cases to consider:

Case 1 When $\alpha = 0$ (Fig. 2b)

For this case R will be normal to the track, hence there will be no road friction, i.e. $F_1 = F_2 = 0$ and $N_1 = N_2$. Also $\tan\alpha = 0$. Thus equation (2.7) becomes

$$\tan\theta = \frac{v^2}{gr} \quad \text{----------(2.8)}$$

This equation gives the angle of bank θ for which skidding will not occur, friction being zero. Also since $N_1 = N_2 \neq 0$, the vehicle will not overturn.

Case 2 When $\tan\alpha = a/h$ (Fig. 2c)

In this case the reaction R acts entirely at the outside wheels and the vehicle is on the point of overturning.

Putting $\tan\alpha = \frac{a}{h}$ in (2.7) gives

$$v^2 = gr \frac{\tan\theta + a/h}{1 - \tan\theta . a/h} \quad \text{----------(2.9)}$$

If $\phi > \alpha$, i.e. $\tan\phi > \tan\alpha$, i.e. $\mu > \frac{a}{h}$, friction is sufficient to allow the vehicle rotate about its outer wheels (i.e. to overturn).

But if $\phi < \alpha$, i.e. $\mu < \frac{a}{h}$ friction is not sufficient and the vehicle will skid instead of overturning. Hence the limiting conditions for skidding is when $\tan \phi = \tan \alpha$ or $\mu = \frac{a}{h}$. Thus the minimum speed for skidding is

$$v^2 = gr \frac{\tan \theta + \mu}{1 - \mu \tan \theta} \qquad \text{----------(2.10)}$$

A comparison of equations (2.4) with (2.10) and (2.6) with (2.9) will show that for the banked track the minimum velocities for skidding and overturning are higher than those for the unbanked track.

2.3. FACTORS AFFECTING SKIDDING AND OVERTURNING VELOCITIES

A study of the above equations will show that three main factors affect the minimum velocities at which skidding will occur. These are:

(a) Superelevation rate ($\tan \theta$)

(b) Coefficient of friction between tyres and road surface (μ).

(c) Radius of curvature of road (r).

A short discussion of each of these factors follows:

(a) Superelevation Rate ($\tan \theta$)

A study of equation (2.10) will show that the higher the superelevation rate (i.e. the higher the banking angle θ), the higher the minimum velocity at which skidding

occurs. However, experience has shown that superelevation rates cannot be increased indefinitely. This is because when a vehicle is travelling slowly around a curve with a high superelevation rate it is held in a proper path only when the driver steers up the slope or against the direction of the horizontal curve. This is an unnatural maneuver on the part of the driver. Furthermore, some trucks have high body loads and when travelling slowly on steep bankings a high percentage of the weight is carried by the inner wheels with a consequent reduction in vehicle stability.

The maximum rates of superelevation usable on highways are controlled by several factors;

(i) climatic conditions. (High rates of superelevation cannot be used in regions where icing occurs);

(ii) terrain condition (flat or rocky);

(iii) type of area (rural or urban);

(iv) frequency of very slow moving vehicles - since as stated earlier, a slow moving vehicle requires a lesser elevated curve than a fast moving one.

The following table gives values of superelevation rates often used by Highway Design Engineers [2].

TABLE 1. SUPERELEVATION RATES.

	Superelevation Rates (m/m).
Maximum for urban streets and expressways with snow and ice	0.06
Maximum for rural roads with snow and ice	0.08
Maximum for urban expressways	0.10
Maximum for rural roads	0.12

The above values are, however, operational only in countries that have established transport policies and the legal machinery to control vehicle reliability, method of loading, speed of operation, etc.

Since these conditions do not hold very well on Nigerian roads, values for the 0.08 rate are most often used [2] p.7.

For any particular region, only one of these values holds; though, of course, different values could be used for different road systems.

(b) Coefficient of Friction (or Side Friction Factor μ)

The coefficient of friction at which side-skidding is imminent depends on the speed of the vehicle, type and condition of the road surface and type and condition of the vehicle tyres. Since this factor depends on the speed of

the vehicle, it can only be selected on the basis of the speed for which the road is designed (design speed).

Values of this factor for good dry pavements range from about 0.5 at low speeds to about 0.35 at fairly high speeds. For a wet pavement and smooth tyres, the value is about 0.35 at low speeds.

In general, it was discovered that the friction factor decreases as the speed of the vehicle increases. For most practical purposes, values of μ range from 0.16 at 50 km/h to 0.11 at 130 km/h. [2]

(c) Radius of Curvature of Road (r)

The minimum radius of curvature that could be used is determined from the maximum rate of superelevation and the maximum coefficient of friction. This is clear from equation (2.10) which when solved for r gives

$$r = \frac{v^2(1 - \mu \tan \theta)}{\tan \theta + \mu}$$

Here, v is the design speed. Use of sharper curvature for this design speed would call for superelevation beyond the limit considered practical or for operation with tyre friction beyond safe limits, or both. Sharper curvature below minimum stipulated values are often encountered in mountainous regions where the provision of large radii of curvature could be expensive.

The table below shows different values of minimum radii for different values of design speeds [3].

TABLE 2. MIN. CURVE RADII.

Assumed Design Speed km/h	Areas of Operation	Radius of Curvature	
		Desirable Minimum (m)	Absolute Minimum (m)
50		90	70
70	Rural roads	160	125
80	Urban roads	250	200
100	Expressways	350	300
120	Freeways	600	450

The Design Speed

This is the speed selected for designing the road and all factors such as superelevation rates, side friction factors and radii of curvature are selected on the basis of this speed. The speed is selected on the basis of the type of road and the area of operation (rural, urban, freeway or expressway).

As a result of interviews with a number of road design engineers, it is found that design speeds range from 80 km/h to 110 km/h. Thus travelling at any speed beyond the design speed exposes the vehicle to chances of overturning and/or skidding. As was mentioned in the introductory chapter,

the purpose of this work is to design an instrument that will give a warning to the driver of the possibilities of occurence of overturning or skidding by giving a measure of the rate at which the turn is negotiated.

An instrument which has found widespread application in air and marine vehicles is the gyroscope (or gyro for short). This same instrument, because of its peculiar characteristics, presents itself as a promising building block for land transport instrumentation.

The object of the present work is restricted to designing a suitable gyroscopic device which could be used in land vehicles to assist the driver in his evaluation of some critical road and speed conditions.

CHAPTER 3

INTRODUCING THE GYROSCOPE

3.1. DEFINITION

In essence, a gyroscope is a very fast rotating wheel whose spin axis has the ability of staying fixed in space under certain conditions which will be mentioned shortly. This ability of the gyroscope (or gyro for short) is a direct consequence of its angular momentum. This quantity is given by the relation

$$H = I\omega \qquad \text{----------(3.1)}$$

where

H = angular momentum ($kg\text{-}m^2/s$).

I = moment of inertia of the wheel about the spin axis ($kg\text{-}m^2$)

ω = spin angular velocity of the wheel (rad/s.)

From dynamics, the sum of all the external moments acting on a body is equal to the rate of change of angular momentum. That is

$$\bar{M} = \frac{d\bar{H}}{dt} \qquad \text{----------(3.2)}$$

In the absence of external moments ($M = 0$), there follows

$$\frac{d\bar{H}}{dt} = 0$$

If we integrate this, we get

$$\bar{H} = I\omega = \text{constant} \quad \text{----------(3.3)}$$

This equation shows that in the absence of external moments (or when the sum of all external moments vanish) the angular momentum vector (and hence the spin vector) stays in a fixed direction in space. Thus the spinning body stays fixed in space so long as two conditions are satisfied:

1. The sum of all the external moments is zero.
2. The angular velocity of spin (ω) remains constant.

If disturbing torques are applied to the spinning wheel, the reaction is an angular velocity whose direction is such that it is perpendicular to the plane containing the vector of the disturbing torque and the vector of the spin velocity. This angular velocity is given as

$$\Omega = \frac{T_d}{H} \quad \text{----------(3.4)}$$

where

T_d = disturbing torque (N -m)

H = angular momentum ($kg\text{-}m^2/s$)

Ω = drift rate (or precession) (rad/s).

In the design of a gyroscope for which the property of 'staying put' in space is required, the major design

task is centred on eliminating as much as possible the occurence of these spurious torques.

Although we defined a gyroscope as a very rapidly rotating wheel, there is of recent years introduced a different type of gyro that does not use a rapidly rotating wheel but uses the vibrating characteristics of a tuning fork tines to measure rate of turn. This type of gyro is called a VIBRATING RATE GYRO. Details of its design and construction are given in [10] and [23].

Fig. 3 shows the two main types of gyros so far mentioned.

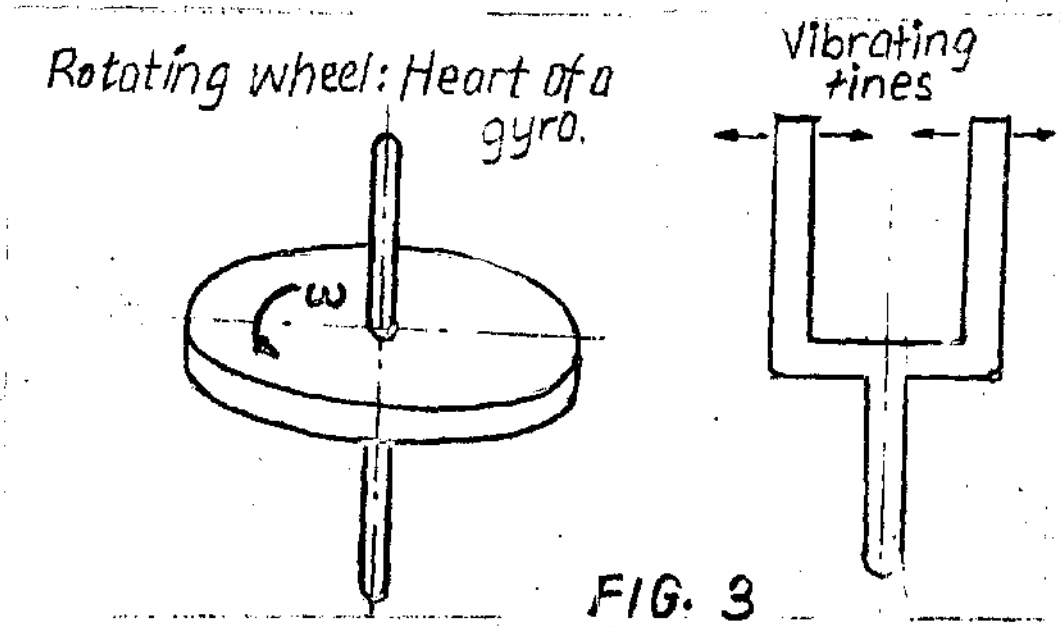


FIG. 3

3.2. CLASSIFICATION

There are a number of ways of classifying gyros:-

(i) According to the number of degrees of freedom(df)

(ii) According to the geometrical configuration (Horizontal or Vertical Spin Axis).

(iii) According to the function (Rate measurement, Integrating or displacement measurement).

(iv) According to the overall function (instrument or non-instrument).

(i) Classification According To The Number Of Degrees Of Freedom

Before the rapidly rotating wheel mentioned earlier could be used it has to be mounted on a frame. This frame is called a gimbal. Fig. 4a shows a typical arrangement in which the wheel is mounted on a gimbal. This arrangement could further be mounted on another gimbal.

The first configuration is called a single-degree-of-freedom (sdf) gyro since the gimbal is capable of rotating about axis xx only (shown in Fig. 4a).

The second configuration (Fig. 4b) is called a two-degree-of-freedom gyro since it can rotate about both axes xx and yy.

Many more gimbals could be added to give more degrees of freedom.

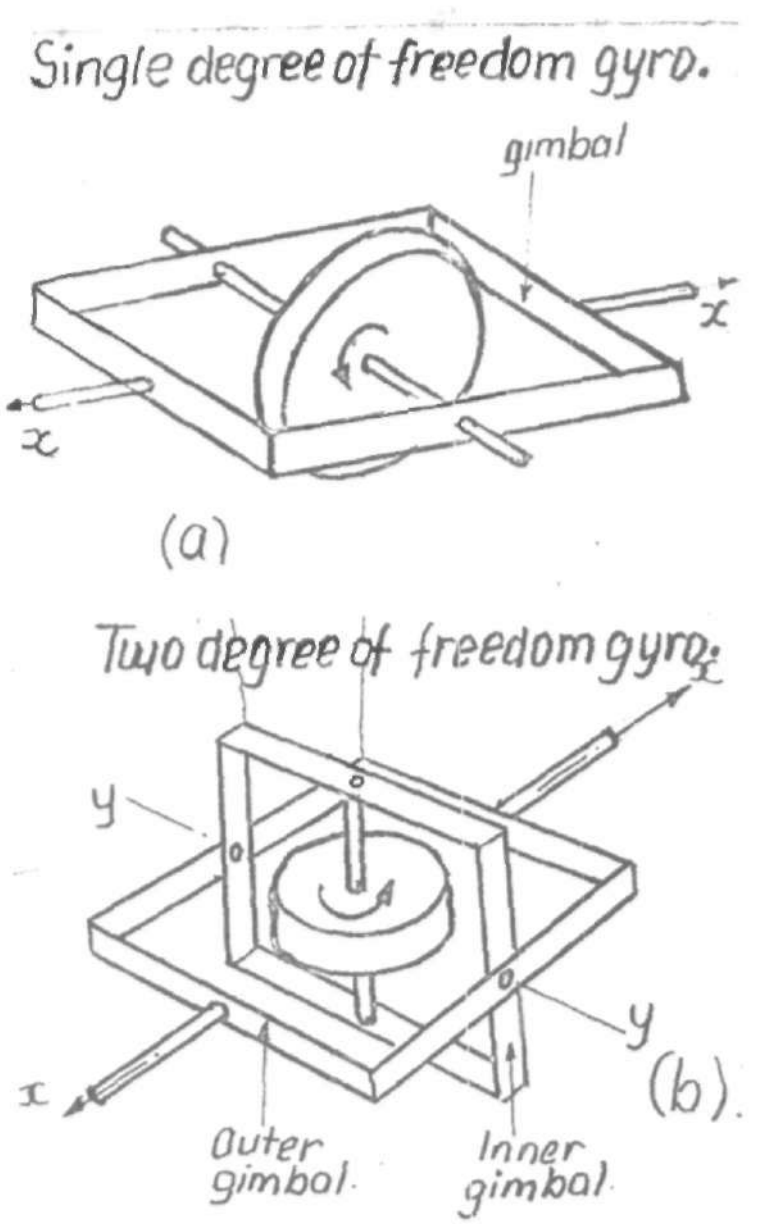


FIG. 4

(ii) Classification According To The Geometrical Configuration

The orientation of the spin axis could be such that it lies in the vertical plane or in the horizontal plane.

If the spin axis is stabilized in the vertical plane, the gyro is called a VERTICAL GYRO. But if the axis is stabilized with the spin axis in the horizontal plane, the gyro is called a DIRECTIONAL GYRO. Fig. 5 shows these two geometric configurations.

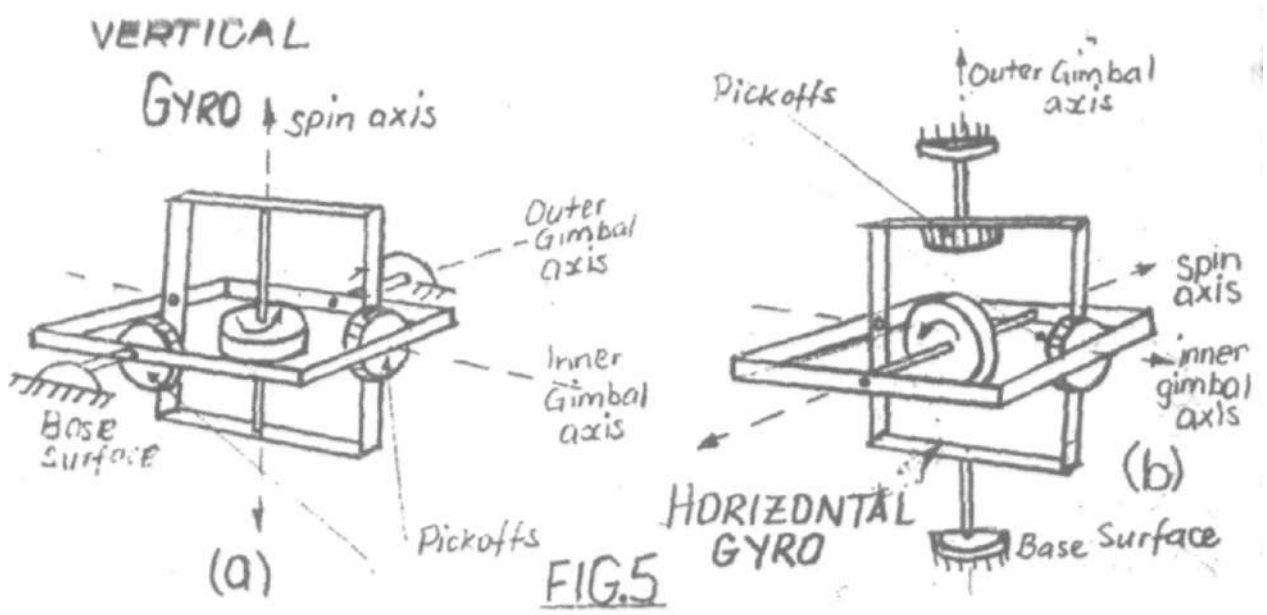


FIG.5

The vertical gyro is used to establish a vertical reference aboard a moving vehicle. Its practical applications appear in the following forms:

(a) pitch and roll indicator (artificial horizon) used to help an aircraft pilot maintain a level flight under blind flying conditions;

(b) Autopilots for automatic stabilization of aircraft;

(c) Stabilizer for guns, optical devices, radar antennas and search lights aboard Navy combat vessels.

The constructional features of these instruments are treated in detail in [7].

The directional gyro forms the basic element for gyrocompasses which are used to tell directions accurately especially when magnetic compasses cannot be relied upon (as when the vehicle is involved in a maneuver).

Details of the construction of a gyrocompass are also given in [7].

(iii) Classification According To Function

Gyros could also be classified according to the particular function they perform. There are basically three functions:-

(a) Measurement of Displacement

The gyro that performs this function can be either a two-degree-of-freedom gyro or a single-degree-of-freedom gyro (Figs. 5a and 6).

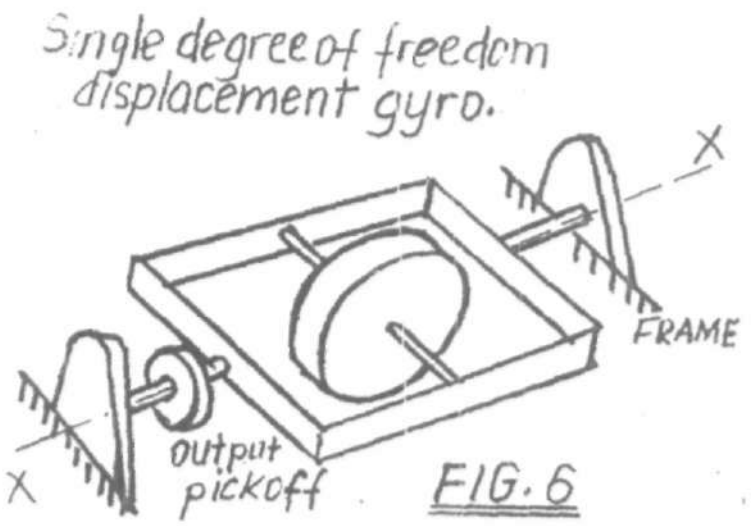


FIG. 6

Consider the 2df gyro shown in Fig. 5a. Since the spin axis remains stablized in inertial space (assuming no external torques), then motion of the frame about the outer gimbal axis will produce a signal at the pick-off on that axis which is a measure of the angular displacement of the frame with respect to the gyro wheel spin axis (or inertial space).

If the frame were to move about the inner gimbal axis, then it will rotate with the outer gimbal, leaving the inner gimbal and the spin axis in the vertical plane. The

pickoff on the inner gimbal axis will give a signal which is proportional to the angular displacement between the inner gimbal and the outer gimbal or the angular displacement between the outer gimbal and inertial space.

Thus the two-degree-of-freedom gyro can provide information on the angular displacement of the frame about two mutually perpendicular axes.

The single-degree-of-freedom gyro shown in Fig. 6 can provide information on the angular displacement of the frame about the A XX axis only. Thus by using three of these with their spin axes pointing in three mutually perpendicular directions the set can provide information on the angular displacement of the frame along three mutually perpendicular axes in space. This arrangement finds extensive application in the stabilization of platforms for Inertial Navigation.

(b) Measurement of Rate

A rate gyro is a single-degree-of-freedom gyro whose motion about the gimbal (or output) axis is restrained with the aid of an elastic member (such as spring, torsion wire, etc.). Fig. 7 shows a schematic of a rate gyro.

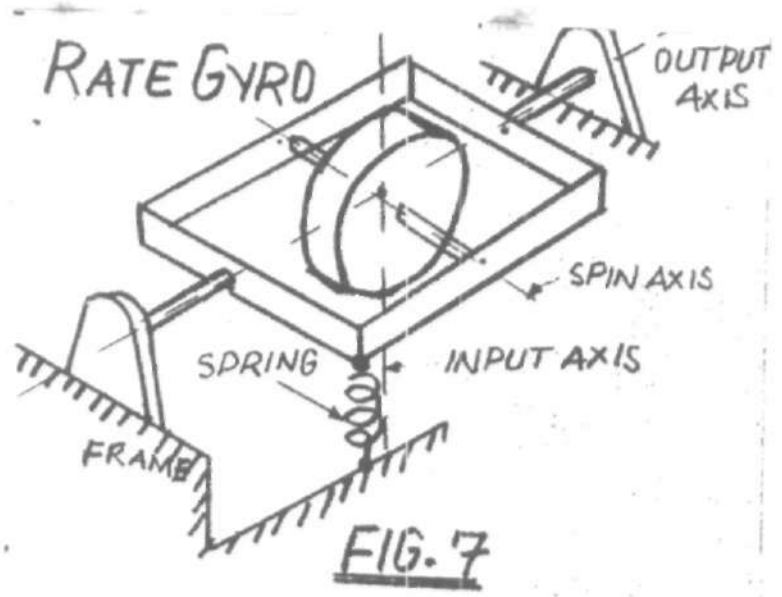


FIG. 7

If the frame carrying the gyro is made to rotate about the vertical (or input) axis, the gyro will respond with an angular displacement about the gimbal (or output) axis, which is directly related to the rate of rotation of the frame. Thus if it is mounted on a vehicle, the gyro will provide information on the rate at which the vehicle is traversing a curve.

Quite often, a damping system is connected along the output axis to minimise oscillations of the gimbal when subjected to an input signal.

(c) Integration

An integrating gyro is a single-degree-of-freedom gyro for which a damping device is connected along the output axis. (Fig. 8).

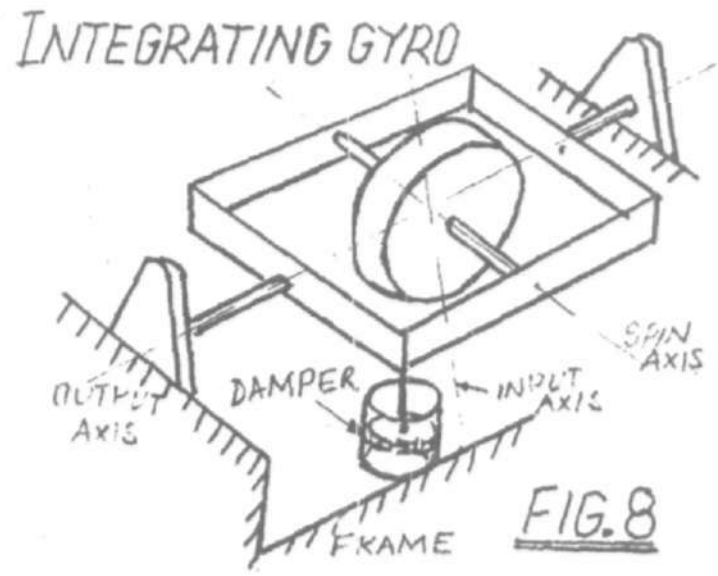


FIG. 8

In this type of gyro, angular velocity about the input axis will cause the gyro to rotate with some angular velocity about the gimbal axis (or output axis). This gimbal (or output) angular velocity will always be directly proportional to the angular velocity about the input axis. Thus at any given time the total angle through which the gimbal rotates about the output axis will be directly proportional to the total angle through which the gyro rotates

about the input axis.

Integrating gyros find widespread application in Inertial Navigation where they are used in stabilizing platforms and acting as vertical references. Details of these applications are given in [6].

(iv) Classification According To Overall Function

In this classification, gyros are divided into two basic groups - instrument and non-instrument. The former group refer to the applications of the gyros as sensing devices in a control system, while the later refer to their applications as direct stabilizing elements. This last group of gyros is almost vanishing due to the discovery of better means of stabilization, which utilize the sensing ability of the instrument gyros, in conjunction with appropriate servomechanisms.

3.3. SUMMARY OF APPLICATIONS

The gyro in the various forms mentioned above finds extensive applications in Marine, Aeronautical, Land, Inertial, Military and other fields.

A list of the various applications is given below. Details of these applications can be obtained from [4], [5], [6] and [7].

Marine Applications

(i) Gyrocompass

(ii) Stabilization of ships

(iii) Automatic steering of ships.

Aeronautical Applications

(i) Directional gyros

(ii) Artificial horizon

(iii) Rate of turn indicators

(iv) Automatic pilots.

Military Applications

(i) Naval gunnery

(ii) Aircraft Bombsights and Gunsights

(iii) Control of Missiles.

Inertial Navigation

(i) Stabilization of Inertial Platforms.

(ii) Integrating accelerometers. [6]

Land and Other Applications

(i) Stabilizing Monorail Vehicles

(ii) Binocular stabilizer [6]

(iii) Direction finders used to provide stabilized line of sight for surveying oil wells. [6]

3.4. ASPECTS OF GYROSCOPE DESIGN

Since the major part of this work involves the design of a gyroscope, it will not be out of place to mention the critical factors that affect the design of a gyroscope.

Fig. 9 shows the most essential parts of a gyro. Some of the parts may be removed, depending on the functional requirements of the gyro.

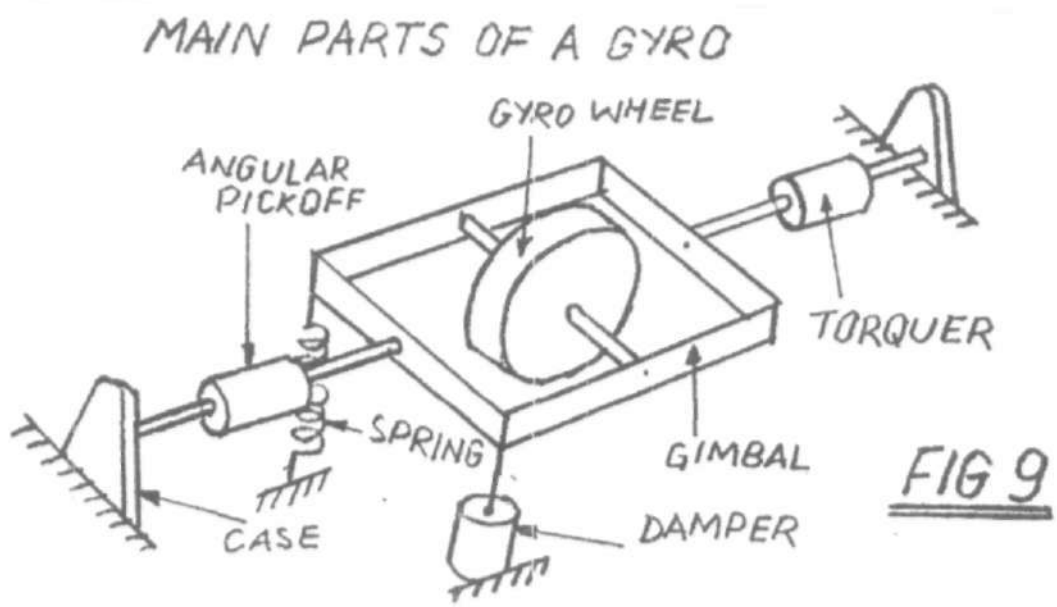


FIG 9

The three main factors that govern the design of a gyro are:

1. Performance Requirements - meeting the specifications covering function, accuracy and environmental conditions.

2. Producibility Requirements - capable of being produced within certain cost and time limitations.

3. Reliability Requirements - ability to maintain operational capability within performance specifications even after exposure to various conditions of handling, test, service, use and storage.

The principles governing the design for producibility and reliability demand the application of standard rules coupled with good judgement based on past design experience. Thus there are no rigid mathematical analysis in these areas. However, the principles governing performance requirements are wide open to analysis.

The major areas of consideration when performance requirements are involved are:

(a) reducing as much as possible gimbal disturbing torques. The effects of these torques were mentioned earlier on in this chapter (Equation (3.4))

(b) maximizing angular momentum

(c) providing accurate pickoff and torquing systems.

Each of these conditions will be treated in great detail:

(a) Gimbal Torques (Suspension Torques)

The most important design problem in meeting performance requirements is to minimize as much as possible,

disturbing torques acting on the gimbal. The extent to which this must go depends on the precision requirements of the gyro.

Basically, there are two classes of disturbing torques:

(i) Systematic torques

(ii) Random torques.

Systematic torques can be measured and their characteristics can be correlated with some parameter. Thus it is theoretically possible to compensate for these torques either directly or indirectly. Random torques, however, cannot be measured with any degree of certainty. The magnitude of random torques thus clearly establishes the level of uncertainty in the gyro performance.

Details of these torques and their effect on gyro performance are treated in detail in [8].

(b) Angular Momentum

Equation (3.4) of this chapter gives the relationship between the drift rate of the gyro and the gimbal torques.

$$\Omega = \frac{T_d}{H}$$

or

$$\text{Drift rate} = \frac{\text{Gimbal torque(unwanted)}}{\text{Angular momentum}}$$

From this equation it is clear that to minimize the drift rate, the unwanted gimbal torques should be minimized and the angular momentum maximized.

From equation (3.1), the angular momentum H is given by

$$H = I\omega = \omega MK^2$$

where

ω = gyro wheel spin speed

M = mass of wheel

K = radius of gyration of wheel about its spin axis.

The angular momentum can be maximized by maximizing any or all of the above three parameters. However, there are limitations to this approach:

Rotor Spin Speed

If the gyro wheel is driven by an electric motor, then as the spin speed requirement increases, power needed to overcome windage and bearing friction also rises. Thus a large motor becomes necessary. This introduces increased heating effects (this is detrimental to gyros floated in fluids). Also, the life span of the bearings is greatly reduced.

Rotor Mass

The mass of the gyro wheel could be increased by using higher density material or increasing the size of the rim. This large mass will call for the use of bigger bearings and hence increased friction. Increased friction means the need for a larger motor with its accompanying increased power and heating.

Radius of Gyration

To increase the radius of gyration, the diameter of the gyro wheel must be increased. However, this cannot be done indefinitely since space requirements are always imposed on the overall gyro design.

(c) Pickoff And Torquing Systems

Pickoffs are certain transducers which are connected to the gyro along its output axis. Their main function is to detect the relative angular displacements between the gimbal and the supporting case.

Torquers on the other hand are used to compensate for certain types of errors and also to allow for the use of a single-degree-of-freedom gyro as a rate sensing device.

It goes without saying, that any of these two devices could introduce unwanted torques about the gimbal axis.

SUMMARY

From the above analysis it is clear that the design of a gyro involves a number of conflicting factors. Thus if the mass of the rim is increased (to increase its angular momentum) the inertia of the gyro about the output axis increases. This has the effect of making the system less dynamically stable. In this case, gyro manufacturers use a certain figure of merit f_m given by

$$f_m = \frac{I_s}{I_o} \qquad [6]$$

where

I_s = inertia of gyro wheel about spin axis.

I_o = inertia of gyro wheel about output axis.

The higher the value of this figure of merit the more satisfactory is the gyro.

In the design of very high precision gyros, optimization techniques could be utilized to maximize the desired parameters and minimize the unwanted parameters.

Also in these high precision gyros, the bearings carrying the gimbal are replaced with air-bearings or magnetic suspension bearings. Additionally, by floating the gyro gimbal in a fluid, the load carried by the suspensions is markedly reduced and hence smaller and more precise suspension systems can be used.

CHAPTER 4

THE GYRO AS A RATE OF TURN SENSOR

4.1. FUNDAMENTAL EQUATION OF THE RATE GYRO

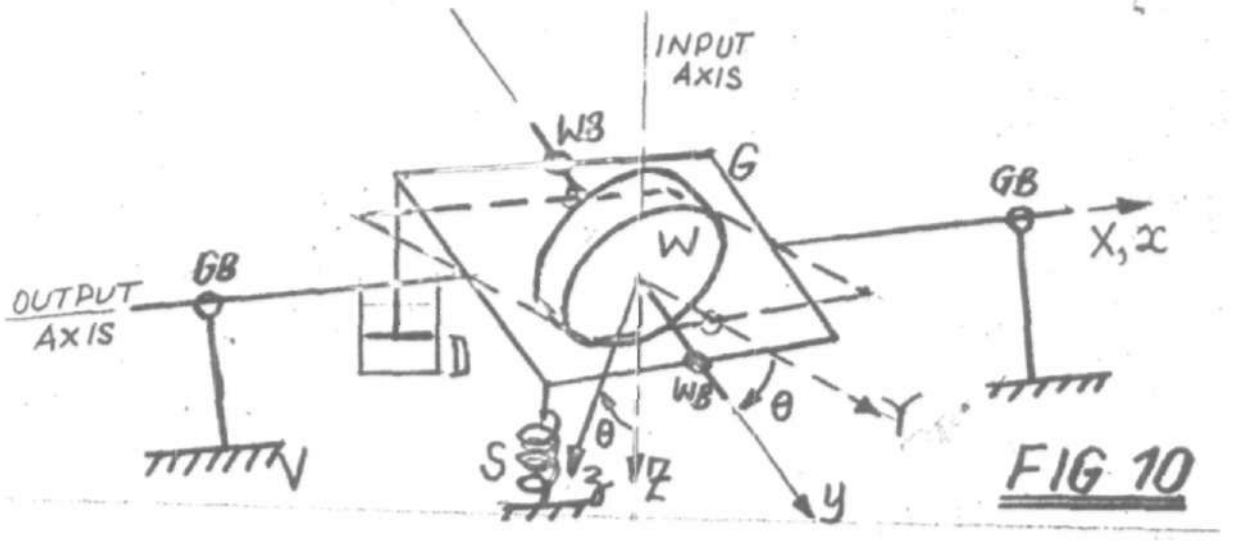


Fig. 10 shows in schematic form the main features of a rate gyro mounted on a vehicle or platform (V).

In this diagram,

G = gimbal ring

W = gyro wheel

S = spring or elastic restraint

D = damper

WB = gyro wheel bearings

GB = gimbal ring bearings.

Let the axes OX, OY and OZ represent the principal axes of the vehicle, while O_x, O_y and O_z represent the principal axes of the gyro.

When the vehicle is moving along a straight line (in the direction OX), there is no angular velocity input hence the two sets of axes mentioned above point in the same direction. For this same condition the gyro has only one degree of freedom - about O_x. Consequently, rolling of the vehicle about OX and pitching about OY have no effect on the gyro.

Let the vehicle enter a bend under the following conditions:

R = radius of curvature of bend

v = velocity of vehicle in bend

ω = spin speed of gyro wheel

Ω = rate of turn of the vehicle round the bend

$(\Omega = \frac{v}{R})$

θ = angle of tilt of gyro due to the angular rate input Ω about OZ (assumed to be small).

Let K = torsional constant of elastic restraint

C = damping coefficient

I = inertia of rotor wheel about O_y (spin) axis.

It can be shown (Appendix) that under the action of the rate of turn Ω , the gyro responds with a reaction torque given by

$$T_R = (I\omega)\Omega \qquad \text{----------(4.1)}$$

This torque acts about the output axis (O_x), and causes the gimbal to rotate about that axis until the restraining torque due to the spring or elastic member counters the reaction torque. The elastic torque is given by

$$T_e = K\theta \qquad \text{----------(4.2)}$$

At equilibrium, the two torques (4.1) and (4.2) are equal. Hence

$$K\theta = I\omega\Omega$$

$$\therefore \boxed{\theta = \left(\frac{I\omega}{K}\right)\Omega} \qquad \text{----------(4.3)}$$

This equation is the fundamental equation of the rate gyro. Since I, ω and K are constants for any particular gyro, we see that the output angle is directly proportional to the rate of turn. Thus this angle can be used to give a measure of the rate of turn.

4.2. THE DYNAMIC RESPONSE OF THE RATE GYRO

Since the gyro has appreciable inertia about the output axis, it has the tendency to oscillate when subjected

to an angular velocity input and it may take some time before it finally settles to a steady reading. This type of behaviour is most unwelcome in an instrument where instant values of the output are needed. A damping device is thus added to the gyro along its output axis to minimize the oscillations.

If damping is introduced, the fundamental equation of the rate gyro can be shown (Appendix) to become;

$$\theta = \frac{I\omega\Omega}{K}\left\{1-\exp.\left[-\zeta\omega_1 t\right]\mathrm{Cos}\left(pt - \tan^{-1}\frac{\zeta}{\sqrt{1-\zeta^2}}\right)\right\} \quad \text{--(4.4)}$$

Here ζ = damping ratio,

$$= \frac{C}{2\ Ix\ \omega_1} \quad \text{----------(4.5)}$$

where

C = damping constant

Ix = inertia of gyro (wheel, gimbal and other attachments) about O_x.

ω_1 = natural frequency of oscillation of the system

p = natural damped frequency of oscillation of the system.

A study of equation (4.4) shows that it contains two terms. The first one is a steady value and is the same as equation (4.3); while the second term is a rapidly decaying term which soon vanishes, leaving only the steady value.

In practice, the degree of damping depends on the requirements of the instrument, but ζ is usually taken less than unity. Values of ζ from 0.4 - 0.7 are most often used [6_7]. Increasing ζ makes the oscillations reduce to a given level in fewer cycles but increases the periodic time (or time taken for the system to reach a steady value).

4.3. CROSS COUPLING ERROR

A very important facet of Rate Gyro design is the concept of cross-coupling error. Consider the gyro shown in Fig. 11, which has responded to an angular velocity input Ω .

Since under the input angular velocity Ω the gimbal will tilt through an angle θ, then the input axis, the output axis and the spin axis are no longer mutually orthogonal. But the first two together with the component of ω in the horizontal plane are orthogonal.

Hence

$$I(\omega \cos\theta)\Omega = K\theta$$

$$\therefore \quad \dot{\theta} = \left(\frac{I\omega}{K}\right) \cos\theta . \Omega$$

Cross coupling error.

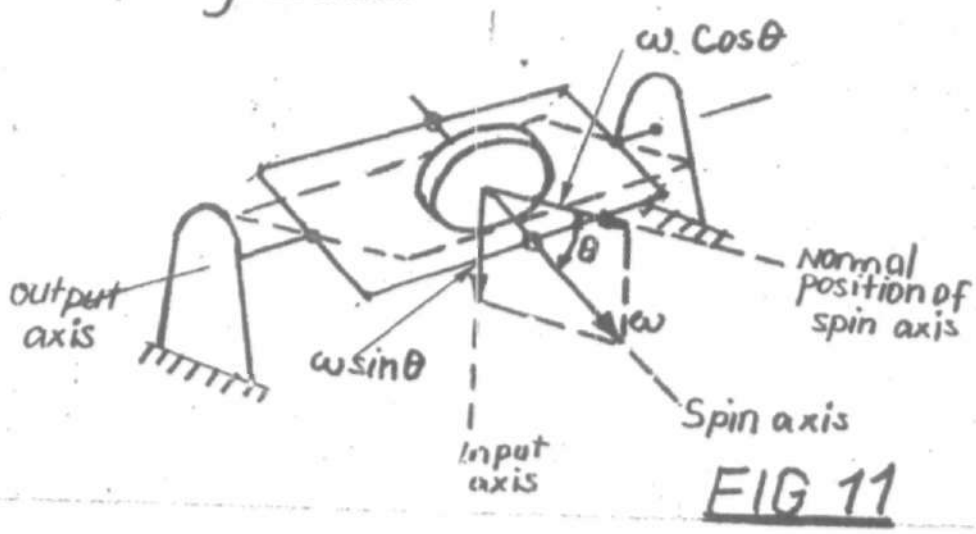


FIG 11

Now, it could be noticed that there is a component of spin along the input axis = ω Sin θ. If there is any angular velocity input along the horizontal axis (Ω_h , say), then this, together with ω Sin θ will cause a torque along the output axis given by

$$T = I(\omega \text{ Sin } \theta).\Omega_h$$

This will cause a spurious output angle θ^1 given by

$$\theta^1 = \frac{I \omega \Omega_h}{K} \text{ Sin } \theta$$

This angle constitutes an error in the actual output θ and is called a cross-coupling error.

Note:

In the case of land vehicles, this error can be shown to be negligible since the pitching movements of these vehicles are small ($\Omega_h \approx 0$).

Hence large output angular deflections can be utilized to enhance the accuracy of the instrument.

4.4. RATE GYRO DESIGN

Fig. 12 shows once again a schematic arrangement of the rate gyro highlighting the main areas of design consideration. Each of these elements will be treated separately in the subsequent chapters.

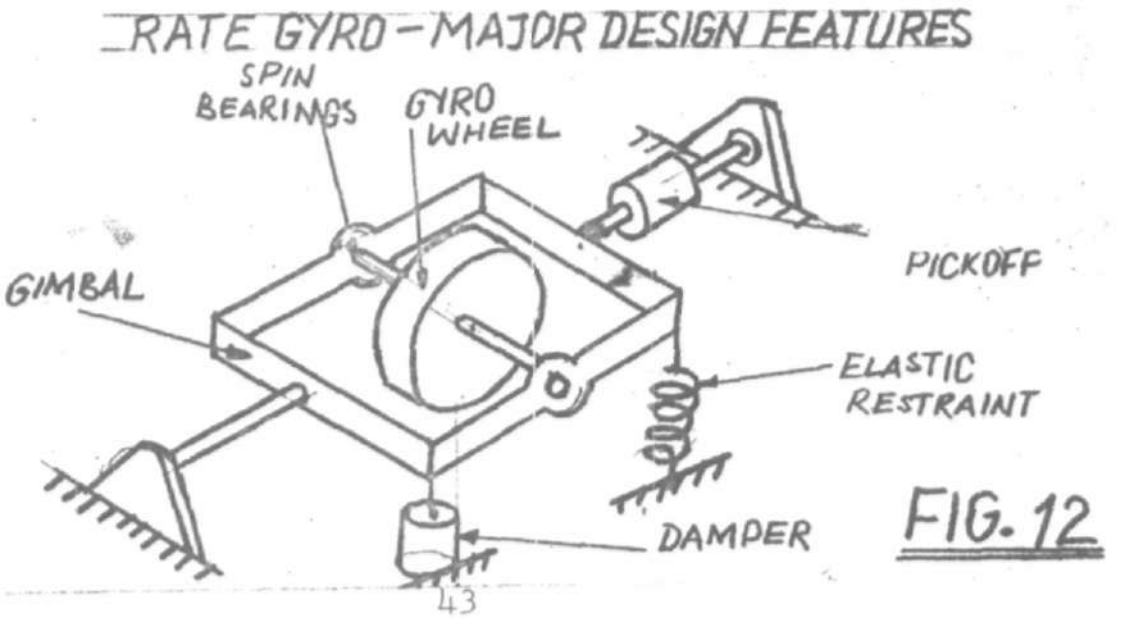


FIG. 12

CHAPTER 5

GYRO DRIVES

Since the most essential component of a rate gyro is a fast spinning wheel, some device must be employed to impart the spin to the wheel. There are three main methods of doing this:

1. By spiral spring
2. By air blast
3. By electric motor.

Each of these will be considered in greater detail.

5.1. SPIRAL SPRING DRIVE

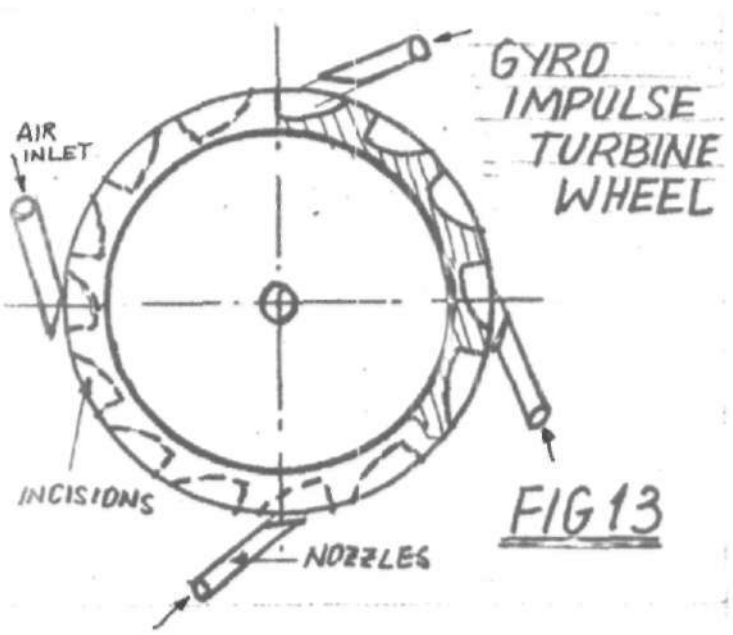
This type of drive is mainly used for short time operations as in the case of torpedo gyros or missile gyros where the gyro is required to guide the vehicle over the short period of its motion. This drive is cheaper and more reliable for these applications.

In essense, the drive consists of the rotor which is driven via gearing from a wound spiral spring (of the clock type). The speed is stored in the spring in the form of potential energy which is released to spin the gyro wheel immediately the weapon is released.

5.2. PNEUMATIC DRIVE

In this case the gyro is driven on the principle of the impulse turbine or Pelton wheel. However, in most designs the fluid impinges on incisions cut around the periphery of the wheel instead of on buckets as in the former machine.

Fig. 13 shows a typical impulse turbine wheel for gyro rotors.



The air-blast needed to drive the wheel can be provided in two ways:

1. The inside of the gyro casing is evacuated to a very low pressure by connecting it to a vacuum pump

which is driven by the engine. As the gyro case is evacuated, fresh air is admitted through a set of nozzles (usually 4) arranged round the periphery of the wheel. The nozzles are arranged such that the air-blast coming in through the nozzles impinges on the buckets causing the wheel to rotate at high speed.

2. Instead of evacuating the casing, air at high pressure is admitted via the nozzles. The high pressure air could be obtained by connecting the gyro to the pressure side of a vacuum pump or from a compressor.

A number of factors render these methods of driving the gyro wheel unsuitable for land vehicle applications:

1. The vacuum pump or compressor will have to be driven by the engine thus increasing engine load.

2. The vacuum pump and other pneumatic accessories make the whole arrangement cumbersome and expensive.

3. The gyro casing must be made air-tight which increases the complexity of the design.

4. The rotor speed cannot be accurately defined since it is a function of air-speed through the nozzles which is itself a function of the vacuum in the casing.

5. The rotor is often subject to small but unpredictable pneumatic couples due to gusts of the incoming air.

Despite these disadvantages, however, pneumatic drives are used for low precision or non-critical gyro designs. This is because by using these drives;

1. the overall gyro design becomes much more simplified;

2. the instrument is more rugged since there are no wires which may sag and introduce unwanted couples.

Finally, it could be worth noting that these drives find extensive usage in aircraft instrumentation where low pressure in the gyro casing can be obtained cheaply by connecting the gyro to the low pressure side of the wings.

5.3. THE ELECTRIC DRIVE

An electric motor (either induction type or synchronous type) is most often used to spin the gyro wheel. In conventional motor design, the rotor rotates within the stator. However, in most gyro motors, this configuration is reversed - the rotor lies outside the stator (Fig. 14).

By arranging for the rotor to be outside the stator, the inertia and hence angular momentum of the gyro is improved.

Although an induction motor could be used to drive the gyro wheel, the type of motor which is almost exclusively used for gyro drives is the synchronous hysteresis motor.

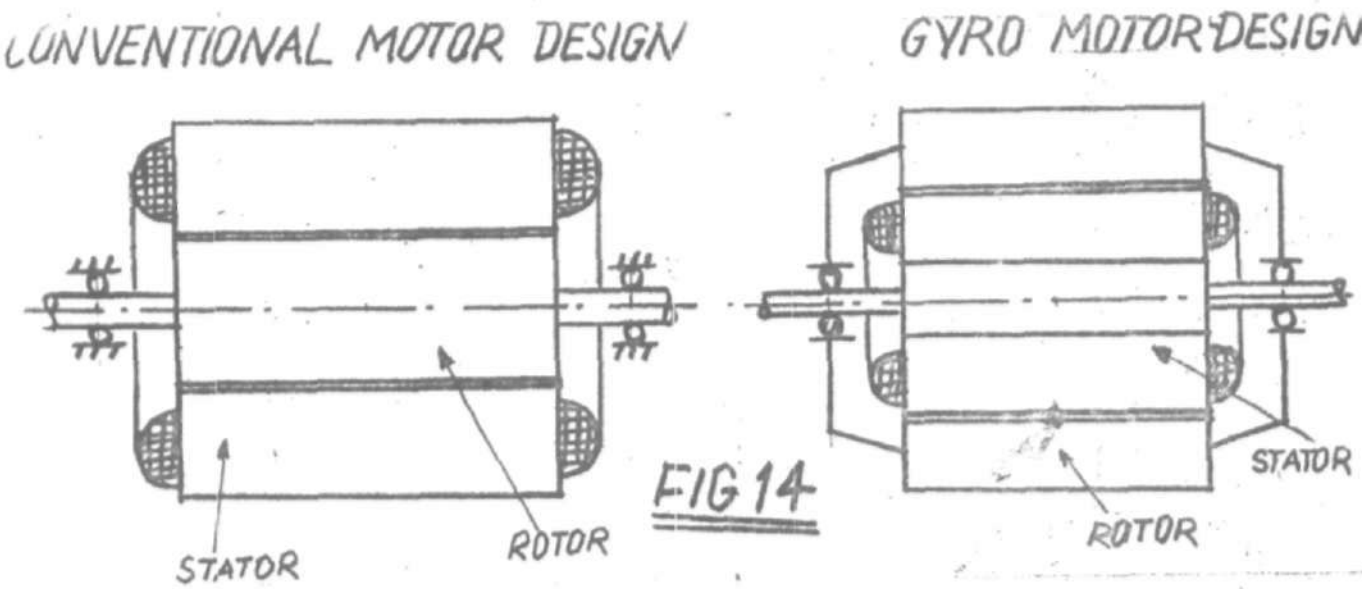


FIG 14

This motor has several advantages over the induction motor and other synchronous motors for gyro driving. Some of these advantages are:

1. It can accelerate a load inertia of any magnitude up to synchronous speed, provided that the load torque opposing rotation arising from bearing friction, windage and similar other causes is not in excess of the hysteresis torque.
2. Its efficiency, power factor, and maximum output can be increased by oversaturation. This is done by

momentarily increasing the applied voltage to between 50 - 100% above its normal value after reaching synchronous speed.

3. Its starting current is only 110 - 115% of full-load current compared to around 300% for an induction motor.

4. It has a comparatively high starting torque.

5. The output speed remains constant even when operating from a $\pm$ 10% voltage source. This is a useful property for a gyro which gets its power supply from a battery, since the output voltage of the battery may be lowered as it gets discharged.

6. The motor is simple and rugged in structure - since the rotor can be made of solid material instead of laminations.

7. Its range of speed adjustment by frequency control is greater than for an induction motor.

8. Its momentum is 6 - 10% higher than for an induction motor because of zero slip.

9. The smooth rotor surface and absence of rotor slots give good mechanical stability, reduces windage loss and vibration at high speeds and makes the motor quiet running.

5.4. SELECTION OF DRIVE

On the basis of the above discussion, a Hysteresis motor will be selected as the drive for the rate gyro to be designed.

One serious disadvantage of the hysteresis motor is its rather low efficiency. However, as will be shown in the next chapter, the efficiency will be greatly improved by introducing certain modifications in the design.

5.5. POWER SUPPLY

Since the hysteresis motor for driving gyro wheels is a very small one (in the fractional horse-power category), it can be driven directly from the battery of the vehicle. It is expected that the power and current that the motor will absorb will not be too large as to affect the battery.

However, the hysteresis motor, being an a.c. motor requires an a.c. source to run it; hence it cannot be connected directly to the battery which is a d.c. source. Thus for the hysteresis motor to utilize the d.c. of the battery, the d.c. will have to be converted to a.c. This is achieved by use of the so-called Power Converters. Details of the theory and design of Power Converters is adequately treated in [12].

One apparent problem is that the output of most converters is a square wave instead of a sinusoidal wave; and motors running on square wave sources require slightly more voltage than when running on a sinusoidal wave.

Another problem is that since the hysteresis motor is a multi-phase motor, it cannot be run from a single phase as is provided by a converter. Some form of phase splitting device like a capacitor is required to convert the single phase from the converter to at least two phases.

A block diagram of the whole arrangement is given in Fig. 15.

Driving a hysteresis motor from d.c. source.

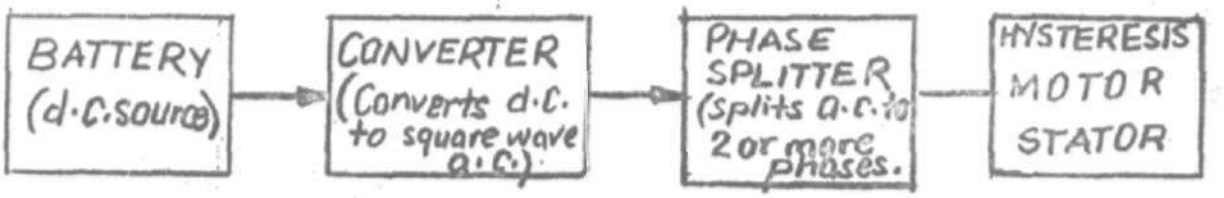


FIG 15

Although the extra attachments (converter and phase-splitter) make the arrangement more complicated, it has been recently discovered that a Hysteresis Motor of the capacitor split-phase type driven from a square voltage source has a unique advantage over other Hysteresis motors (like those driven from a 3-phase sinusoidal voltage source). The unique advantage of this motor is that the synchronous pull-out torque (hence, the maximum synchronous output power) is increased, the input current is decreased and the efficiency greatly improved. For details of this, see [14]

CHAPTER 6

THEORY AND DESIGN ASPECTS OF THE HYSTERESIS MOTOR

6.1. THEORY OF THE HYSTERESIS MOTOR

When an a.c. is used to magnetize a ferro-magnetic material, the complete hysteresis loop is traversed once for every cycle of alternating current. A typical loop is shown in Fig. 16.

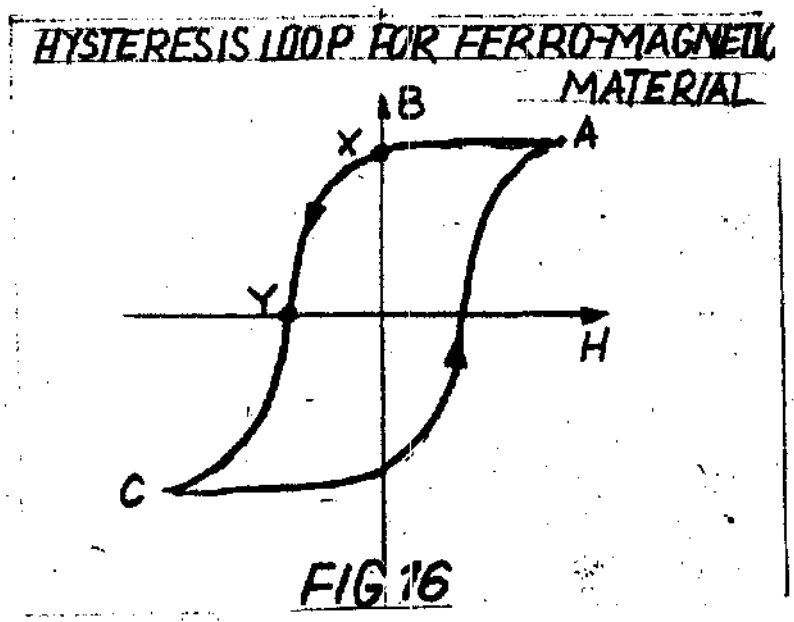


FIG 16

The magnetization force H will be in phase with the current. Now, when the current reaches its maximum (or peak) value, the iron will be magnetized to point A; but when the current has dropped to zero (H = 0), the iron

will still be magnetized to point X. It is thus evident that the point of zero magnetization B will lag the zero of the magnetizing force H (and current) in time. This time lag between B and H is the basis of the operation of the hysteresis motor.

Consider Fig. 17 below:

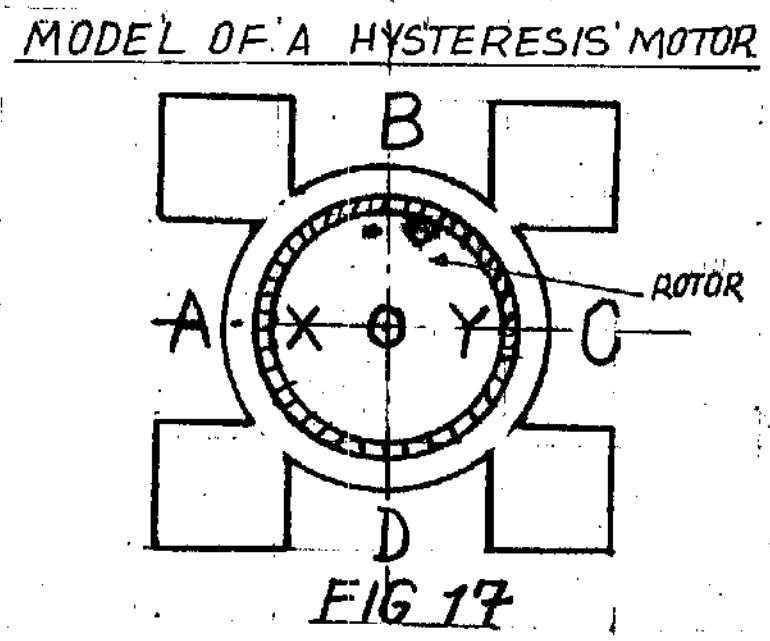


FIG 17

In this figure, A, B, C, D are the four poles of a two-phase field. At one instant A will have N-polarity, C will then have S-polarity while B and D will be neutral.

The rotor, having a hard magnetic material (say Cobalt) ring at its periphery will have a S-pole induced at X and a N-pole at Y. Owing to the field rotation a quarter-cycle

later B will have N-polarity, and D will have S-polarity and A and C will be neutral.

But because of the hysteresis lag in the rotor, X will have some residual S-polarity and Y some residual N-polarity. Thus X will be attracted towards B and Y towards D. This attraction will exert a torque on the rotor that causes it to rotate following the rotating field.

Suppose the rotor is held fixed so that it does not rotate with the field. Then another quarter cycle later, A will have a S-polarity and C a N-polarity while B and D remain neutral. Since X had a residual field of S-polarity, then it will have to realign itself such that it has a N-polarity (opposite polarity to the one now at A). This realignment of the magnetic dipoles requires the expenditure of energy called Hysteresis loss. In practice, however, the rotor tends to resist this realignment by following the rotating stator flux. Thus the rotor utilizes the hysteresis loss that would have been wasted in the form of heat to exert a torque on the motor shaft. It is because of this that this type of motor is called a Hysteresis Motor.

The energy loss (or Hysteresis Loss) is proportional to the area of the hysteresis loop. Thus the hysteresis

motor torque is also proportional to the area of the hysteresis loop. This torque is given by [8]:

$$T = \frac{pVW_h}{4\pi} \qquad \text{----------(6.1)}$$

where

$$W_h = B_m H_m \sin\alpha \qquad \text{----------(6.2)}$$

and

W_h = hysteresis loss per cycle which is proportional to the area of the hysteresis loop.

V = volume of hysteresis material of rotor.

p = number of poles in stator winding.

B_m = flux density in rotor (peak value).

H_m = rotor magnetizing force (peak value).

α = lag angle between H_m and B_m.

Speed-Torque Characteristics

Fig. 18 shows the speed-torque characteristics of a hysteresis motor.

This characteristics shows that the motor runs at synchronous speed for all torques less than the pull-in torque. Thus slight changes of the motor torque (due to drop in supply voltage, say) may not affect the synchronous speed of the motor so long as the remaining hysteresis torque is greater than the bearing and windage torques

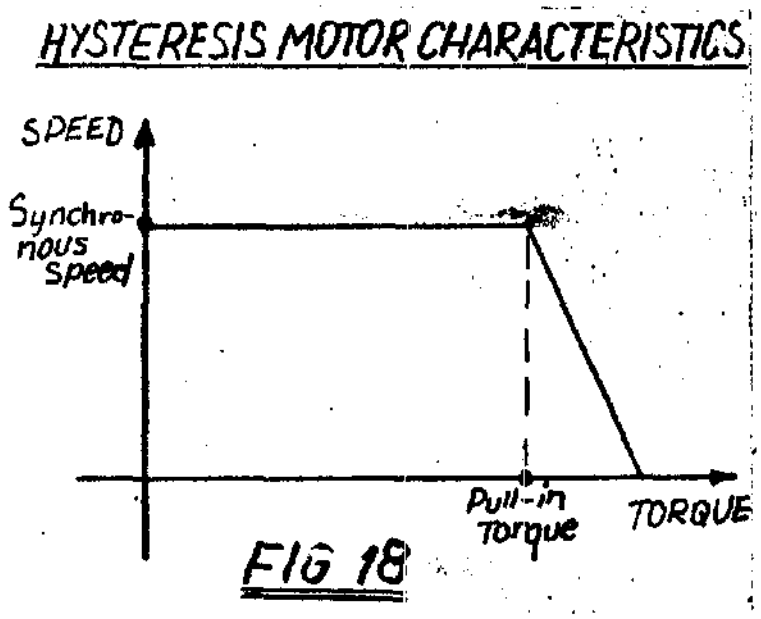


FIG 18

(which are relatively very small). It is this characteristics of the hysteresis motor that makes it most useful for gyro applications where unpredictable fluctuations in the supply is expected.

It is also because of this characteristics that it finds application as the drive for record changers where the increase in load (due to more records dropping on the turntable) does not affect the turntable speed appreciably.

6.2. ASPECTS OF HYSTERESIS MOTOR DESIGN

The main factors that govern the design of a hysteresis motor are:

(a) The number of slots in the stator

(b) The thickness of the stator slot bridge

(c) The rotor material

(d) The radial thickness of the rotor material

(e) The radial length of the air gap.

Each of these will be considered separately.

(a) The Number of Stator Slots

When the stator of a motor is connected to a voltage source, the current in the winding sets up a magnetomotive force (mmf), which in turn sets up the required flux in the air-gap. The mmf is distributed in a wave form according to the distribution of the windings. The most ideal waveform is the sinusoidal one which is achieved only with an infinite number of stator slots. The larger the number of stator slots, the nearer the mmf waveform approaches the ideal sinusoidal form as shown in Fig. 19.

The number of stator slots is, however, limited by the tooth cross-section - to avoid the problem of saturation.

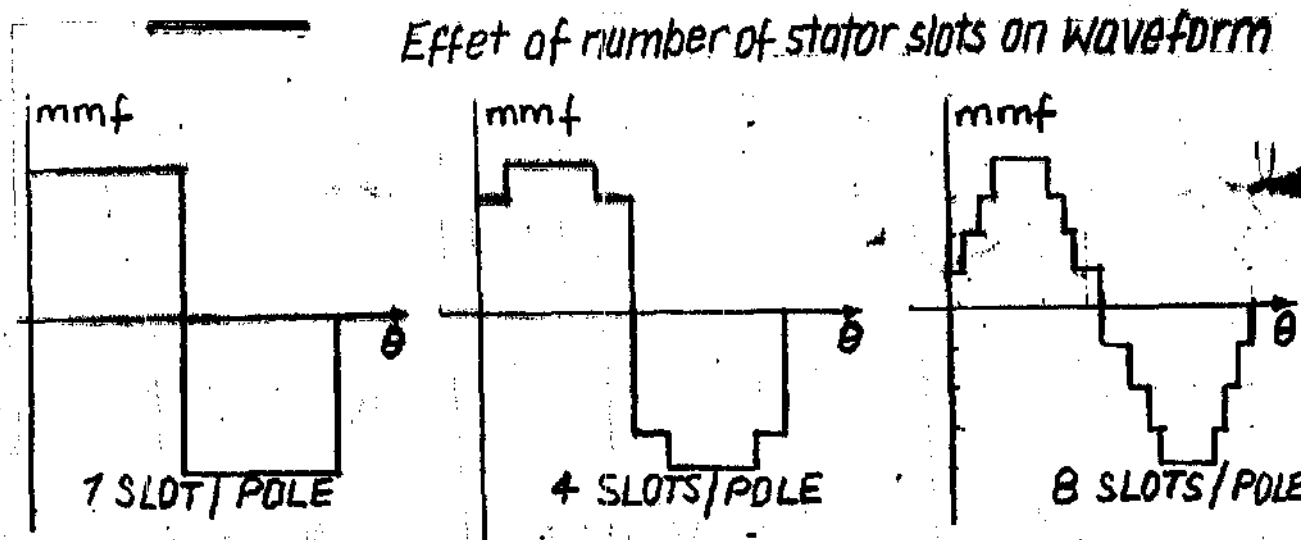


FIG 19

In general, 4 slots/pole represents an ideal value for small motors. Experience has shown that for these motors increasing the number of poles decreases the efficiency - thus a 4-pole-2 phase motor may have only 15 - 20% while a 2-pole-2 phase motor could have 25 - 30% efficiency [15].

(b) The Slot Bridge Thickness

The slot bridge is the material that lies in the gap between two teeth. If the slot bridge is made too thick then most of the useful flux from the stator is shunted away and does not reach the rotor. This leads to reduced output power and hence efficiency. On the other hand, if the slot bridge is made too thin, the bridge becomes very easily saturated and a saturated bridge is equivalent to an open bridge whose characteristics will be discussed shortly.

The actual bridge thickness used in design depends on the following factors:

(i) Number of poles

(ii) radial length of air gap

(iii) radial thickness of rotor.

For most practical purposes, a bridge thickness of 5 - 10% of rotor radial thickness is used.

Since the use of closed slots will make the assembly of coils difficult, it is usual to make the stator laminations of open slot and mounting a bridge ring after the windings have been assembled.

The reason why open slots are not used for these types of motors is because the flux density in the rotor fluctuates as it passes from the shorter gap under a tooth to the longer

gap under a slot. These fluctuations in rotor flux density give rise to minor hysteresis loops superimposed on the major one. These minor loops lead to parasitic losses (heat in the rotor) and thus cause a reduction in the efficiency.

The fluctuations in the flux density due to the open stator slots is more pronounced near the teeth and it decreases further away. Thus one way to reduce the effect of the open slots is to maximize the air gap length. This means, however, that more flux from the stator is required and hence the need for higher stator current which will lead to an increase in copper loss which could more than offset the parasitic losses.

Thus although the use of closed slots causes some of the useful flux to be shunted away from the rotor, it offers a higher output than the open slot. This result is shown graphically in Fig. 20. [16]

(c) Rotor Material

As is evident from equations (6.1) and (6.2), the hysteresis torque depends on the angle of lag between B_m and H_m (i.e. angle α). Also the torque depends on the area of the hysteresis loop - the larger the area, the

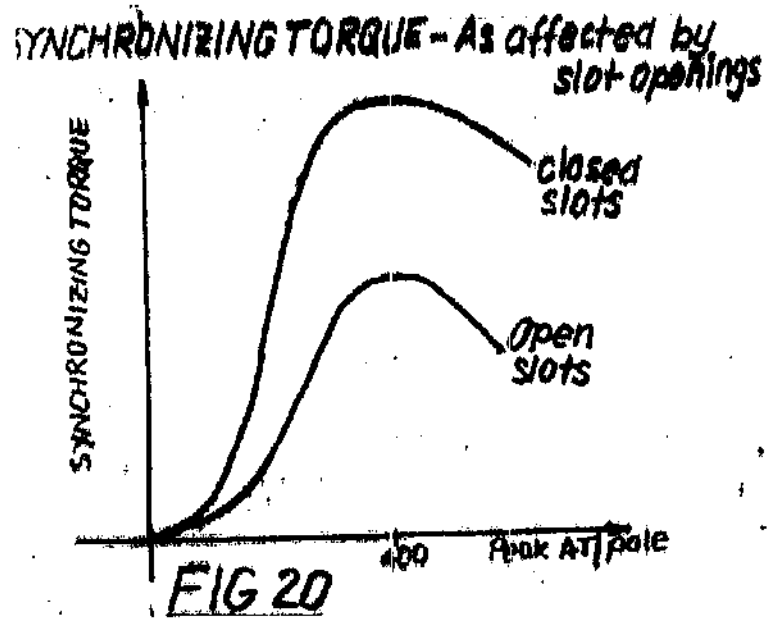


FIG 20

bigger the torque. The area on the other hand is dependent on the remanence (B_r) and coercivity (H_c) of the material. Thus the best rotor materials are those with high remanence and high coercivity. This is the property of the so-called magnetically hard materials. Characteristics of a few of these materials are given in the table below [15]. (See Page 63).

The hysteresis energy loss (W_h) is a function of the area of the hysteresis loop. Although materials with higher value of W_h will give higher values of torque, these materials

TABLE 3

MAXIMUM VALUES OF HYSTERESIS ENERGY LOSS FOR SOME COMMERCIALLY AVAILABLE STEELS

Material	W_h(Joules/m^3/cycle)	$(BH)_{max}$(Tesla-AT/m)
6% W	23,600	2,380
P6	22,500	4,370
36% Co	66,000	7,560
Vicalloy	70,000	8,900
Alnico	130,000	13,500

are seldom used. This is because to produce the value of W_h quoted for them it will require very large magnetizing fields due to their low permeability. The use of high magnetizing fields implies using higher currents which in turn leads to excess copper loss in the form of heat.

It has been found that for small motors of less than 50 W output, 6% tungsten steel or P6 could be used; while for bigger motors Vicalloy is preferrable.

(d) Radial Thickness of Rotor Material

Since in most motor designs the speed and torque are specified initially, then W_h and V must be selected to satisfy equation (6.1).

The choice of rotor inner diameter is often governed by the available stator stampings. The outer diameter is selected such that the flux in the rotor is sufficient to make the rotor rotate without the stator getting saturated due to large flux.

Experience has shown that the best ratio of outer to inner diameters is 1.2 - 1.4 [13], and the best value of rotor flux density should range from 0.5 - 0.8 Tesla [15].

(e) Length of Air-Gap

A short air-gap reduces the reluctance of the gap and hence improves the motor performance by reducing copper losses.

In open slot motors, a short air-gap leads to parasitic losses which may outweigh the above advantage. In the case of closed-slot motors, however, the air-gap length is no more determined by parasitic losses; but by manufacturing tolerances. For most motors a gap of 0.2 - 0.5 mm is used [13].

(f) Stator Design

Details of the design of the stator of the Hysteresis Motor cannot be included in this work, This is because there are a multitude of factors to consider whose

proper selection can only be done by a person experienced in electric motor design.

However, [13] shows a fairly exhaustive list of these factors - such as number of slots, maximum number of conductors in a slot, slot cross-section, number of stator winding turns per phase, specifications for the main winding and auxilliary winding, specification of the capacitance of the series capacitor and so on.

Even then, the selection of such factors as coefficients for determining the maximum field intensity inside the ring and the voltage coefficients necessary to determine the winding specifications were left to the designer's past experience of motor design.

CHAPTER 7

THE ELASTIC RESTRAINT

As was mentioned earlier, an elastic restraint is required along the output axis of the rate gyro. This restraint acts to counterbalance the gyroscopic torque due to a rate input.

The elastic restraint can take one of several forms:

1. Helical spring
2. Spiral spring
3. Torsion wire
4. Elastic restraint Microsyn.

Each of these will be considered separately.

7.1. HELICAL SPRING RESTRAINT

The helical spring (tension type) is attached one end to the gimbal and the other end to the gyro casing. A simplified schematic arrangement is shown in Fig. 21.

If l is the distance of the spring from the output axis and θ the angle through which the gimbal rotates (output angle), then it can be shown that the torque exerted by the spring is

$$T = K l^2 \theta \qquad \text{----------(7.1)}$$

where

K = linear spring constant (N/m).

HELICAL SPRING RESTRAINT

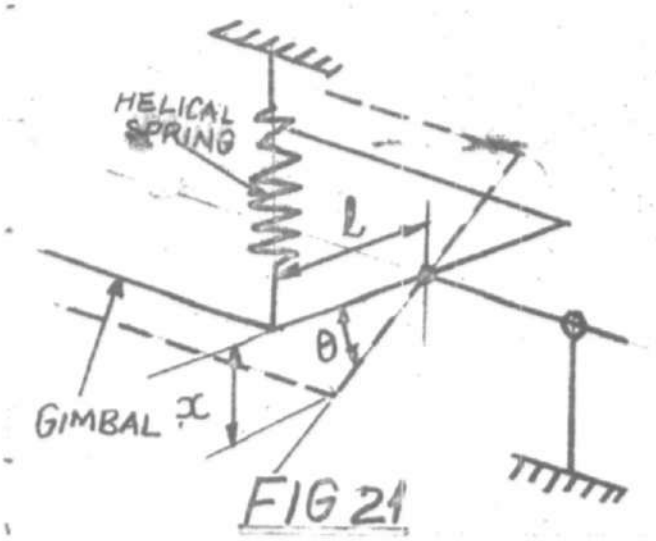


FIG 21

This torque will counterbalance the gyroscopic torque due to an input angular velocity .

Thus equating (7.1) to (L.1), there follows

$$K\, l^2\, \theta = I \omega \Omega$$

$$\therefore \quad \theta = \left(\frac{I\omega}{K\, l^2}\right)\Omega \qquad \text{----------(7.2)}$$

The only way to vary the spring constant (for purposes of calibration) is by pretentioning. This, however, tends to reduce the working life of the spring due to creep.

Another problem with helical springs is that to cater for rotation in two directions, two springs will have to be used; otherwise elaborate linkages will have to be used if only one spring is used.

Finally, unless special steps are taken to secure the spring at its ends, some backlash will be introduced, thus giving rise to errors in the output.

7.2. THE TORSION WIRE RESTRAINT

The use of a torsion wire as an elastic restraint is mainly used in flotation gyros (where the gimbal assembly is floated in a fluid). It is not used for ordinary gyros because a torsion wire of the required stiffness may not be strong enough to carry the motor and gimbal assembly. Its use in flotation gyros is facilitated by the fact that most of the gyro weight is borne by the flotation fluid and only a fraction is carried by the suspension system. In this application, the torsion wire acts both as the elastic restraint and as the suspension system for the gyro and gimbal assembly.

7.3. THE ELASTIC RESTRAINT MICROSYN

The elastic restraint microsyn is an induction type component that produces a torque proportional to the

angle of rotation. The schematic arrangement of this is shown in Fig. 22.

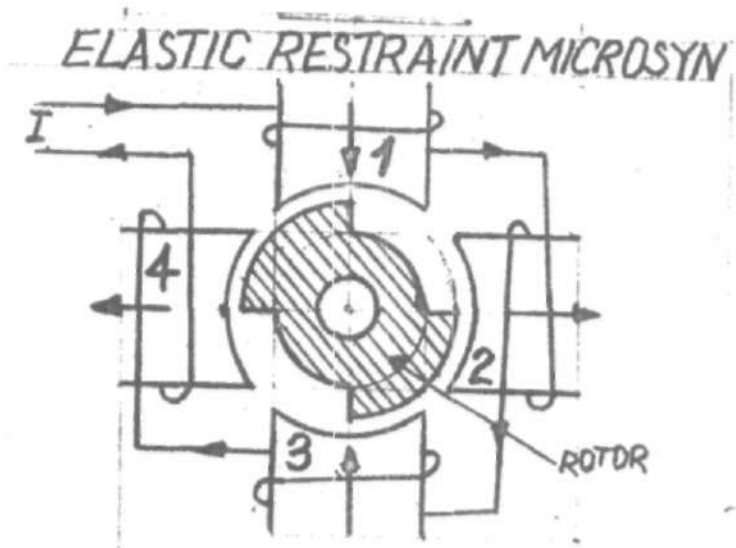


FIG 22

The device consists of a dumb-bell shaped rotor which rotates between the four poles of a stator. Each of the poles has a coil; and all the coils are connected in series. The flux produced is such that the one in each pole is opposite in direction to that of an adjacent pole. In the null position, the rotor aligns itself such that half of each pole is covered. Thus the flux densities under all the poles are equal.

If the rotor rotates clockwise (say), then the flux density under poles 2 and 4 is decreased (due to the increase in area under the pole); while that under poles 1 and 3 is increased. Due to the change in flux density under each pole, a torque is produced which is directly proportional to the square of the flux density under that pole. The total torque can be expressed by an equation of the form (7.3) [8]

$$T = b I^2 \theta \quad \text{----------(7.3)}$$

where

T = total torque developed by the system

b = a constant

I = applied or input current

θ = rotor deflection angle.

The elastic restraint microsyn has the following advantages over other restraints:

1. The elastic constant of the system ($b I^2$) may be varied by simply varying the excitation current I.
2. The torque produced is always a linear function of rotor angular velocity - there is no deviation from Hooke's law.

However, this type of restraint has the disadvantages of complexity and the likelihood of higher cost than the other systems. It is, however, used almost exclusively for precision rate gyros used for inertial navigation.

7.4. HAIRSPRING OR SPIRAL SPRING RESTRAINT

A hairspring has a number of advantages which make it suitable for providing restraining torques in many mechanisms. Some of these advantages are:

(i) It satisfies flat space requirements

(ii) Its torsional constant can be varied by varying the working length - no need to prestress it

(iii) Only one spring is enough for both directions of rotation

(iv) It is relatively cheap and easy to produce.

Because of the above advantages, a spiral spring will be selected for the present design. Details of its design will now be considered.

There are a number of factors that affect a hairspring design [17]

(a) breadth/thickness ratio

(b) number of active coils

(c) length/thickness ratio

(d) maximum total deflection

(e) material of spring

(f) hub design

(g) outer-end fastening.

Each of these factors will be considered separately.

(a) The Breadth/Thickness Ratio (b/x)

Since most spiral springs are made by flattening a round wire in a single pass rolling operation, it has been suggested that the b/x ratio be restricted to from 3:1 to 15:1. If other methods of manufacture are used, however, the length is the only critical dimension and b and x are selected such that with a reasonable length the spring will give the required restoring torque.

(b) Number of Active Coils

To obtain a low spring rate for sensitive operation, the design should be made for maximum length and minimum thickness. However, as the number of turns becomes too large, the spring sags - the upper outer coils tend to lie on their lower counterparts. If the number of coils becomes too few, however, the restraint becomes insensitive to low torques.

Experience has shown that the optimum number of coils for most designs should lie between 4 and 10. For rugged

instruments subject to vibrations, 4 - 6 represents the best number.

(c) Length/Thickness Ratio (l/x)

For instruments in the low sensitive range, an l/x ratio of 1000:1 is ample; while for those in the high sensitive range 3000:1 is used. A spring in the middle range of applications could have l/x = 2000:1 and b/x = 10:1.

(d) Maximum Total Deflection and Caging

The maximum deflection of a hairspring should not exceed 2½ turns (900°), otherwise the spring could move out of its plane to form a ball-like structure. This phenomenon is called 'caging'. For applications where large deflections are expected, this defect is guarded against by using supporting flanges at either side of the spring; although these are expected to produce objectionable friction.

(e) Material Selection

The material for the spring depends on the application. Where the spring is to act both as a restraint and as an electric conductor, phosphor bronze is the best choice. Spring-steel has higher strength but lower conductivity.

Beryllium copper has very high strength and conductivity but it is expensive. For springs that must have a constant rate at all temperatures Nispan C is a good choice.

(f) Hub Design

The most popular type of hub is the spool-like type with a groove just wide enough for the spring to fit in. In other cases, however, plain hubs with no flanges at either side are used.

Where the spring is to carry electric current it is soldered to the hub and the latter is fixed to the shaft with a tight fit.

The usual hub material is brass; but for hard spring materials subjected to repeated stresses and vibrations, stainless steel can be used.

(g) Outer-End Fastenings

A wrong outer end fastening could lead to fracture due to repeated stresses especially where the spring deflects in both directions. Elaborate bends or loops can cause the spring to move out of plane, cause clashing of the coils and result in erratic spring behaviour. Fig. 23 shows a useful comparison of outer end fastenings.

SPIRAL SPRING END CONNECTIONS



(a)

- outer coil looped over post
- when deflected, coils will move to one side and clash.
- relatively expensive.



(b)

- better design
- outer coil has a single flat bend secured in a slotted post
- clashing reduced
- less expensive



(c)

- best design
- outer coil has no bend but is securely fastened.
- minimal clashing
- least expensive.

FIG. 23

CHAPTER 8

THE DAMPING DEVICE

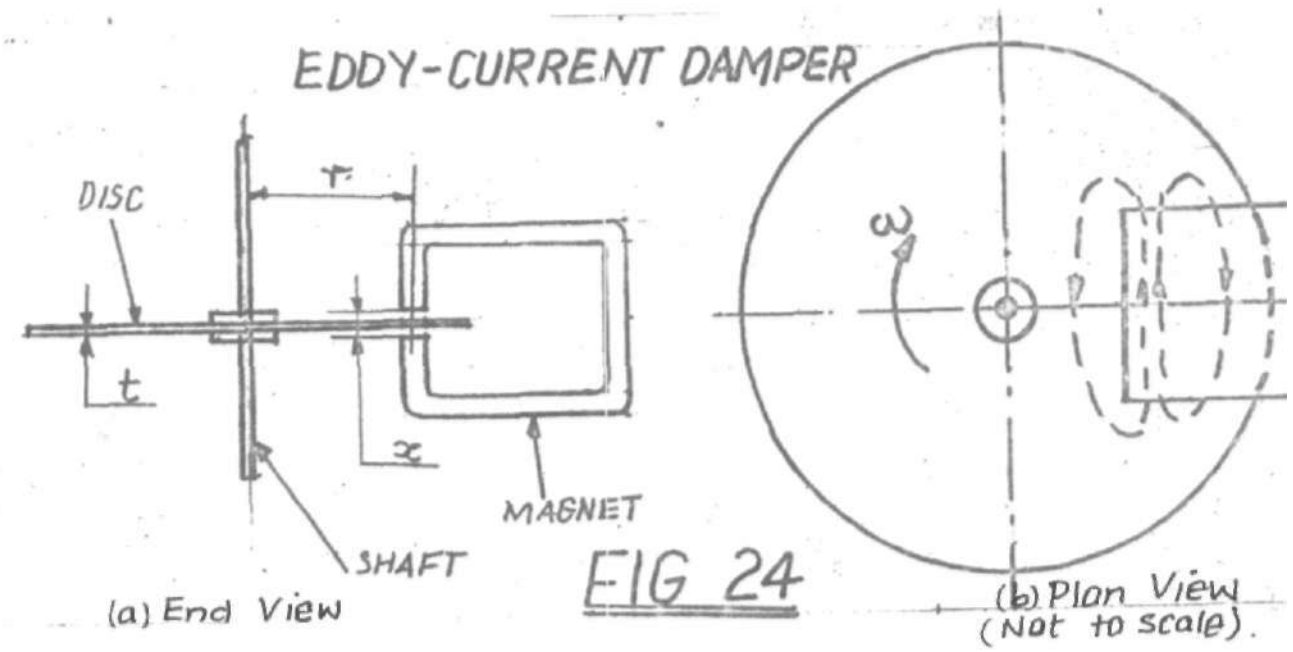
The rate gyro, like most other sensing instruments, will oscillate when subjected to a step angular velocity input. This oscillation about a mean value may take a long time to settle, thus rendering the instrument worthless as a warning device. A means is therefore needed to damp out these oscillations. Basically, three methods of damping are widely used in gyroscopy.

1. Eddy-Current Damping
2. Liquid Damping
3. Air Damping.

8.1. EDDY-CURRENT DAMPING

In this case a magnetic field sets up eddy currents in a moving conductor. The currents react with the field producing them to produce a torque which could be used to damp the oscillations. The field could be set up either by a permanent magnet or an electromagnet.

The disc is made of high conductivity material - either copper or aluminium. Fig. 24 shows a schematic arrangement of the eddy-current damper.



It can be shown that the damping constant in this case is given by [18_7:

$$C = \frac{\phi^2 r^2 t}{K \rho A} 10^{-3} \text{ ----------(8.1)}$$

where

ϕ = flux (Webers)

r = radius from axis to centre of magnet pole(mm)

t = disc thickness (mm)

A = pole area at air-gap (mm^2)

ρ = resistivity of disc material (Ω - m)

K = a certain constant

C = damping constant (Nm/rad/s).

To minimize inertia about the output axis, aluminium is most often selected as the disc material.

The gap between the poles and the disc must be as small as possible for greater effectiveness of the damper. Thus the disc must be rigidly attached to the spindle to prevent contact with the magnet poles. Special reinforcing pieces are used to ensure this.

A study of equation (8.1) shows that the bigger the radius r, the bigger the damping constant. Experience has shown, however, that there is an optimum range of values of r above which the damping constant decreases until it becomes zero at the edge of the disc. This range is 75 - 80% of r [18].

The eddy current damper has a number of advantages over other types of dampers:

1. It strictly obeys a linear law between damping torque and output angular speed.
2. It is very easy to construct and also easy to adjust the damping especially if electromagnets are used.
3. It lends itself to accurate or approximate analysis from first principles.

However, it has the following disadvantages:

1. The maximum damping available is rather small.
2. It is relatively expensive.
3. The stray field from the magnets could affect some other parts of the instrument (especially if these are sensitive to magnetic fields).

8.2. LIQUID DAMPING

In these types of dampers, a paddle or vane is made to rotate in a container of fluid. The drag of the fluid on the paddle provides the necessary damping.

Fig. 25 below shows the schematic arrangement of a typical paddle damper.

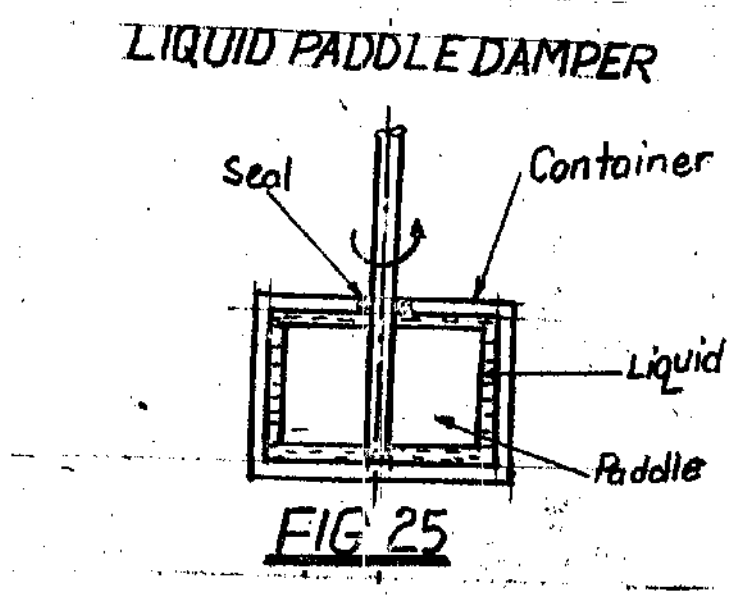


FIG 25

The container must be thoroughly sealed to prevent some of the damping fluid leaking out and fouling the other parts of the instrument. The difficulty of providing such a sealing restricts the use of these dampers to vertical axis instruments only.

Other problems with these dampers include the appreciable changes in damping due to changes in temperature. Also most of the good damping fluids tend to overdamping.

However, for instruments where heavy damping is required they offer the best choice.

Finally, it could be worth noting that despite their disadvantages, liquid dampers are used, in a modified form, in integrating gyros with the gimbal replacing the paddle.

The most widely used damping fluids are the mineral oils - kerosene, paraffin, etc. Beside satisfying the conditions of low vapour pressure, constant chemical and physical properties, non-corrosiveness and good insulation, these oils can have their viscosity adjusted by mixing different grades.

8.3. AIR DAMPING

Air dampers can be divided into three broad categories:

(a) Open Air Vane Damper

(b) Closed Chamber Vane Damper

(c) Piston Damper.

Fig. 26 shows these dampers schematically.

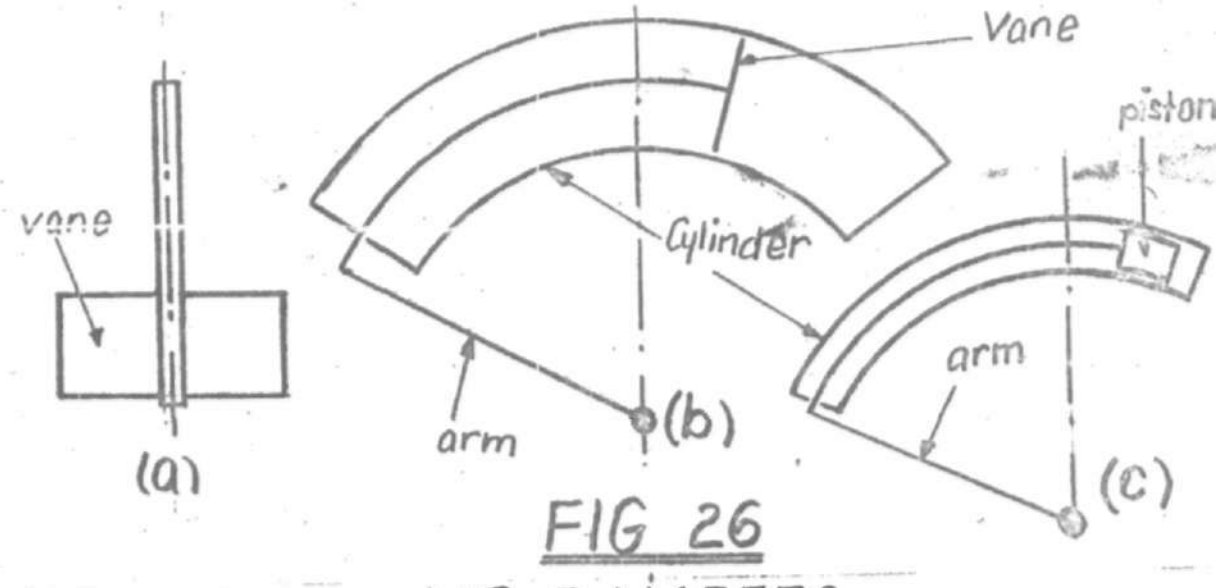


FIG 26

AIR DAMPERS

The open air vane damper consists essentially of two or more vanes attached to the spindle of the instrument. It resembles a liquid vane damper in structure; but the drag in this case is provided by air friction. This type of damper is only useful for very low inertia instruments where the amount of damping required is very small. It is completely useless for gyro applications.

In the case of the closed chamber vane damper (b), appreciable damping could be obtained especially if certain steps are taken:-

(i) a very smooth finish for the interior of the chamber

(ii) using as small a gap as possible.

Both these two factors present manufacturing difficulties. The amount of damping could also be improved if the edges of the vane are upturned.

The piston damper (c) is similar in operation to the enclosed vane damper except that the vane is replaced by a long piston. But the piston damper provides higher damping than the vane damper; although it has a rather bigger inertia. Thus it is most exclusively used in instruments with heavy movements of high inertia which require considerable damping and in which the extra inertia of the piston is relatively negligible.

The performance of the piston damper can also be improved by using smooth surface finish for the piston and inner part of the chamber. Also, the air gap should be as small as possible.

All the air dampers have a common problem - they do not lend themselves to accurate mathematical analysis from

first principles. Their design is based on certain empirical relationships which were experimentally derived. For details of these empirical equations for air dampers, see [18].

8.4. SELECTION OF DAMPER

On the basis of the above discussion an Eddy Current Damper will be selected for the rate gyro.

Eddy Current Damper Design

The main problem in eddy-current damper design is the design of a magnet (or magnets) that will supply the flux ϕ given in equation (8.1).

The Damper will use simple U-shaped magnets to ease the design.

Owing to the complex nature of a permanent magnet, it is not easy to start from given values of flux ϕ and get from this the dimensions of the magnet required. The usual method of design is to guess values of dimensions of an arbitrary magnet, analyze this magnet and find out by how much its performance compares with the required value.

The arbitrary dimensions could be obtained by considering the overall space restrictions in the gyro.

CHAPTER 9

THE PICKOFF AND OUTPUT DISPLAY

9.1. INTRODUCTION

For the rate gyro to be effective as a rate of turn indicator the output axis must be parallel to the longitudinal axis of the vehicle. Thus the instrument panel must be vertical as shown in Fig. 27.

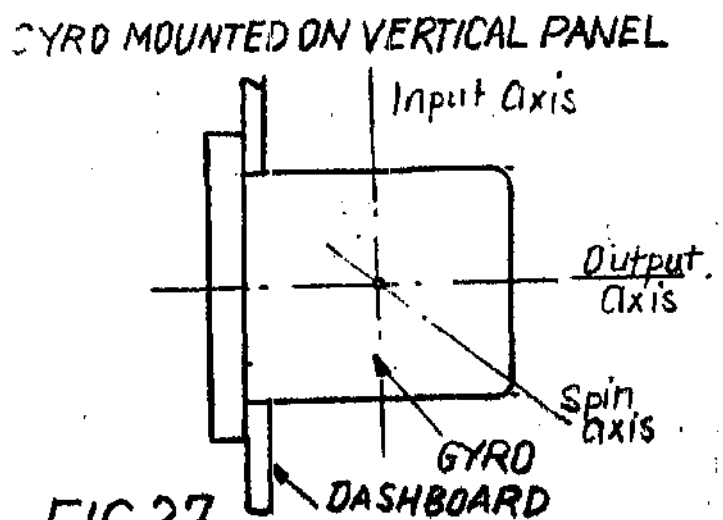


FIG 27

The instrument panel of most automobiles, aircrafts and trains is oriented in this way. Hence the gyro could be mounted directly; and rate of turn readings directly read from the gyro face.

However, modern truck design tends to place the panel in a semi-horizontal or inclined position [7]. A gyro directly mounted on this type of panel will not give any readings of rate of turn since the input axis will not be vertical. For the rate gyro to be used on these types of vehicles, a transducer will have to be used to transfer the output of the gyro, which is placed somewhere with its input axis vertical, to a display unit on the dashboard. A shematic of this arrangement is shown in Fig. 28.

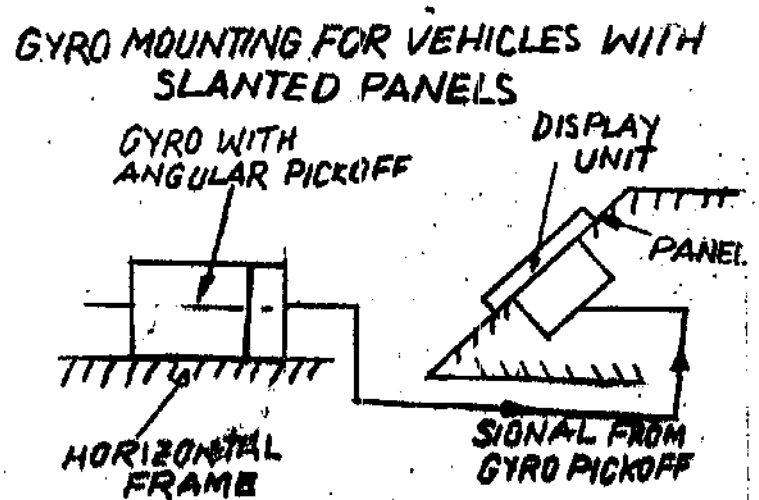


FIG 28

The transducer which is used to convert the gyro angular rotation about the output axis to either an electrical or mechanical signal to be transferred to the display unit is called a pickoff.

9.2. GYRO-SIGNAL PICKOFFS

The main types of pickoffs used on gyros are:

1. Capacitive Type
2. Electrolytic Type
3. Resistive Type
4. Inductive Type.

Each of these classes will be treated separately.

1. Capacitive Type Pickoffs

These types of pickoffs work on the principle that mechanical displacement can cause a change in capacitance which can be measured. The capacitance between two parallel plates is given by

$$C = \frac{\epsilon A}{d} \qquad \text{----------(9.1)}$$

where

C = capacitance

ϵ = dielectric constant of material between the plates

A = area of plates

d = distance between the plates.

From equation (9.1) it is clear that the capacitance can be varied by varying either ϵ, A or d.

Capacitive pickoffs based on varying d must, however, be subjected only to very small mechanical displacements.

This is because from equation (9.1), the capacitance is inversely related to d; thus the relationship is a hyperbolic one, and only over very small ranges around the origin is the relationship linear. If this unit is mounted on a gyro, limit stops must be used to prevent excess deflection and shorting of the plates.

Capacitive pickoffs based on varying A give a linear relationship between the capacitance and the cross-sectional area. They are used in certain devices where space restrictions are not rigidly imposed.

Capacitive pickoffs based on varying ϵ are rarely used. This is because to change ϵ, the material between the plates must be changed. This is not very practical to achieve, since most gyros either contain air or flotation fluids. The later is selected on the basis of its buoyant force rather than its dielectric constant. Use of capacitive pickoffs for flotation gyros is limited by the viscous drag between the moving and stationary parts.

Finally, the use of capacitive pickoffs is limited by the following factors:

1. They require high frequency (5,000 - 10,000 H_z) for satisfactory operation. Thus extra circuitry might be needed.

2. Their performance is greatly reduced by the stray capacitances of the cables in the circuit.

3. The high output impedance of the circuit containing these pickoffs causes the output to be sensitive to electrical noise.

2. Electrolytic Type Pickoffs

These types of pickoffs work on the principle of change in resistance as the distance between two electrodes is varied.

Fig. 29(a) shows the design features of an electrolytic pickoff.

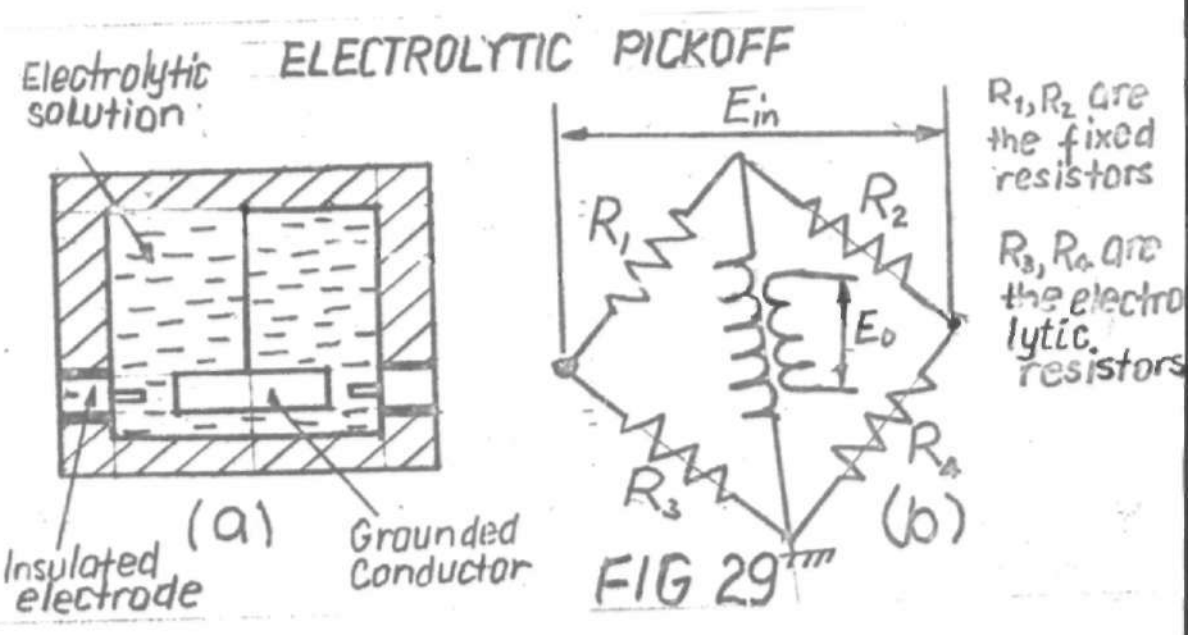


FIG 29

The electrolyte conducts electric current according to Ohm's Law:

$$R = \frac{L}{\sigma A} \qquad \text{----------(9.2)}$$

where

R = resistance of electrolyte

L = length of conducting path

σ = conductivity of electrolyte

A = cross-section of path.

From equation (9.2) it is clear that R varies linearly with L.

The electrolytic circuit must be connected to a high frequency (1,000 H_z or above) a.c. supply to avoid electroplating of the electrodes.

Fig. 29(b) shows the way this pickoff is connected - to form two arms of a bridge. The transformer is a step-down type which is used to reduce the high output impedance (high electrolyte resistance). However, the output voltage will also be stepped down.

The main problem associated with electrolytic pickoffs is that of getting an electrolyte that will have the proper resistivity and which can be stable for long periods of time under varying temperature conditions.

3. Resistive Type Pickoffs

The most prominent members of this group are the Potentiometers. These pickoffs produce an electrical signal which is proportional to the change in resistance between two points. Different types of potentiometers are available - single turn, multi-turn, slide-wire, deposited-film, metal-film, conducting-plastic-film, etc. Details of the design of potentiometers can be obtained from [22].

Fig. 30 shows the schematic of a single turn potentiometer and the equivalent electrical circuit.

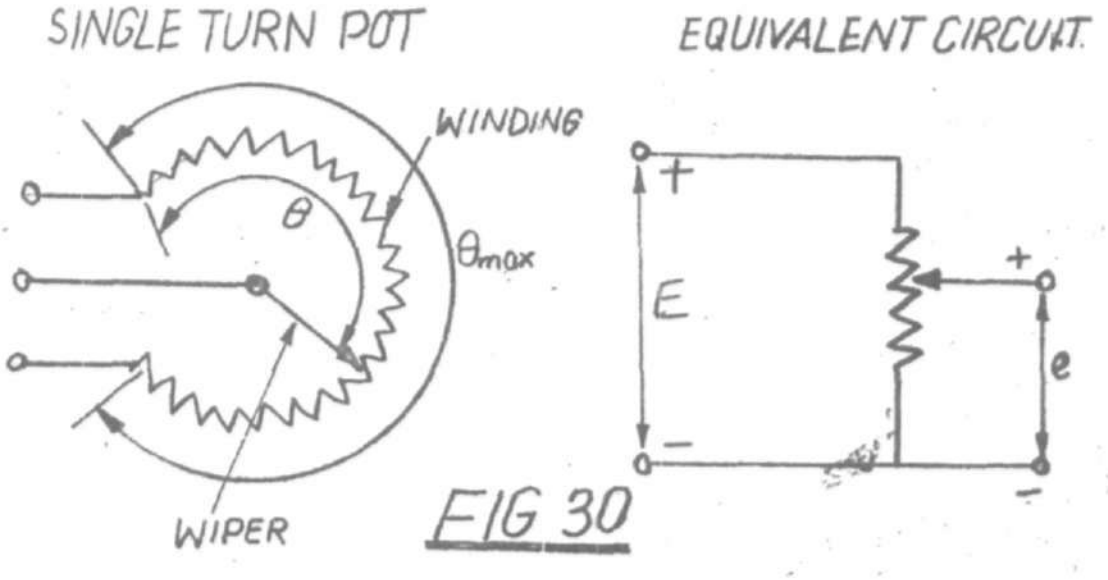


FIG 30

For this, the output signal is given by

$$\frac{e}{\theta} = \frac{E}{\theta_{max}}$$

or $$e = (\frac{E}{\theta_{max}})\theta \quad \text{----------(9.3)}$$

Thus the output electrical signal is directly proportional to the angle of rotation of shaft (or output of gyro).

The main advantages of potentiometer pickoffs are:

1. they are economically available in compact sizes
2. they are simple in design and construction.

Their major drawbacks are:

1. Since the slider contacts the resistive wire, objectionable friction is introduced and this is not good for precision gyro work.
2. The transfer function is not a continuous curve but a series of steps. This is because the slider does not move over a continuous wire.
3. The voltage applied to the pickoff must be as low as possible to avoid heating effect on the resistance wire (and consequent change in resistance). Thus the voltage gradient of this type of pickoff is very small.
4. The parts are subjected to wear due to contact friction between slider and wire.

Many design variations have been created to make potentiometers suitable for precision work. However, their use is still restricted to the low precision gyros.

4. Inductive Pickoffs

These pickoffs work on the principle of a voltage output due to change in magnetic coupling between two coils.

The main types of inductive pickoffs are:

(a) E-pickoff

(b) Synchro pickoff

(c) Microsyn pickoff.

(a) E-Type Pickoffs

Fig. 31 shows the design features of an E-type Pickoff.

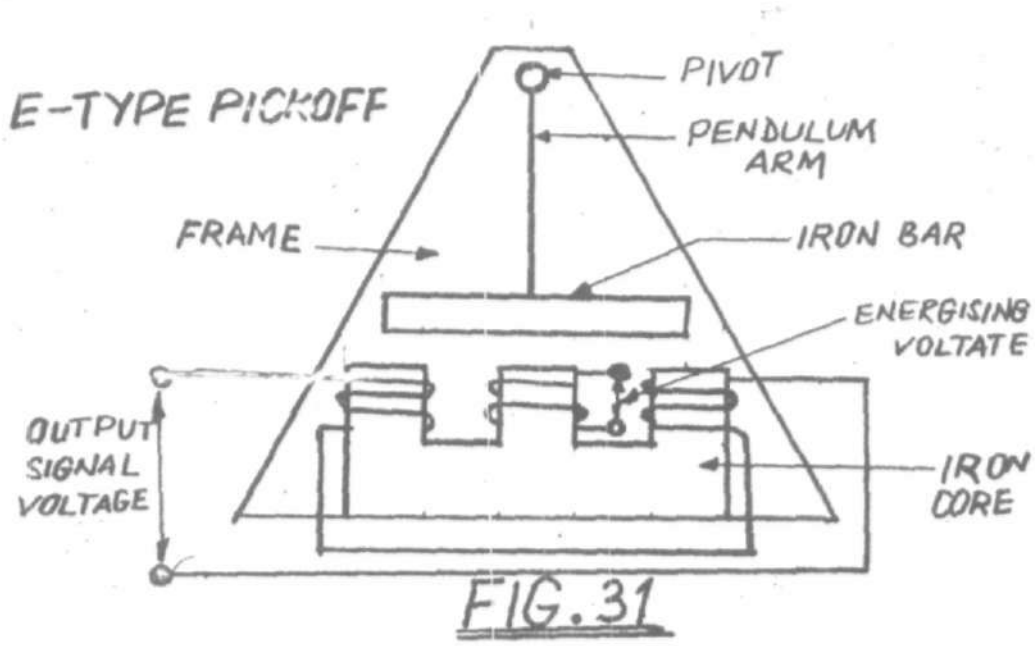


FIG. 31

Essentially, the unit consists of an iron bar which is suspended from a pivot connected to the output shaft of the gyro. The iron bar is positioned over the E-shaped stationary core which is made of steel laminations. The central arm of the core has a winding which is excited by an a.c. supply. The two outer arms carry the pickoff windings. When the iron bar is in the central position, the voltages induced in these outer arms are equal. The windings on the outer arms are connected in series, but such that their resultant voltage at zero deflection of the bar cancel out.

If the pendulum is displaced by rotation about the output axis say, then the voltage in one arm increases while that in the other decreases and hence an output voltage is obtained which is proportional to the deflection of the pendulum.

The main advantage of these types of pickoffs is that they are very sensitive and can detect very small movements. However, their output power is very small (in the order of milliwatts). Hence power amplifiers are needed to increase the output signal to working values.

Another disadvantage is that the iron bar tends to increase the inertia of the gyro about the output axis.

Finally, it cannot be used effectively in gyros because the pickoff will give an erraneous output when the carrying vehicle tilts, say at the banking of a bend.

(b) Synchro Pickoffs

These types of pickoffs are widely used in control systems where a gyro is used as the sensing device.

Essentially, the synchro consists of two units - the Gyro Unit and the Remote Unit. The two units can be as far apart as required (Fig. 32).

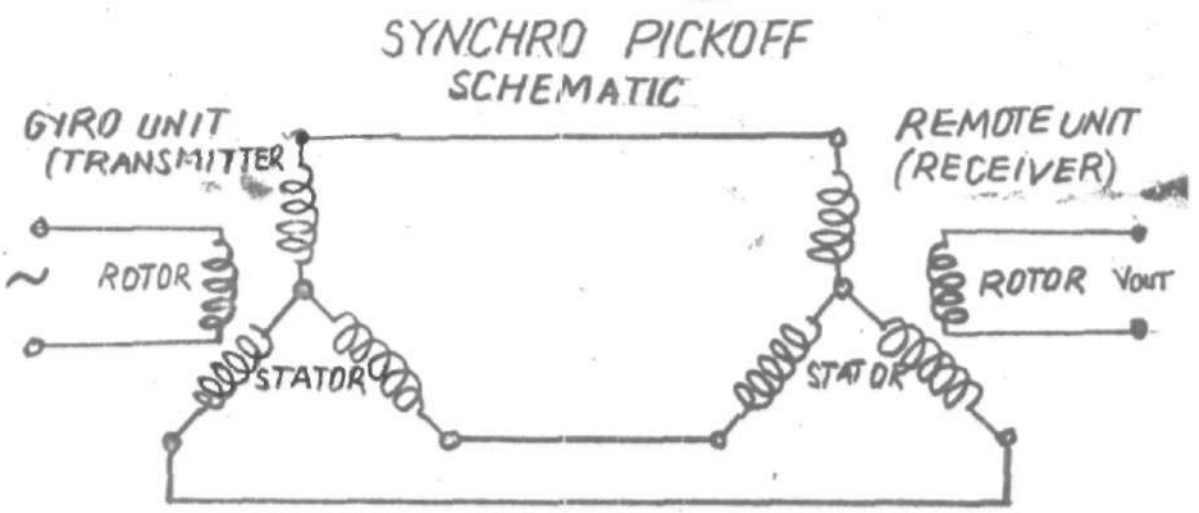


FIG 32

In each unit, the rotor has one winding while the stator has three windings. The rotor of the Gyro unit is attached to the gimbal of the Gyro and is excited by an a.c. supply.

The stator is attached to the gyro casing.

With the rotor of the Gyro unit excited by an a.c. supply, varying (rotating) voltages are induced in the stator windings - depending on the rotor position.

The output from the gyro stator windings is fed to the windings of the Remote Unit. If the rotor of the Remote unit is not aligned with its stator (as the rotor of the Gyro Unit is aligned with its stator), then a voltage is induced in the Remote Unit rotor windings. The value of this voltage is proportional to the misalignment and is thus proportional to the gyro output.

The main advantages of synchro pickoffs are:

1. There are no rubbing parts, hence stray torques due to friction are eliminated.
2. They are relatively insensitive to stray cabling capacitance.
3. They have a very high accuracy.
4. They have a useful operating angle of 360° and are capable of continuous rotation.

Their main disadvantages are:

1. Relatively expensive due to the need for two units.
2. The presence of windings in the rotor means that

stray torques may be induced in the gyro due to coil wire sagging and shifting.

c. Microsyn Pickoffs

Fig. 33 shows the essential features of a Microsyn Pickoff.

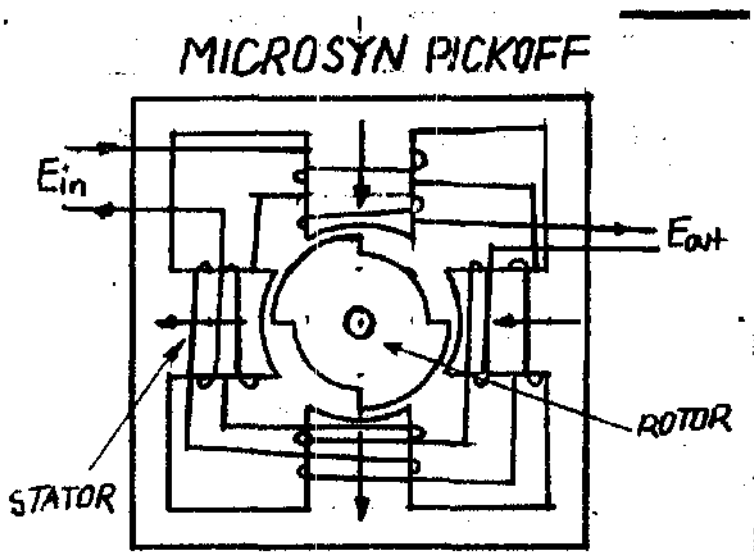


FIG 33

Basically, the Microsyn consists of laminated stator and rotor. The stator has four (or more) poles each of which carries a primary and secondary winding. The rotor has no winding. Its main purpose is to vary the reluctance of the flux paths between the stator poles. All the primary windings

are in series. They are connected such that when they are excited by an a.c. voltage flux flows from pole 2 to pole 4 and from pole 3 to pole 1 as shown in the figure. The secondary windings are also connected in series but in such a way that the induced voltage in the windings of poles 2 and 4 oppose those in the windings of poles 1 and 3.

The rotor is so shaped such that the resultant voltage output of the secondary is zero if the rotor is in its neutral position. Any deviation of the rotor from the neutral position results in a proportional voltage output.

In gyro applications, the stator is mounted rigidly in the casing, while the rotor is attached to the output shaft.

The absence of windings on the rotor of the Microsyn makes it the most versatile unit for gyro applications. Also, unlike the synchro, it has only one unit instead of two. This makes it relatively less expensive. Another thing is that the Microsyn has a fairly high voltage gradient (0.5 volts/degree).

9.3. SELECTION OF PICKOFF

The following factors are the necessary characteristics of a good pickoff and are used as aids in selection.

1. The pickoff must be able to convert angular motion to electrical signals with adequate sensitivity to operate the associated circuitry.
2. It must have a high resolution so that it can detect very small increments of motion as is often encountered in gyros.
3. The input power must be as low as possible to avoid internal heating and overloading of the power supply.
4. It must have no self-generated noise that could mask an output signal.
5. It should introduce no spurious torques about the gyro output axis.
6. It should be robust and fairly cheap to produce and run.

In view of the above requirements and the cases considered in section 2 of this chapter, a Microsyn pickoff will be selected for this design.

9.4. ASPECTS OF MICROSYN DESIGN

The main factor that governs the design of a Microsyn Pickoff (and also any other angular displacement pickoff) is the voltage gradient (i.e. the output voltage per unit angle of rotation). This parameter is calculated

from the change in reluctance or its reciprocal the change in permeance. For the evaluation of these, consider the geometrical relationships shown in Fig. 34.

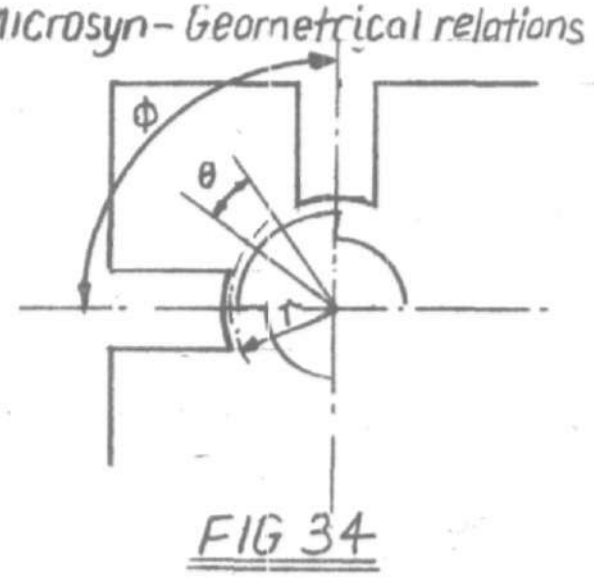


FIG 34

The area A of the rotor under one pole is given by

$$A = rt \left[\frac{\phi}{2} + (-1)^p \theta \right] \quad \text{---------(9.4)}$$

where

r = radius of rotor at centre of air gap

t = thickness of rotor

ϕ = pole angle

p = number of poles in stator (even or odd number)

θ = displacement of rotor from null position.

The reluctance is given by

$$R = \frac{L}{\mu A} \qquad \text{----------(9.5)}$$

where

L = length of magnetic path

μ = permeability of air-gap

A = area of magnetic path.

The reciprocal of reluctance (permeance) for the microsyn air-gap is thus

$$P = \frac{\mu A}{L} = \frac{\mu rt}{h}\left[\frac{\phi}{2} + (-1)^p \theta\right] \qquad \text{--------(9.6)}$$

where

A is substituted for its value from (9.4).

h = radial length of the air-gap.

The change in permeance of the air-gap due to a differential angular displacement is given by

$$\frac{dP}{d\theta} = (-1)^p \frac{\mu rt}{h} \qquad \text{----------(9.7)}$$

The voltage gradient can be expressed in terms of this change in permeance by the relationship

$$\frac{dE_o}{d\theta} = \omega p\, I_p N_p N_s \frac{dP}{d\theta} \qquad \text{----------(9.8)}$$

where

p = number of poles in stator

I_p = primary current

N_p = number of turns in primary

N_s = number of turns in secondary

ω = frequency of supply current (rad/s).

Equation (9.8) is the fundamental equation of Microsyn design.

From this equation, it is apparent that there are many variables which can be used to improve the voltage gradient of the pickoff. However, there are a large number of factors that tend to discourage this. Some of these restrictions are:

1. The frequency of the supply should as much as possible be the same as for the other parts of the system.
2. Increasing the number of stator poles tend to decrease the reliability of the pickoff and increase the cost of production.
3. Increasing the number of turns tend to increase the impedence of the system; and this may cause problems with the rest of the circuit due to lack of impedence matching.
4. Increasing the primary current increases the reaction torque between the poles and the rotor given by

$$T = (N_p I_p)^2 \frac{dP}{d\theta}$$

5. From equation (9.7), the only way to increase $\frac{dP}{d\theta}$ is by maximizing r and t and minizing h. The values of r and t are obviously restricted by space requirements, while h is limited by manufacturing tolerances.

9.5. THE OUTPUT DISPLAY UNIT

Since the signal from the pickoff will take the form of an electrical signal, then any voltage or current measuring device can be used as the output display unit. Thus a centre-zero galvanometer can have its scale converted to rate of turn, calibrated and used as the display.

Some form of lighting (like a small bulb) can be placed inside the output display unit and connected to the gyro or to the voltage signal such that it shows a red warning when the output exceeds a pre-set safe-value. Details of this will be discussed in the next chapter.

CHAPTER 10

MISCELLANEOUS DESIGN ASPECTS

10.1. LIMIT STOPS

Limit stops are integrated into the design to serve three basic functions:

1. To limit the deflection of the gimbal about the output axis thus preventing overstressing the spiral spring.
2. Their position can be varied to make the instrument suitable for different vehicles.
3. They can act as contacts to trigger on either an audio or a visual signal, thus giving warning of overshooting of a pre-set safe rate of turn.

The last two points deserve further explanation. A close study of equation (2.9) of Chapter 2 will show that the minimum velocity for overturning is a function of the geometry of the vehicle (wheel-base 2a and height of centre of gravity h shown on Fig. 1).

Thus different vehicles will have different velocities of overturn (as shown in equation (2.6)). Although knowledge of overturn velocities is impossible to come by, approximations can be made - either intuitively on the basis of the possible loading capacity of the vehicle, or

by carrying out a statistic of accidents which resulted in overturning due to exceeding the allowable speed at bends. These approximations can then be used to calibrate the gyro. Incidentally, the calibration could be done on the basis of the skidding velocity (given by equation (2.4)). This latter calibration will be most useful for vehicles which are lesser prone to overturning but more prone to skidding - like the motor cars. The former calibration can be used for trucks, trailers, tankers and train wagons which are more prone to overturning (due to their apparently high centre of gravity especially when fully loaded).

The fundamental equation of the rate gyro - equation (4.3) is:

$$\theta = \frac{I\omega}{K}\Omega = \frac{I\omega}{K} \cdot \frac{v}{R} \quad \text{----------(10.1)}$$

A close study of this equation shows that there are exactly four different ways to make the gyro adaptable for different vehicle velocities v at the same bend of radius R. These are:

(i) varying the inertia (I) of the gyro spin wheel

(ii) varying the angular spin velocity

(iii) varying the spring constant K

(iv) varying the maximum allowable deflection angle on the basis of the type of vehicle used.

The only way to vary the inertia of the gyro wheel is by varying the diameter or by changing the material of the rotor. None of these is practically feasible and hence the first method is discarded. The angular spin velocity for an electric motor is given by

$$\omega = \frac{120\ f}{p}\ (\text{rpm}) \qquad \text{----------(10.2)}$$

where

f = supply frequency (H_z)

p = number of poles.

Present-day gyroscopic equipment operate on a standard frequency of 400 H_z [8]. Moreover, varying the frequency of a motor will require additional equipment and hence add to the overall cost and complexity of the system. Finally, it is not feasible to vary the number of stator poles of an electric motor. Hence the second method is also discarded.

Now, consider the method that involves varying the spring constant K. It can be shown [18] that the spring constant for a spiral spring is given by

$$K = \frac{Ebx^3}{12\ I} \qquad \text{----------(10.3)}$$

where

b = breadth of spring

E = Young's Modulus for material of spring

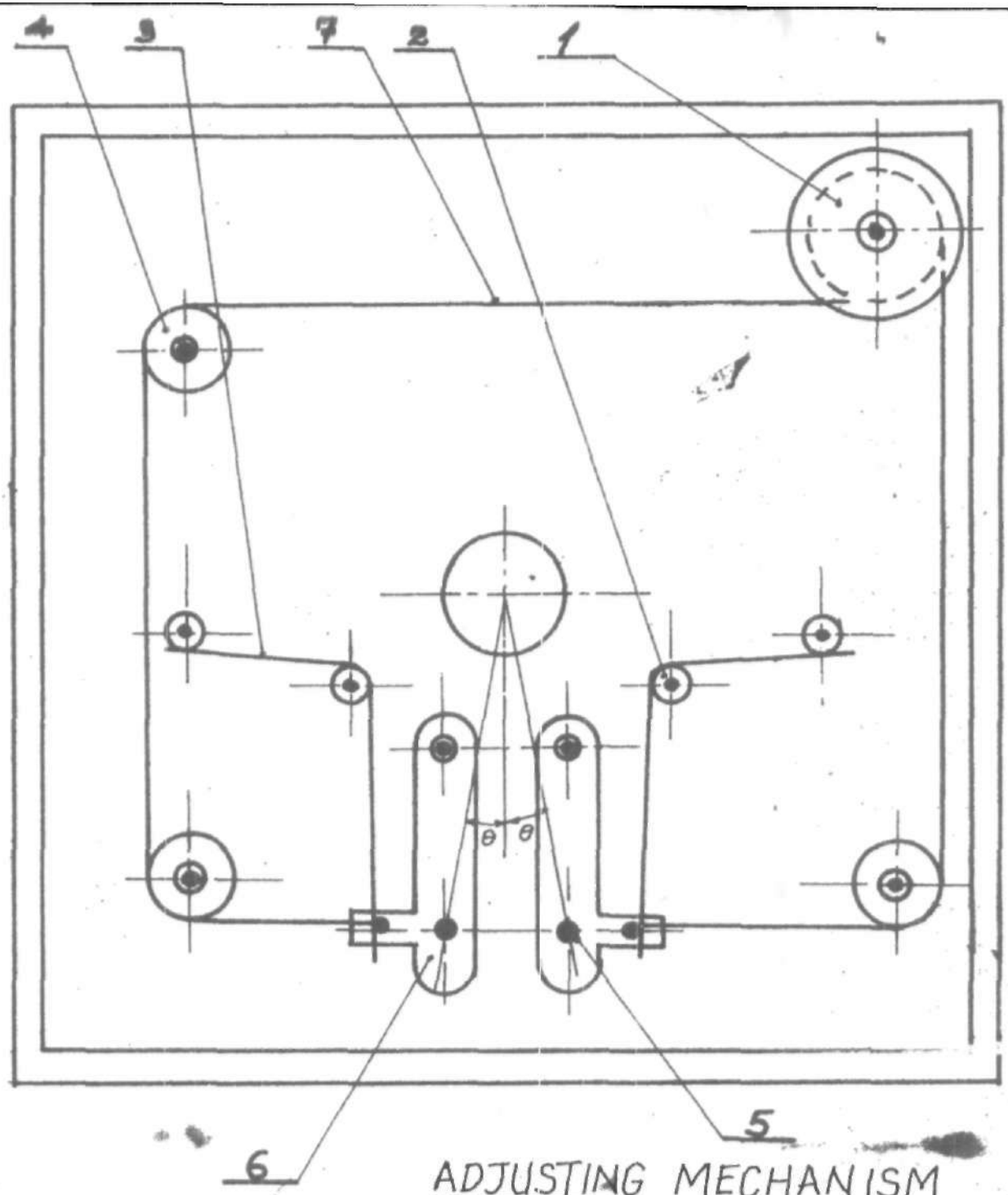
x = thickness of spring

l = length of spring.

Obviously, varying b, E or x are not physically feasible. The only promising parameter for variation is the length l. Incidentally, the method of changing spring characteristics by varying the length l is used to vary the resonant frequency of a clock hairspring; and is discovered to cause a movement of the coils to one side. This may have the detrimental effect of disturbing the linearity of the spring. Thus this method will not be used in this work.

The last method involves varying the maximum allowable deflection angle θ. The main advantage of this method is that it does not involve varying any of the geometrical or physical parameters of the main gyro, as the first three methods do. For this reason, this method will be adopted for this work.

Figure 35 shows one way by which varying the maximum allowable angle of deflection can be achieved. This figure shows two levers 6 which are carrying the limit stops 5 which define an angle θ on either side of the output axis.



ADJUSTING MECHANISM

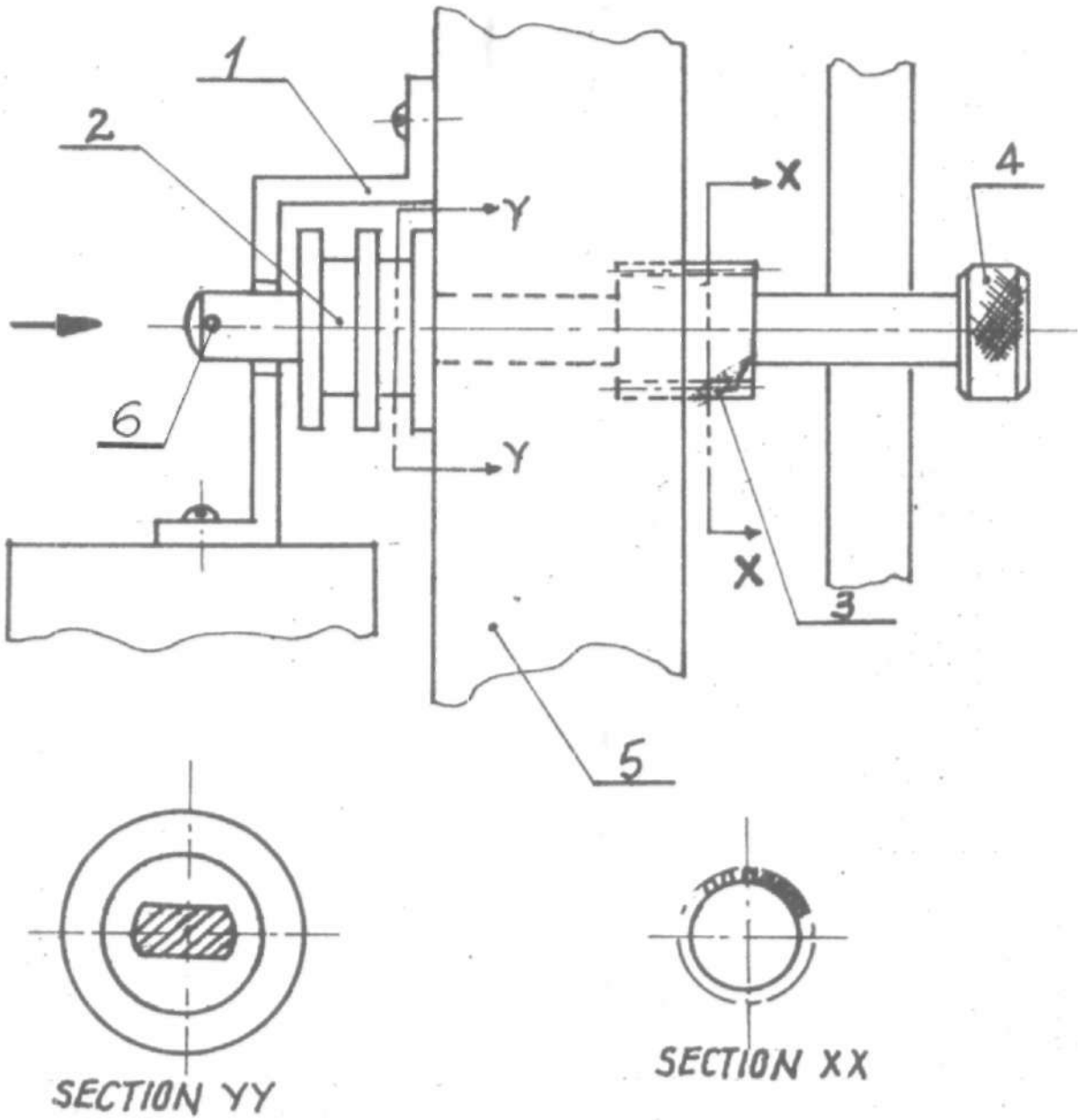
1	MAIN ROLLER (SPOOL)	5	LIMIT STOPS
2	SPRING SUPPORTS	6	LEVER
3	WIRE SPRING	7	STRING
4	ROLLERS		

FIG. 35

The angular position of the levers and hence the stops can be varied equally and simultaneously by turning the spool 1 clockwise thus winding up the string. A counterclockwise rotation can be obtained by releasing the spool 1 thus allowing the levers to 'move in' under the action of the wire springs 3. The springs also prevent the stops from moving out under the impact of the gimbal due to a rate input.

For this system, a means is required to prevent the spool 1 from unwinding under the action of the springs 3. This is achieved by the device shown in Fig. 36. In this figure, the spool 2 is the same as spool 1 of Fig. 35. The spool is held in place by a bracket 1 and it can be rotated by turning the spindle through the knob 4. However, free rotation of the spindle is prevented by the engagement of the toothed (splined) sections of the spindle and the support structure 5.

To increase the maximum allowable deflection angle θ, the spindle is pulled in the direction of the arrow until the splined sections are disengaged. This can be felt by the stop-pin 6 bearing on the bracket 1. The knob is then rotated counterclockwise until the desired angle is obtained.



1	BRACKET	3	TOOTHED SECTION OF SPINDLE
2	SPOOL	4	TURNING KNOB
6	STOP PIN	5	SUPPORT STRUCTURE

FIG. 36 ADJUSTING SPINDLE

This angle is given by

$$\theta = \left(\frac{r}{l}\right).\ \phi \qquad \text{----------(10.4)}$$

where

r = radius of spool 1 in Fig. 35

l = height of the pivots of the levers 6 from the limit stops 5.

ϕ = angle of rotation of knob 4 in Fig. 36.

To decrease the maximum angle θ, the spindle is again disengaged and the spool allowed to rotate freely under the action of the springs 3 of Fig. 35.

To lock the mechanism, the required angle θ is defined and the spindle is moved opposite the direction of the arrow to engage the toothed sections.

In conclusion, it should be mentioned that this device prevents free movement of the limit stops only in discrete steps. However, it provides positive locking of the system. To use a device that prevents free movement of the stops in continuous steps would involve the use of friction stops which are rejected for this work because of the possibility of slip under the action of the springs 3. Depending on the number of splines, fairly good accuracy of the position of the limit stops can be obtained.

The Alarm

Since the gyro will be used to warn the driver of a critical driving condition (overspeed at bends), then it will not be sufficient to have only a scale on the output display unit mentioned in Chapter 9. This is because the driver may not have the opportunity to keep his eyes always on the scale.

This problem is solved by using the limit stops as contacts for switches that will trigger on either an audio or a visual alarm to warn the driver that he has exceeded the pre-set angle θ (and consequently a safe maximum velocity v). The electrical circuit for this alarm could be as depicted in Fig. 37.

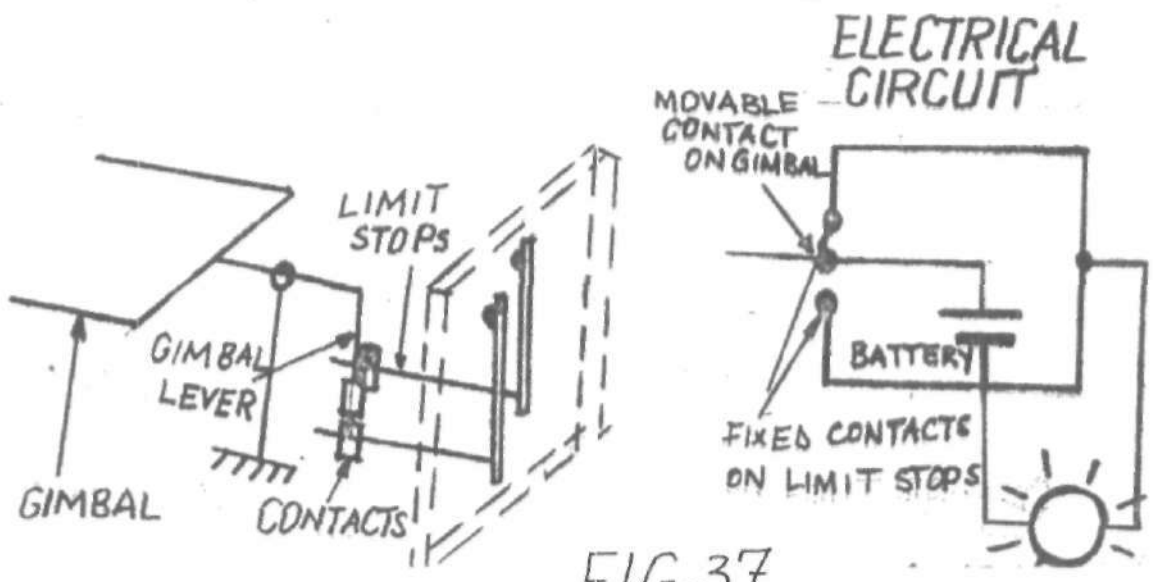


FIG.37

This figure shows the gimbal carrying a lever which can make contact with the limit stops under the action of an angular velocity input. Such contact means the required maximum has been reached and the alarm is triggered on. By this artifice, the output display unit now plays a secondary role - the primary role now taken over by the alarm.

10.2. DAMPING ADJUSTMENT

Since values of damping obtained by calculation are not necessarily the values obtained in practice, it will be good if during calibration and testing of the gyro the position of the damping magnets is varied and the dynamic response of the gyro for each position noted. In this way, the position that gives the best damping is obtained and the magnets locked in that position. Slots are thus provided for the screws that hold the magnets so that this can be done.

10.3. BALANCE WEIGHTS

These can be screws made from a fairly high density material like brass and are mounted on the gimbal on either side of the output axis. By screwing them in or out during calibration, the gyro gimbal can be balanced statically in the horizontal position.

To prevent the screws getting loose during operation, very fine threads (UNF) should be used. Also some locking adhesive like araldite may be used to lock the screws after balancing.

10.4. GYRO TESTING AND CALIBRATION

Before the gyro can be used, it has to be tested and calibrated. A controlled rotating table (called a rate table) is used to calibrate rate gyros. A simple schematic of this table is shown in Fig. 38.

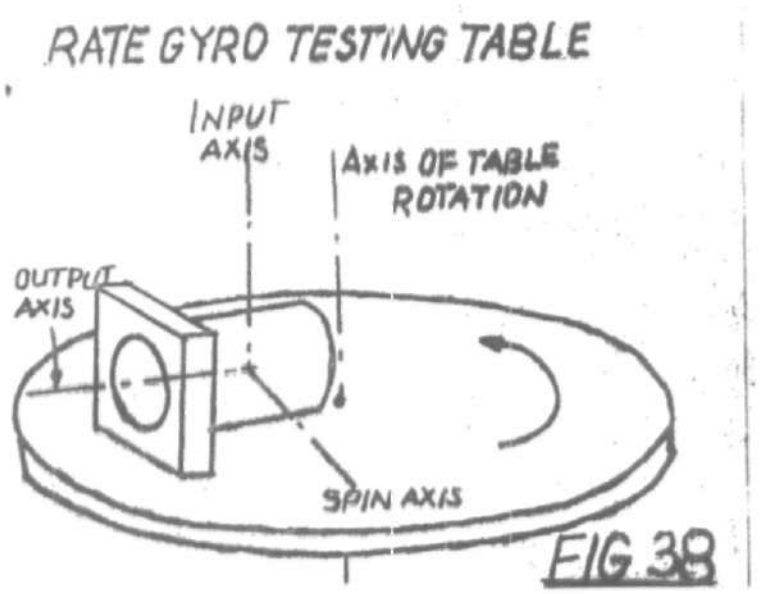


FIG 38

Testing is carried out by mounting the gyro on the table as shown with the input axis parallel to the axis of rotation of the table. The table is made to rotate at

various rates and the gyro output is measured.

To calibrate the gyro, rates of turn that simulate rates of turn of different vehicles are induced in the gyro via the testing table; and the output of the gyro noted.

Other important tests that could be done on the gyro include damping control, power consumption, pickoff sensitivity, sensitivity to linear and angular accelerations, sensitivity to vibrating movements, etc.

The results of all these tests should then be analysed to be used in modifying and improving the overall design.

CHAPTER 11

THE DESIGN CALCULATIONS

11.1. THE ELECTRIC MOTOR DESIGN

(a) The Design Approach

There are two ways to design the gyro motor:

1. The output requirements of the motor (torque, speed, etc.) could be specified and the dimensions of the motor needed to satisfy these requirements are calculated.
2. Arbitrary dimensions (to satisfy space requirements) are assigned to the various components of the motor and the performance of this motor calculated and compared with the required values.

The latter method of design is chosen for this work because it offers two advantages. First, data for calculating all the dimensions of a capicitor split-phase hysteresis motor driven by square voltage source is not readily available - particularly for the stator. Secondly, we notice from the fundamental rate gyro equation (4.3) of Chapter 4), the sensitivity of the gyro could be improved by maximizing on its angular momentum $I\omega$. The design of

the motor by the second approach helps in deciding at the outset the amount of inertia that could be used to satisfy a required input-output relationship.

(b) Motor Rating

The rating of a motor is determined by the expected maximum load it will pull in practice. The main torques that a gyro motor is expected to overcome are:

(i) accelerating torque to pull the motor from rest to synchronous speed (pull-in torque);

(ii) bearing friction torque;

(iii) windage torque.

(i) Acceleration Torque

One of the characteristics of the hysteresis motor is that it does not make its final pull-in effort by impulse; but accelerates smoothly into synchronism [15]. Thus we can assume a constant angular acceleration.

Let ω_s = synchronous spin speed (rad/s)

ω_o = initial spin speed (rad/s)

α = constant angular acceleration (rad/s^2)

t = time taken to reach synchronism from ω_o (s)

I = inertia of rotor (kg-m^2)

n = synchronous speed (rpm).

From kinematics of rotation

$$\omega_s = \omega_o + \alpha t$$

For most practical purpose, the motor starts from rest. Hence $\omega_o = 0$.

$$\therefore \alpha = \frac{\omega_s}{t}$$

$$= \frac{\pi n}{30\, t}$$

The power expended in accelerating the rotor to synchronism is

$$P_a = I \alpha . \omega_s$$

$$= (0.011\, n^2 I)/t \quad [W] \text{ ----------(1)}$$

(ii) Bearing Friction Torque

The bearing friction torque for ball-bearings is given by

$$T = \frac{W \mu d}{2} \quad [N\text{-}m]$$

where

W = radial load on bearing (N)

μ = coefficient of friction between balls and races (ranges from 0.002 to 0.02)

d = inner diameter of bearing.

The power absorbed is thus

$$P_b = \frac{W \mu d}{2} \cdot \frac{2\pi n}{60} \times 2 \quad (W)$$

$$= 0.1047\ W \mu dn \quad (W) \text{ ----------(2)}$$

(iii) Windage Torque

In general, the windage losses are so much smaller than the bearing losses that for preliminary design purposes they may be neglected [20]. Hence

$$P_W = 0$$

The motor rating will be specified after the dimensions that satisfy the input-output requirements have been specified.

(c) Rotor Dimensions

For the gyro to qualify as a panel instrument the following maximum outside dimensions are considered ample:

Total length 140 mm

Outside diameter 80 mm.

Out of the 80 mm outside diameter an approximate 50 mm will be used as the maximum outside diameter of the rotor,

The synchronous pull-out power of the hysteresis motor can be written as

$$P = T\omega_s = T \cdot \frac{2\pi n}{60}$$

$$= 0.1047\ Tn \quad [W] \text{ ----------(3)}$$

where

T = hysteresis torque (N-m)

n = synchronous speed (rev/min).

But from equation (6.1) of Chapter 6, the hysteresis torque is given by

$$T = \frac{pVW_h}{4\pi}$$

where

p = number of poles

V = volume of rotor hysteretic material (m^3)

W_h = hysteresis energy loss/cycle/m^3.

Substituting this equation into (3) gives

$$P = (8.33 \times 10^{-3})\ pVW_h n \quad \text{----------(4)}$$

Thus the pull-out power depends on the volume of the rotor hysteretic material.

Experience has shown that the dimensions of the rotor hysteretic material are restricted by the following relationships [13]:

$$D_2/D_1 = 1.2 - 1.4$$

$$L/D_2 = 0.5 - 1.2$$

$$\delta = 0.2 - 0.5 \times 10^{-3}\ m^3$$

where

D_2 = outer diameter of hysteretic material

D_1 = inner diameter

L = axial length

δ = air-gap length.

Let D_1 = 30 mm

Thus, if we use

D_2/D_1 = 1.33, D_2 = 40 mm

L/D_2 = 0.625, L = 25 mm

Thus the volume of the material is

$$V = 0.786\ L\ (D_2^2 - D_1^2)$$

$$= 1.38 \times 10^{-5}\ m^3$$

As a tentative design, assume the following parameters specified on the basis of the discussion in Chapter 6 section 6.2:

Spin speed n = 9000 rpm

No. of poles p = 2

Rotor Material = P6

Hence W_h = 22,500 (J/m^3/cycle)

Overall efficiency η = 60%

Substituting into (4) gives

$$P = 45.6 \text{ W.}$$

Thus the input power to the motor is

$$P_i = \eta P = 77.7 \text{ W}$$

So the input power to the motor is approximately 80 W, which places it in the fractional-horsepower category.

(c) Total Inertia of Rotor

Inertia of the Hysteresis ring (Ir)

The inertia of a hollow cylinder is given by

$$I = \frac{\rho \pi L}{32} (D_2^4 - D_1^4)$$

For P6, $\rho = 8200 \text{ kg/m}^3$

$D_1 = 30 \text{ mm}$

$D_2 = 40 \text{ mm}$

$L = 25 \text{ mm}$

$\therefore$ $Ir = 3.523 \times 10^{-5} \text{ kg-m}^3$

Inertia Actually Needed (I_t)

To evaluate the total inertia needed in the gyro, certain approximations on the gyro output requirements must be made.

1. A good working value of a spring constant for small gyros is

$$K = 0.012 \text{ Nm/rad.}$$

2. Assume a maximum truck speed of 60 km/h. Based on Table 2 of Chapter 2, the minimum radius of curvature most likely to be encountered is 125 m. Thus the maximum rate of turn for such trucks is

$$\Omega = \frac{v}{R} = \frac{60}{(3.6)(125)} \approx .1\ 4 \text{ rad/s.}$$

Let the gyro response due to this input be an output angle θ of $\frac{\pi}{4}$ rad. Substituting these into equation (4.3) of Chapter 4 gives

$$I_t = \frac{K\theta}{\omega\Omega} = \frac{(0.012)(\pi)}{(4)(300\pi)(0.14)}$$

$$= \underline{7.15 \times 10^{-5} \text{ kg-m}^2}$$

Extra Inertia Needed (I)

The extra inertia needed is given by

$$I = I_t - Ir$$

$$= (7.15 - 3.523)\ 10^{-5}$$

$$= 3.63 \times 10^{-5} \text{ kg-m}^2.$$

A brass ring will be used to provide this extra inertia. For this ring,

Outer diameter $D = ?$

Inner diameter $d = 40$ mm

Axial length $L = 25$ mm

density $\rho = 8390$ kg/m^3.

Substituting into the equation

$I = 0.0982 \rho L (D^4 - d^4)$ gives

$D = 46$ mm.

(d) Check For Motor Rating

The power needed for acceleration and to overcome bearing and windage can now be calculated and compared with the total output power of the motor. The main power relations are (1) and (2):

$$P_a = (0.011\ n^2 I)/t$$

$$P_b = 0.1047\ W \mu\ dn \qquad (W)$$

For this motor,

$n = 9000$ rpm

$I \simeq 8.0 \times 10^{-5}$ kg-m^2

take $t = 5$ s.

Then

$$P_a = 14.26\ W,$$

and assuming $\mu = 0.02$, $d = 5$ mm, and from the above dimensions $W \simeq 4$ N, then $P_b \simeq 0.4$ W.

Thus the total power needed is about 15 W. Hence the motor output (45 W) is ample enough to overcome the load.

11.2. THE SPRING DESIGN

(a) SPECIFICATIONS

The spring constant K = 0.012 Nm/rad. The spring is to be made of phosphor bronze; and is to be rectangular in cross-section. The inner end of the spring is to be fitted into a slot made on the hub, whose diameter is 10 mm. The outer end is also to be clamped at a radius of 35 mm. For phosphor bronze, Young's Modulus E = 118 x 10^9 N/m^2, and Maximum bending stress S = 59 x 10^6 N/m^2.

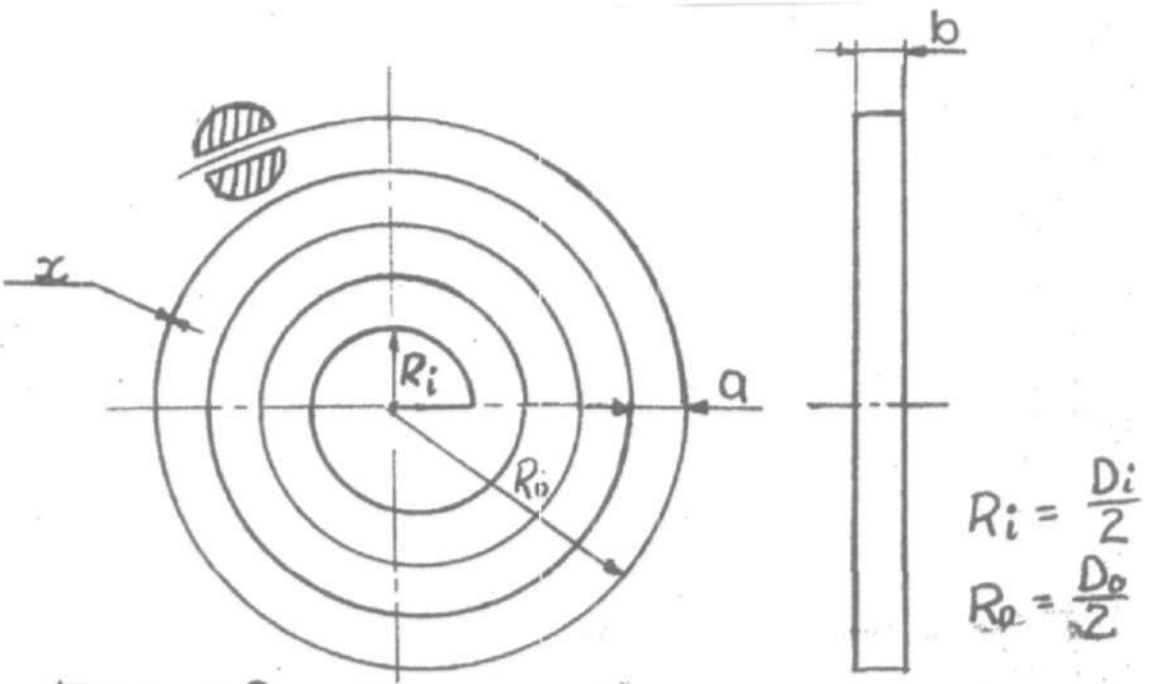


FIG. 39. SPIRAL SPRING

(b) DESIGN PARAMETERS (See Fig. 39)

x = thickness of spring material (mm)

b = width of spring material (mm)

D_o = outer diameter of spring (mm)

D_i = inner diameter of spring (mm)

ϕ = maximum angle of spring deflection (rad)

S_m = maximum working stress of spring (N/m^2)

a = spacing between the coils (mm)

n = number of convolutions.

(c) DESIGN EQUATIONS [17] and [18]

$$S_m = \frac{E\,\phi}{2(l/x)} \leq S \qquad \text{----------(1)}$$

$$x^3 = \frac{12\,Kl}{E\,b} \qquad \text{----------(2)}$$

$$l = \frac{n\pi(D_o + D_i)}{2} \qquad \text{----------(3)}$$

$$n = \frac{D_o - D_i}{2\,a} \qquad \text{----------(4)}$$

The limit equations are:

$$3 \leq b/x \leq 15 \qquad \text{----------(5)}$$

$$1000 \leq l/x \leq 3000 \qquad \text{----------(6)}$$

$$S_m \leq S = 59 \times 10^6\ N/m^2 \text{ (for phosphor bronze)} \qquad \text{----(7)}$$

$$\phi \leq 900^o \qquad \text{----------(8)}$$

$$4 \leq n \leq 10 \qquad \text{----------(9)}$$

(d) DESIGN CALCULATIONS

The following tentative values will be used:

$K = 0.012$ Nm/rad

$b = 3$ mm

$E = 118 \times 10^9$ N/m^2

$D_o = 65$ mm

$D_i = 10$ mm

$\phi = \pi/4 \quad (45^\circ)$

$n = 6$

From equation (3)

$$L = \frac{(6)(\pi)(75)}{2}$$

$$= 700 \text{ mm}.$$

From equation (2)

$$x^3 = \frac{(12)(0.012)(.700)}{(118 \times 10^9)(0.003)}$$

$$\therefore \quad x = 0.7 \text{ mm}$$

(e) CHECKING THE DESIGN

Check for l/x ratio from equation (6)

$$l/x = \frac{700}{0.7} = 1000$$

Check for b/x ratio from equation (5)

$$b/x = \frac{3}{0.7} = 4.3$$

Check for stress from equation (1)

$$S_m = \frac{(118 \times 10^9)(\pi)}{8(1000)}$$

$$= 46.3 \times 10^6 \text{ N/m}^2 \quad \text{S}$$

Hence all the limit equations are satisfied.

(f) SPACING BETWEEN COILS

This is given by equation (4)

$$a = \frac{D_o - D_i}{2}$$

$$= \frac{55}{12}$$

$$= 4.6 \text{ mm}$$

11.3. THE DAMPER DESIGN

(a) SPECIFICATIONS

As was stated in Chapter 8, the damper will be of the Eddy-Current type. The damping will be provided by four powerful U-shaped permanent magnets. Thus instead of a single-gap magnet of the horse shoe type which is suitable for bending from low coercivity alloy steel rolled bar, it is usual to use two short cast magnets of high coercivity alloy one mounted above and one below the disc, so that the flux intersects the disc twice [24].

In this design, four magnets are used as shown diagramatically in Fig. 40.

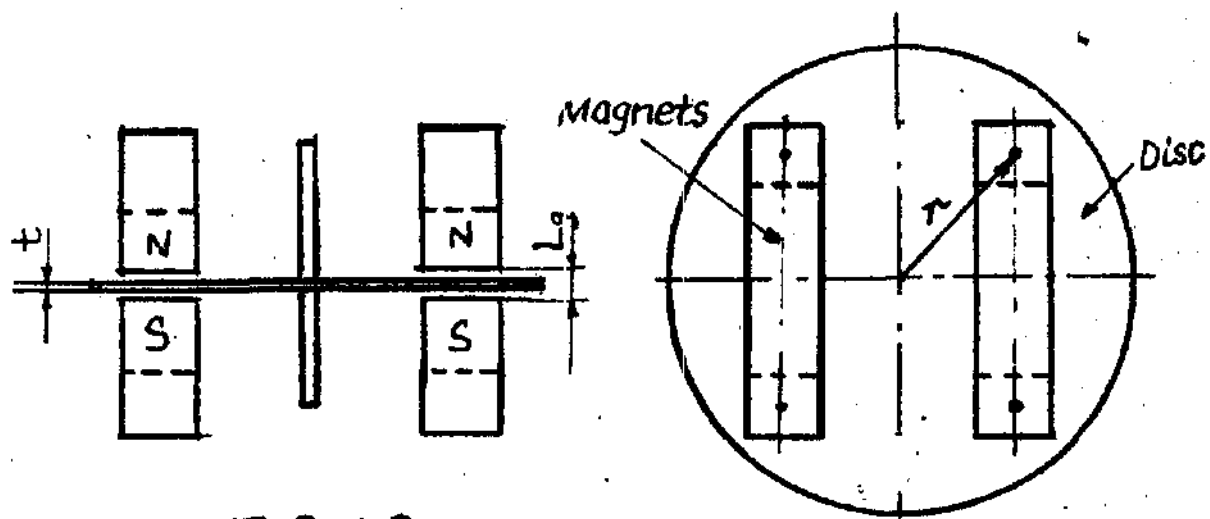


FIG 40. Eddy Current Damper.

(b) DESIGN PARAMETERS

C = damping coefficient (N-m/rad/s)

ζ = damping ratio

K = spring constant (N-m/rad)

I_o = inertia of gimbal and motor and other attachments about gyro output axis ($kg\text{-}m^2$)

ϕ = flux in magnets (W b)

ρ = resistivity of disc material (Ω-m)

A_g = area of magnet at air-gap (mm^2)

A_m = area of magnet (mm^2)

r = radius of action of pole of magnets (mm)

t = thickness of disc (mm)

L_m = length of magnet (mm)

L_g = length of air-gap (mm)

B_m = flux density in the magnet (Wb/m^2)

H_m = magnetizing force of magnet (AT/m)

μ_o = permeability of air-gap($= 4\pi \times 10^{-7}$)

K_1, K_2 = constants used in magnet design to take into account fringing and leakage, with K_1 ranging from 1 - 10 and K_2 ranging from 1.05 - 1.45.

(c) THE DESIGN EQUATIONS [24]

The main damper design equations are:

$$C = 2\zeta\sqrt{K I_o} \quad \text{----------(1)}$$

$$C = \frac{2\phi^2 t r^2}{5\rho A_g} \times 10^{-3} \quad \text{----------(2)}$$

(d) DESIGN CALCULATIONS

$I_o \simeq 9.5 \times 10^{-5}$ kg-m^2

K = 0.012 N-m/rad.

As a tentative design, let $\zeta = 0.7$. Then substituting in (1) gives

$$C = 2(0.7)\sqrt{(9.5 \times 10^{-5})(0.012)}$$

$$= 1.5 \times 10^{-3} \text{ N-m/rad/s.}$$

Equation(2) gives the value of damping for the flux under one pair of poles. Since we have 4 pairs of poles in this case, the damping is multiplied four times [24]. Thus

$$C = \frac{8 \phi^2 t r^2}{5 \rho A_g} \times 10^{-3}$$

From this, $$\phi^2 = \frac{625 C \rho A_g}{r^2 t} \quad \text{----------(3)}$$

Assume that the disc material is aluminium; then

$$\rho = 2.82 \times 10^{-8}$$

Assume also that

$$A_g = 25 \text{ mm}^2$$

$$r = 28 \text{ mm}$$

$$t = 1 \text{ mm}$$

Substituting in (3) gives

$$\phi^2 = \frac{(625)(1.5 \times 10^{-3})(2.82 \times 10^{-8})(25)}{(28)^2(1)}$$

$$\therefore \quad \emptyset = 2.9 \times 10^{-5} \text{ Wb}$$

The flux density under each pair of poles is thus

$$B_g = \frac{\emptyset \times 10^6}{A_g}$$

$$= \frac{(2.9 \times 10^{-5})(10^6)}{25}$$

$$\therefore \quad \underline{B_g = 1.16 \text{ Wb/m}^2}$$

(e) DESIGN OF THE MAGNET

The design equation for a simple U-magnet is

$$\frac{B_m}{H_m} = \mu_o \frac{K_1 A_g L_m}{K_2 A_m L_g} \quad \text{----------(4)}$$

Owing to the complex nature of a permanent magnet, it is not usually easy to start from the value of flux density required under each pole and to establish from this the dimensions of the magnet required. It is usually necessary to make an intelligent guess of the dimensions of the magnet and to analyse the resulting design to ascertain how close its performance comes to that required [18].

On the basis of the above argument, the following dimensions are selected to satisfy space requirements in the gyro:

$$L_m = 62 \text{ mm}$$

$$A_m = 64 \text{ mm}^2$$

$$L_g = 3 \text{ mm}$$

Take $K_1 = 5$

$K_2 = 1.2$

Substituting these values in (4) gives

$$\frac{B_m}{H_m} = -\frac{(4\pi \times 10^{-7})(6)(25)(62)}{(1.2)(3)(64)}$$

$$= \underline{\underline{-0.51 \times 10^{-4}}}$$

For this value of permeance, the chart shown below shows that 15% Cobalt Steel can provide a flux density of 0.5 Wb/m^2 very near to its operating point. If this steel is selected for the magnets, we have

$$B_m = 0.5 \text{ Wb/m}^2.$$

To find out the flux density at the air-gap, we use

$$\phi = B_m A_m = B_g A_g$$

$$\therefore B_g = \frac{B_m A_m}{A_g} = \frac{(0.5)(64)}{25}$$

$$= \underline{\underline{1.28 \text{ Wb/m}^2}}$$

This shows that 15% cobalt steel can provide flux density at the air-gap slightly above the required value of 1.16 Wb/m^2.

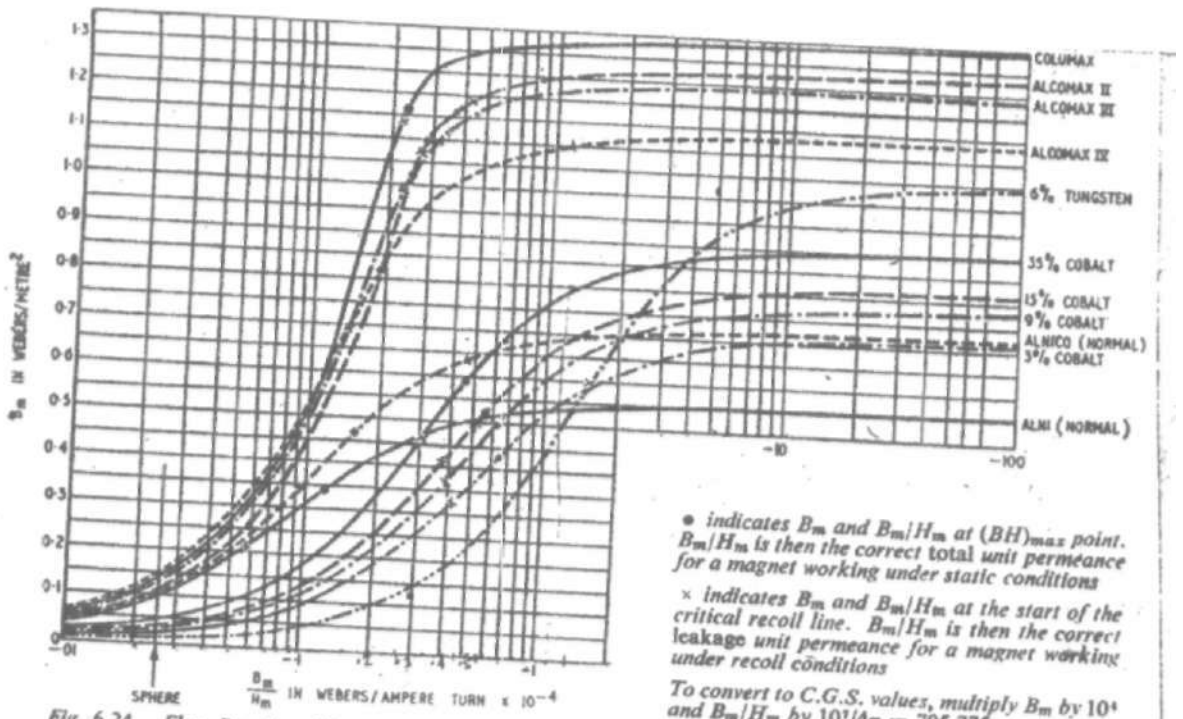


Fig. 6.24. *Flux Density: Unit permeance curves for magnet alloys. This is the basic design chart for permanent magnets. Calculate B_m/H_m from the dimensions of the magnet and the airgaps, allowing for leakage. Find the corresponding value of B_m for any alloy shown on this chart. Finally calculate H_m*

Chart for Permanent Magnet Design. [Ref. 24 p217]

This is, however, not too large since after all, the constants K_1 and K_2 were only selected arbitrarily.

The actual damping can only be obtained experimentally; although the calculations give very useful guidelines.

11.4. THE DESIGN OF THE PICKOFF

On the basis of the discussion in Chapter 9, a Microsyn Type Pickoff was selected. The power to the microsyn will be obtained from the inverter which supplies the gyro hysteresis motor.

The design will be based on the calculated performance of a Microsyn whose dimensions are dictated by the overall dimensions of the rate gyro under consideration.

(a) THE DESIGN PARAMETERS ARE:

r = radius of rotor (mm)

t = thickness of rotor (mm)

ϕ = pole angle (deg.)

θ = displacement of gyro from null position(deg.)

p = number of poles on stator

P = permeance

μ = permeability of air-gap

h = radial length of air gap (mm)

f = supply frequency (H_z)

I_p = primary winding current (amp.)

N_p, N_s = number of turns on primary and secondary windings respectively

E_o = output voltage (V)

$dP/d\theta$ = rate of change of permeance with deflection

angle

$dE_o/d\theta$ = voltage gradient (volts/deg.).

(b) THE MAIN DESIGN EQUATIONS [8]

$$\frac{dP}{d\theta} = (-1)^p \frac{\mu rt}{h} \quad \text{---------- (1)}$$

$$\frac{dE_o}{d\theta} = \frac{1}{2\pi} f\ p\ I_p N_p N_s \frac{dP}{d\theta} \quad \text{---------- (2)}$$

(c) DESIGN CALCULATIONS

From the space requirements of the gyro, we have

$p = 4$

$\mu = 4\pi \times 10^{-7}$

$r = 10$ mm

$t = 10$ mm

$h = 0.5$ mm

$$\therefore \frac{dP}{d\theta} = \frac{(4\pi \times 10^{-7})(10)(10)\ 10^{-6}}{0.5 \times 10^{-3}}$$

$$= \underline{2.513 \times 10^{-7}}$$

To calculate the voltage gradient, we need to know f, I_p, N_p and N_s. The first two can be deduced from the output of the converter to be used. The last two, however, will be selected on the basis of experience.

C L O S I N G R E M A R K S

In conclusion, I will like to mention that the work as presented here should act only as a stepping stone for more refined design of the rate gyro - not necessarily for land vehicle application but for other applications as well. Many modifications might need to be made especially during production. Thus the rotor width might need to be increased depending on the length of the overhung part of the stator windings. However, special care has been taken to ensure that all or most of the elements of the rate gyro can be produced cheaply by either casting or extrusion followed by machining. Also many of the parts were designed to ensure easier production and assembly. For example, where two mating parts are splined (as 21 and 22 on the assembly drawing), the mating part is made as a bronze insert not only because it is stronger than the aluminium support, but because it is easier to cut the splines in an insert than in the support. Most of the production work is expected to be carried out in an instrument workshop.

It might also be noted that the detailed design of many of the parts like the suspension shafts, the axle, etc., has been omitted. However, I have carried out special

checks to ensure that the dimensions of these elements are ample enough to withstand the loading imposed by the gimbal and rotor assembly.

The spin bearings are the special instrument bearings with flange on the outer race. They were selected from a Handbook using conventional methods of selection. The suspension bearings were selected in a similar manner, though they are not flanged.

All the screws are to be those with fine threads. Thisis to ensure that they do not come loose in practice. All the screws, nuts, bolts and wire springs could be selected from a manufacturers catalogue. In keeping with conventional instrument assembly, special adhesives may be used to help keep the screws of such critical parts as the rotor in place.

It will be difficult to present a complete cost analysis for the gyro as this will involve computing the material cost, labour cost, machining cost, advertising cost, etc. The following are average prices for gyros of similar dimensions as the one designed here which are used on aircrafts:

Turn and Slip Indicator - ₦300.00

Directional Gyro - ₦200.00

Artificial Horizon - ₦200.00

The lower cost of the last two could be dueto the fact that they are air-driven and hence have a simplified rotor construction. The higher cost of the first instrument could be due to two reasons. First, the rotor is electrically driven and secondly there are two instruments integrated in one - the rate of turn indicator and the slip indicator.

Based on the above prices, it can be estimated that the design presented here will cost about ₦300.00 $\pm$ 50. This represents only about 2% of the cost of an empty truck.

APPENDIX

DERIVING RATE GYRO EQUATION

Consider the rate gyro shown in Fig. 10.

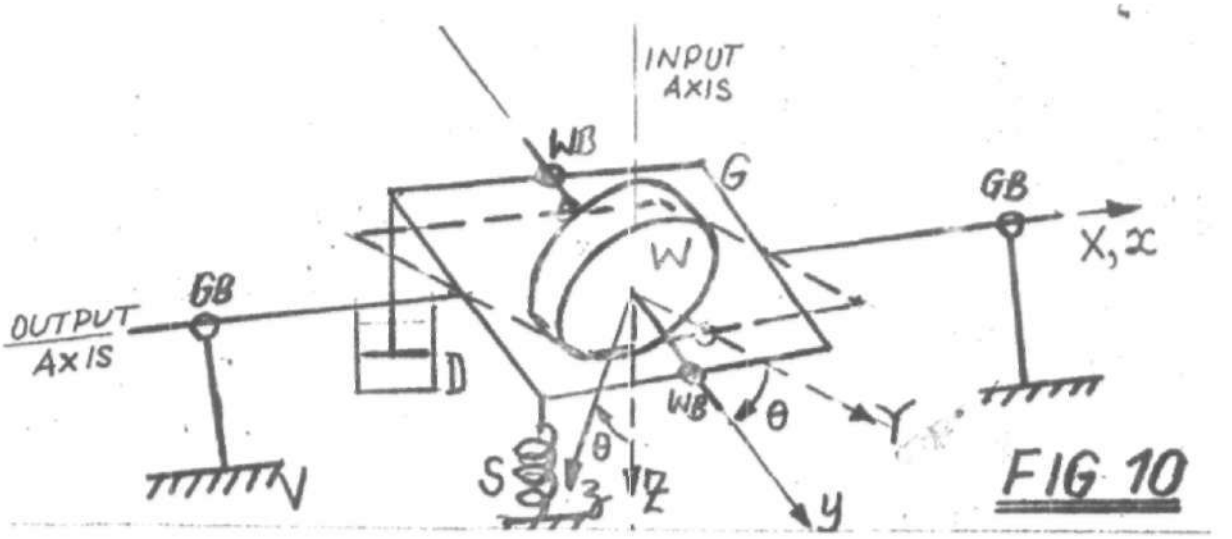


FIG 10

Let I_x, I_y, I_z = inertia of rotor about axes O_x, O_y and O_z.

I_{gx}, I_{gy}, I_{gz} = inertia of gimbal and other attachments about the same axes.

Let $I_{ox} = I_x + I_{gx}$

$I_{oy} = I_y + I_{gy}$

$I_{oz} = I_z + I_{gz}$

The other parameters are as defined in Chapter 4.

The components of angular velocity of the gyro about axes O_x, O_y and O_z are:

$$\left.\begin{aligned} \omega_x &= \dot{\theta} \\ \omega_y &= \Omega \sin\theta \\ \omega_z &= \Omega \cos\theta \end{aligned}\right\} \quad \text{----------(1)}$$

The components of angular velocity of gyro wheel about same axes are:

$$\left.\begin{aligned} \omega_x &= \dot{\theta} \\ \omega_y &= \Omega \sin\theta - \omega \\ \omega_z &= \Omega \cos\theta \end{aligned}\right\} \quad \text{----------(2)}$$

The components of angular momentum are:

$$H_x = I_{ox}\,\omega_x = I_{ox}\,\dot{\theta}$$
$$H_y = I_{oy}\,\omega_y = I_{oy}\,\Omega \sin\theta - I_y\omega$$
$$H_z = I_{oz}\,\Omega \cos\theta$$

Assuming that Ω is a constant, we get

$$\left.\begin{aligned} \dot{H}_x &= I_{ox}\,\ddot{\theta} \\ \dot{H}_y &= I_{oy}\,(\Omega\,\dot{\theta} \cos\theta) \\ \dot{H}_z &= -\,I_{oz}(\dot{\theta}\,\Omega \sin\theta) \end{aligned}\right\} \quad \text{----------(3)}$$

Assume in the subsequent analysis that both $\dot{\theta}$ and Ω are small quantities so that such products as $\dot{\theta}\,\Omega$ could be neglected.

In the light of a gyro mounted on a road vehicle, these assumptions are acceptable since $\dot{\theta}$ being the response velocity is a fairly transient quantity. Thus for a large part of the working of the gyro (steady state), $\dot{\theta} \simeq 0$. With this assumption,

$$\dot{H}_y = \dot{H}_z = 0$$

The equations of motion are:

$$\left.\begin{aligned} M_x &= \dot{H}_x - H_y \Omega_z + H_z \Omega_y \\ M_y &= \dot{H}_y - H_z \Omega_x + H_x \Omega_z \\ M_z &= \dot{H}_z - H_x \Omega_y + H_y \Omega_x \end{aligned}\right\} \text{----------(4)}$$

Substituting (1) and (3) into (4) gives

$$M_x = I_{ox} \ddot{\theta} - \Omega \operatorname{Cos}\theta (I_{oy} \Omega \operatorname{Sin}\theta - I_y \omega) + I_{oz} \Omega \operatorname{Cos}\theta (\Omega \operatorname{Sin}\theta)$$

$$M_y = - I_{oz} \dot{\theta} \operatorname{Cos}\theta + I_{ox} \dot{\theta} \operatorname{Cos}\theta$$

$$M_z = - I_{ox} \dot{\theta} (\Omega \operatorname{Sin}\theta) + (I_{oy} \Omega \operatorname{Sin}\theta - I_y \omega) \dot{\theta}$$

Or for $\dot{\theta}$ and Ω small,

$$\left.\begin{aligned} M_x &= I_{ox} \ddot{\theta} - (I_{oz} - I_{oy}) \Omega^2 \operatorname{Sin}\theta \operatorname{Cos}\theta \\ M_y &= 0 \\ M_z &= - I_y \omega \dot{\theta} \end{aligned}\right\} \text{---(5)}$$

In the steady state $\ddot{\theta} = \dot{\theta} = 0$

Hence the equation reduces to:

$$M_x = (I_{oz} - I_{oy}) \Omega^2 \operatorname{Sin}\theta \operatorname{Cos}\theta + I_y \Omega \omega \operatorname{Cos}\theta$$

It can be shown that the inertia I_{oz} is of the order of I_{oy} and Ω being a small quantity, makes the first part of this equation negligible compared to the second. Hence

$$M_x = I_y \omega \Omega \cos \theta$$

But $M_x = - K \theta - C \dot{\theta}$

$$\therefore \quad I_y \omega \Omega \cos \theta = - K \theta - C \dot{\theta} \qquad \text{---------(6)}$$

In the steady state, $\dot{\theta} = 0$, so the equation reduces to

$$I_y \omega \Omega \cos \theta = K \theta$$

or

$$\theta = \frac{I_y \omega \Omega}{K} \cos \theta \qquad \text{----------(7)}$$

For small values of θ, $\cos \theta \simeq 1$

$$\therefore \quad \boxed{\theta = \frac{I_y \omega \Omega}{K}} \qquad \text{----------(8)}$$

<u>The dynamic response of the rate gyro</u>

The dynamic response of the instrument could be obtained from (5):

$$- K \theta - C \dot{\theta} = I_{ox} \ddot{\theta} - (I_{oz} - I_{oy}) \Omega^2 \sin \theta \cos \theta + I_y \omega \Omega \cos \theta$$

Neglecting the second quantity on the right hand side and rearranging gives

$$I_{ox} \ddot{\theta} + C \dot{\theta} + K \theta = - I_y \omega \Omega \cos \theta$$

The negative sign on the right hand side could be neglected since the direction of ω could be reversed.

The above equation is a non-linear differential equation. To make it linear we have to assume that θ is amall.

With this assumption, the equation becomes

$$I_{ox}\ddot{\theta} + C\dot{\theta} + K\theta = I_y \omega \Omega \quad \text{---------(9)}$$

Equation (9) can be rearranged thus:

$$\ddot{\theta} + \frac{C}{I_{ox}}\dot{\theta} + \frac{K}{I_{ox}}\theta = \frac{I_y \omega \Omega}{I_{ox}}$$

Substitute

$$\frac{C}{I_{ox}} = 2a$$

$$\frac{K}{I_{ox}} = \omega_1^2$$

$$\frac{I_y}{I_{ox}} = I$$

$$\therefore \ddot{\theta} + 2a\dot{\theta} + \omega_1^2\theta = I\omega\Omega \quad \text{--------(10)}$$

Consider the auxilliary equation

$$\ddot{\theta} + 2a\dot{\theta} + \omega_1^2\theta = 0 \quad \text{----------(11)}$$

Assuming that $a^2 < \omega_1^2$, the solution of (11) is of the form

$$\theta_a = e^{-at}\left[A_1 \text{ Cos } pt + A_2 \text{ Sin } pt\right] \quad \text{-------(12)}$$

where

$$p^2 = \omega_1^2 - a^2$$

This can be written as

$$\theta_a = C\, e^{-\zeta \omega t} \cos (pt - \phi) \quad \text{----------(13)}$$

where

$$\zeta = \frac{c}{C_c} = \frac{a}{\omega_1} = \text{damping ratio}$$

$$p = \omega_1 \sqrt{1 - \zeta^2} = \text{natural damped frequency}$$

$$\omega_1 = \sqrt{K/I_{ox}} = \text{natural undamped frequency}$$

Thus the complete solution is

$$\theta = \frac{I \omega \Omega}{K} + C\, e^{-\zeta \omega_1 t} \cos (pt - \phi) \quad \text{-------(14)}$$

We have to solve for the constants C and ϕ.

If we choose for (14) the initial conditions

$\theta_o = \dot{\theta}_o = 0$, then

for $\theta = 0$ at $t = 0$, we get

$$C \cos \phi + \frac{I \omega \Omega}{K} = 0 \quad \text{-------------(15)}$$

From (14), $\dot{\theta} = -\zeta \omega_1 C\, e^{-\zeta \omega_1 t} \cos (pt - \phi)$

$$- C\, p\, e^{-\zeta \omega_1 t} \sin (pt - \phi)$$

For $\dot{\theta} = 0$ at $t = 0$, this gives

$$-\zeta\omega_1 C \cos\phi + C p \sin\phi = 0$$

$$\therefore \tan\phi = \frac{\zeta\omega_1}{p}$$

But $$p = \omega_1\sqrt{1-\zeta^2}$$

$$\therefore \tan\phi = \frac{\zeta}{\sqrt{1-\zeta^2}} \qquad \text{----------(16)}$$

$$\therefore \cos\phi = \sqrt{1-\zeta^2}$$

Substituting this value in (15) gives

$$C\sqrt{1-\zeta^2} = -\frac{I\omega\Omega}{K}$$

$$\therefore C = -\frac{I\omega\Omega}{K\sqrt{1-\zeta^2}} \qquad \text{----------(17)}$$

Substituting (16) and (17) in (14) gives

$$\theta = \frac{I\omega\Omega}{K} - \frac{I\omega\Omega}{K\sqrt{1-\zeta^2}} e^{-\zeta\omega_1 t}\cos\left[pt - \tan^{-1}\frac{\zeta}{\sqrt{1-\zeta^2}}\right]$$

$$\therefore \theta = \frac{I\omega\Omega}{K}\left[1 - e^{-\zeta\omega_1 t}\cos\left(pt - \tan^{-1}\frac{\zeta}{\sqrt{1-\zeta^2}}\right)\right]$$

------(18)

REFERENCES

1. INSTRUMENTATION FOR TRUCKS
   Smiths Industries Ltd., Automobile Engineer, July, 1971, pp. 46 - 47.
2. A POLICY FOR THE APPLICATION OF SUPERELEVATION
   Ove-Arup and Partners, P. O. Box 571, Kano, Nigeria. July, 1974.
3. HIGHWAY ENGINEERING (3rd Edition)
   C. H. Oglesby, John Wiley and Sons, N.Y.
4. THE GYROSCOPE AND ITS USES
   by Tatan: Engineering Materials and Design, June, 1961, pp. 347 - 350.
5. BASICS OF GYROSCOPES (VOL. I)
   Carl Machover, J. F. Ryder Publishers, Inc. N.Y.
6. BASICS OF GYROSCOPES (VOL. II)
   Carl Machover, J. F. Ryder Publishers, Inc.N.Y.
7. THE GYROSCOPE APPLIED
   K. I. T. Richardson, Hutchinson's Books, London.
8. GYROSCOPES - THEORY AND DESIGN
   P. H. Savet (Editor), McGraw-Hill Book Co. Inc.N.Y.
9. THE GYROSCOPE - THEORY AND APPLICATIONS
   J. B. Scarborough, Interscience Pubs., Inc., N.Y.

10. GYRODYNAMICS

R. N. Arnold and L. Maunder, Academic Press, London.

11. GYROSCOPIC THEORY, DESIGN AND INSTRUMENTATION

W. Wrigley, et al., The M. I. T. Press, Cambridge, Massachusetts.

12. SELECTED SEMICONDUCTOR CIRCUITS HANDBOOK

S. Schwartz (Editor), J. Willey and Sons, Inc., N. Y., Part 9.

13. DESIGN OF HYSTERESIS MOTOR

S. Nakamura, K. Okawa and T. Kato, Electrical Eng. in Japan, Vol. 88, No. 6, 1968, pp. 11 - 20.

14. OPERATING CHARACTERISTICS OF CAPACITOR SPLIT-PHASE HYSTERESIS MOTORS DRIVEN BY SQUARE VOLTAGE SOURCE

G. Wakw, Electrical Eng. in Japan, Vol. 94, No. 6, 1974, pp. 87 - 95.

15. DESIGN AND APPLICATION OF THE HYSTERESIS MOTOR

N. R. Capaldi, Design Engineering (London) September, 1975, pp. 43 - 45.

16. THE HYSTERESIS MOTOR

H. C. Roters, A.I.E.E. - Electrical Engineering, March, 1948, pp. 241 - 245.

17. A PRACTICAL GUIDE FOR HAIRSPRING DESIGN

T. M. Raedy, Machine Design, May 12, 1966, pp. 202 - 207.

18. ELECTRICAL INDICATING INSTRUMENTS

G. F. Tagg, Butterworths, London, pp. 32 - 35 and 44 - 65.

19. HANDBOOK OF PRECISION ENGINEERING (VOL. 6)

A. Davidson (Editor), Macmillan Books.

20. FRACTIONAL-HORSEPOWER ELECTRIC MOTORS

F. G. Spreadbury, Pitman and Sons Ltd., London.

21. FRACTIONAL HORSEPOWER MOTORS

S. F. Philpott, Chapman and Hall Ltd., London.

22. VARIABLE RESISTORS

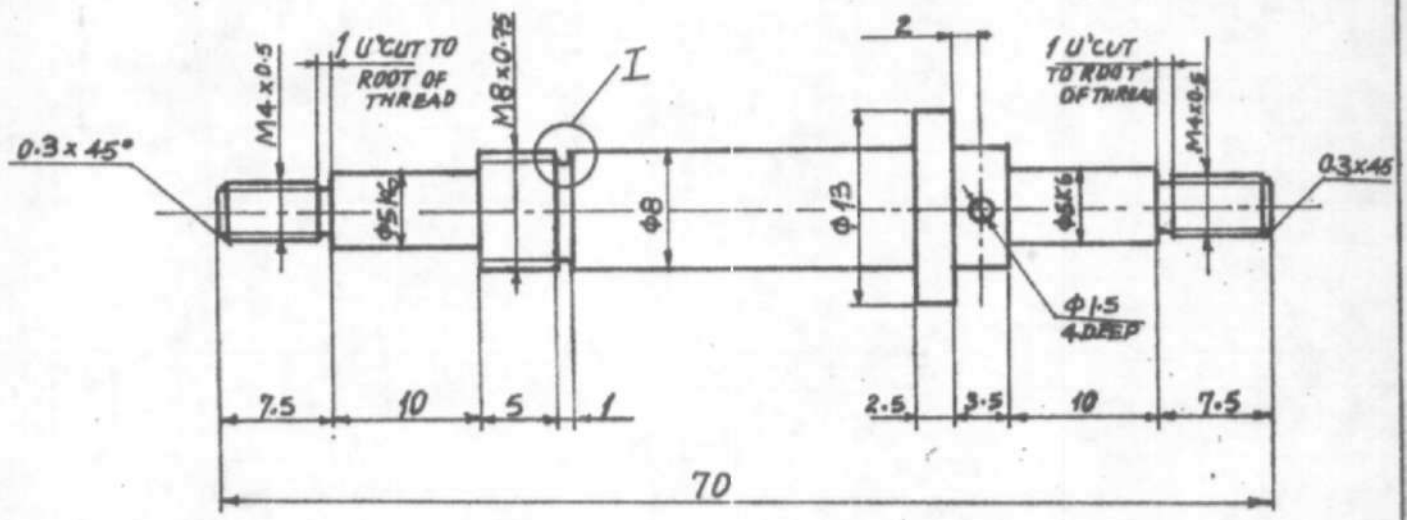
G. W. A. Drummer, Pitman and Sons Ltd., London.

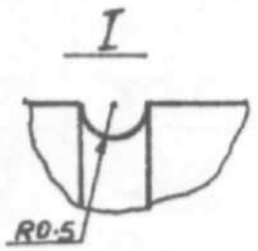
23. GYROS

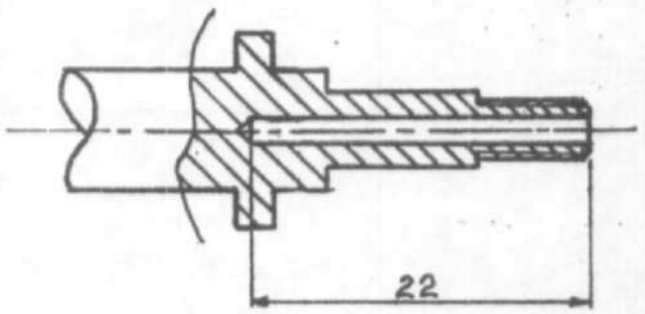
An I.Mech.Engrs.(London) Symposium Proceedings, 1964 - 65, Vol. 179, Part 3E.

24. PERMANENT MAGNETS AND MAGNETISM

D. Hadfield (Editor), pp. 202 - 204, ILIFFE BOOKS LTD., LONDON.

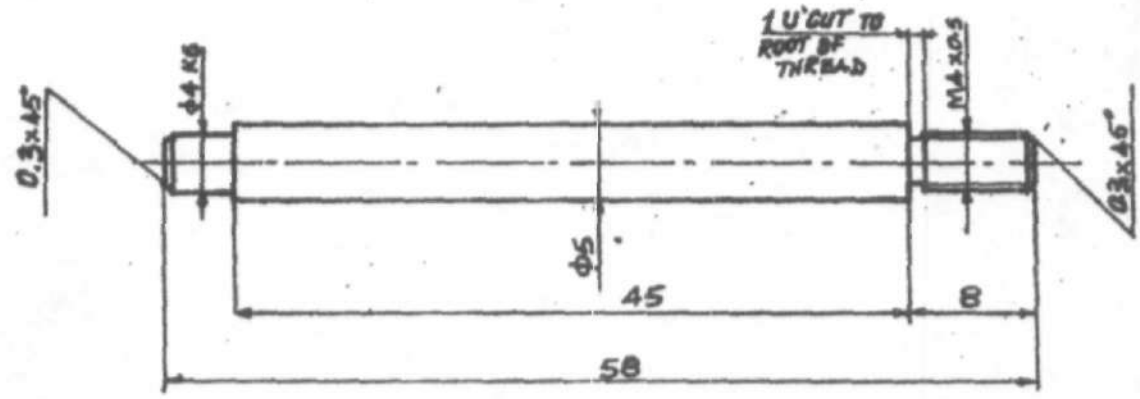






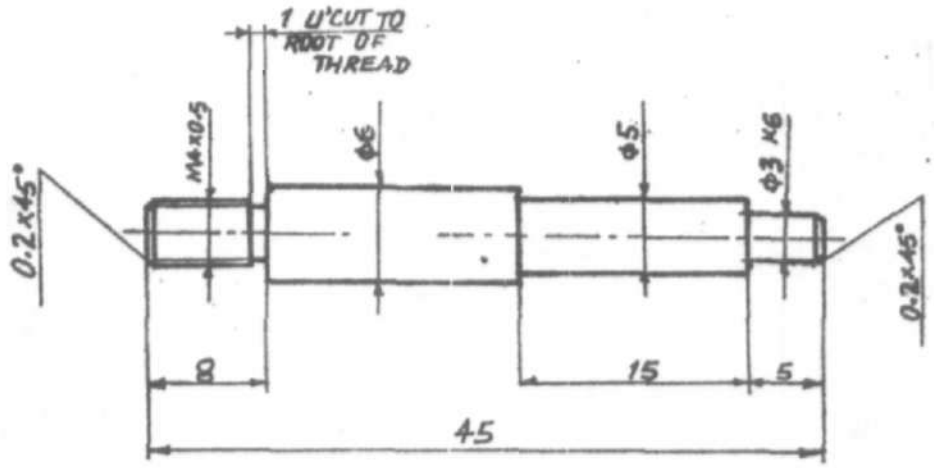
▽8

DRAWN	CHECKED	APPROVED	DESCRIPTION:	RATE GYRO DESIGN		
M.L. AUDU	K.P. Zaclarias		SPIN AXLE	WEIGHT	SCALE	SHEET No.
MATERIAL: STEEL AISI 1045				—	2:1	1



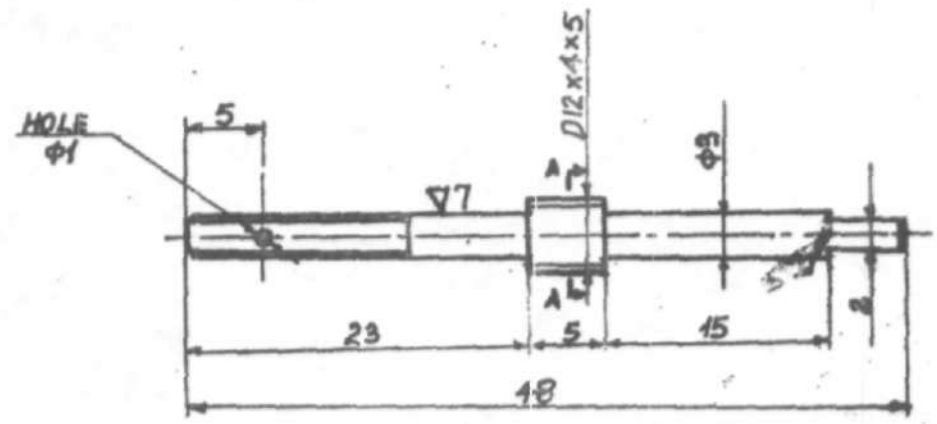
▽8

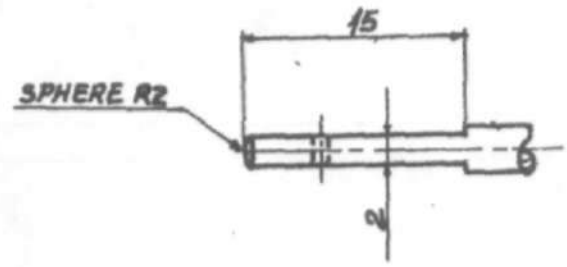
DRAWN	CHECKED	APPROVED	DESCRIPTION:	RATE GYRO DESIGN		
M. L. AUDU	K.P.Z.		REAR GIMBAL SUSPENSION SHAFT	WEIGHT	SCALE	SHEET NO.
MATERIAL: STEEL AISI 1045				—	2:1	2



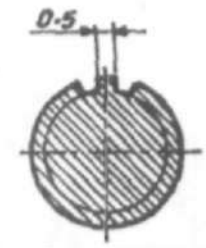
▽8

DRAWN	CHECKED	APPROVED	DESCRIPTION:	RATE GYRO DESIGN		
	K.P.Z.		FRONT GIMBAL SUSPENSION SHAFT	WEIGHT	SCALE	SHEET NO.
MATERIAL: STEEL AISI 1045				—	2:1	3





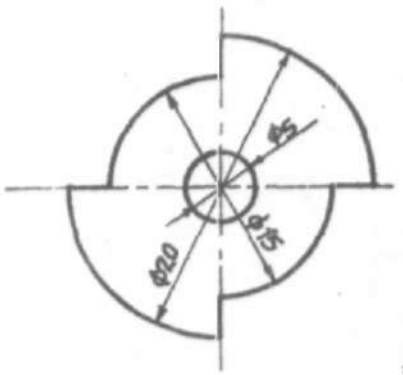


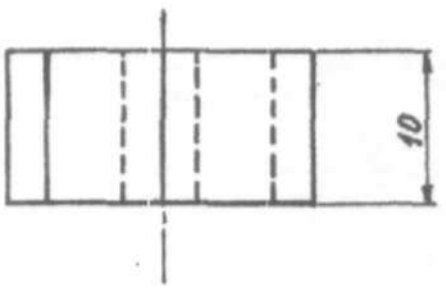


SECTION A-A
(SCALE 1:4)

▽8

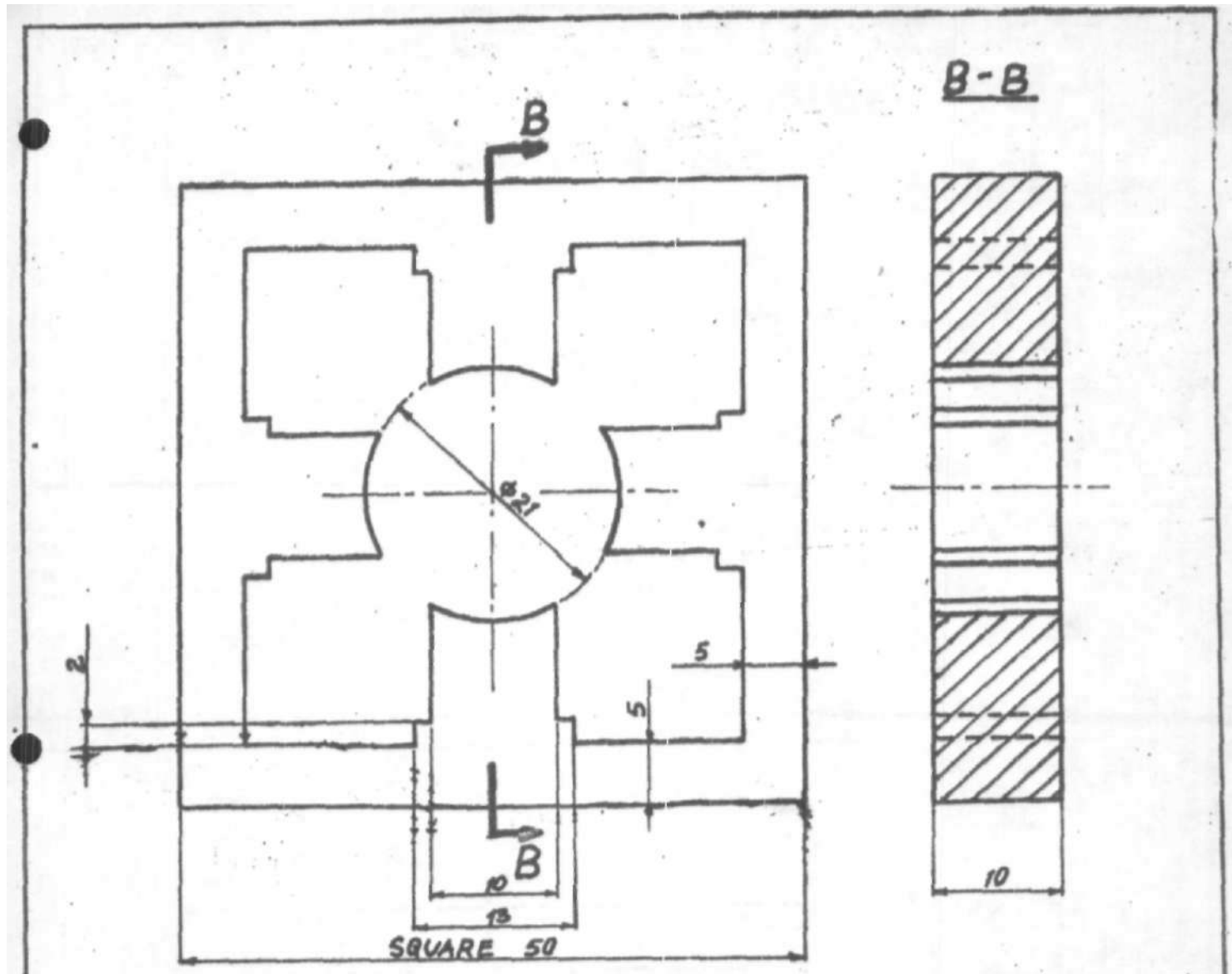
DRAWN	CHECKED	DATE	DESCRIPTION:	RATE GYRO DESIGN		
				WEIGHT	SCALE	SHEET No.
M.L.AUDU	K.P.Z.		SPINDLE FOR ADJUSTING MECHANISM	—	2:1	4
MATERIAL: STEEL AISI 1045						





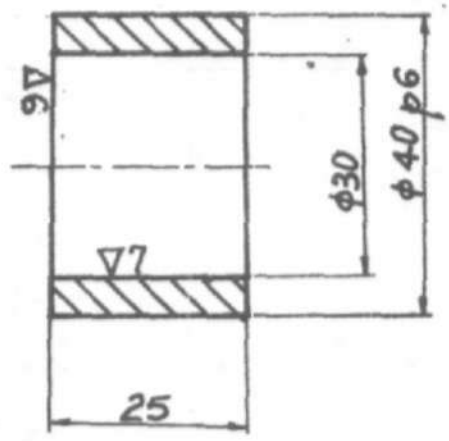
▽8

DRAWN	CHECKED	APPROVED	DESCRIPTION:	RATE GYRO DESIGN		
				WEIGHT	SCALE	SHEET NO.
M. L. AUDU	K.P.Z		ROTOR FOR MICROSYN	—	2:1	5
MATERIAL: TRANSFORMER STEEL						

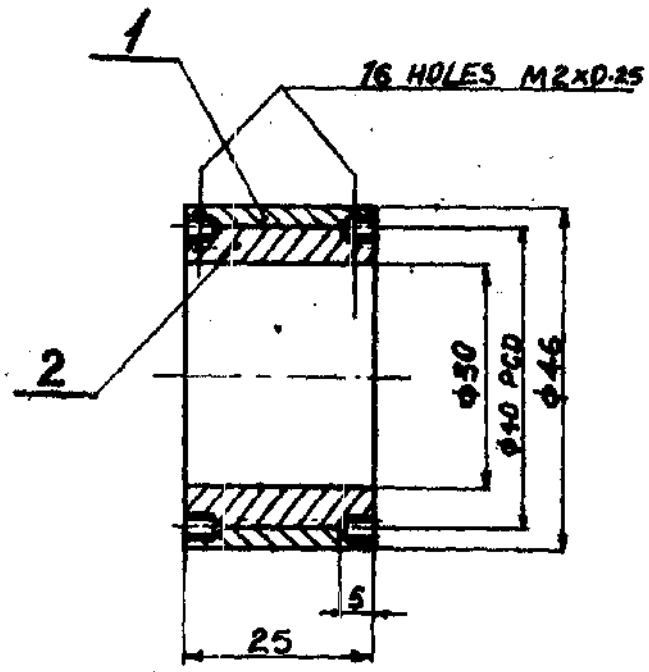


▽5

DRAWN	CHECKED	APPROVED	DESCRIPTION:	RATE GYRO DESIGN		
M.L.AUDU	K.P.Z		MICROSYN STATOR FRAME	WEIGHT	SCALE	SHEET No.
MATERIAL: TRANSFORMER STEEL				—	2:1	6

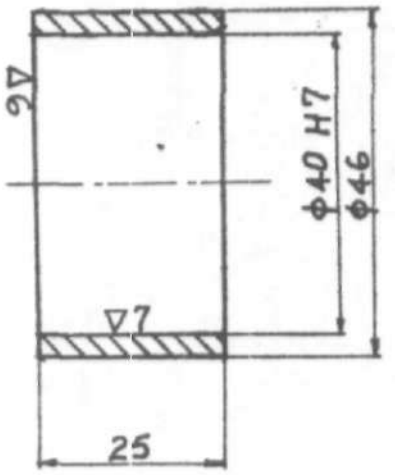


DRAWN	CHECKED	APPROVED	DESCRIPTION:	RATE GYRO DESIGN		
M.L.AUDU	K.A.Z		HYSTERESIS RING	WEIGHT	SCALE	SHEET No.
MATERIAL: P6				—	1:1	7

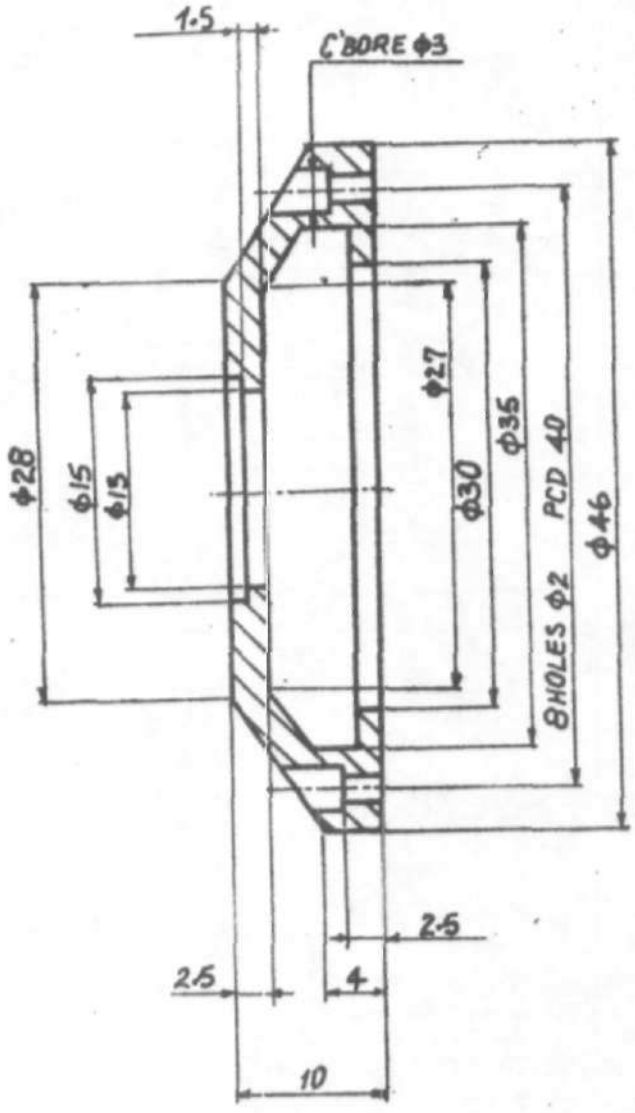


DETAIL / UNIT NO.	DESCRIPTION	NO. OFF	MATERIAL	WEIGHT	NO. OF DRAWING OR STANDARD
2	HYSTERESIS RING	1	P6	—	—
1	INERTIA RING	1	BRASS	—	—

DRAWN	CHECKED	APPROVED	DESCRIPTION:	RATE GYRO DESIGN		
M.L.AUDU	K.P.Z		ROTOR RING ASSEMBLY	WEIGHT	SCALE	SHEET NO.
MATERIAL: —				—	1:1	8

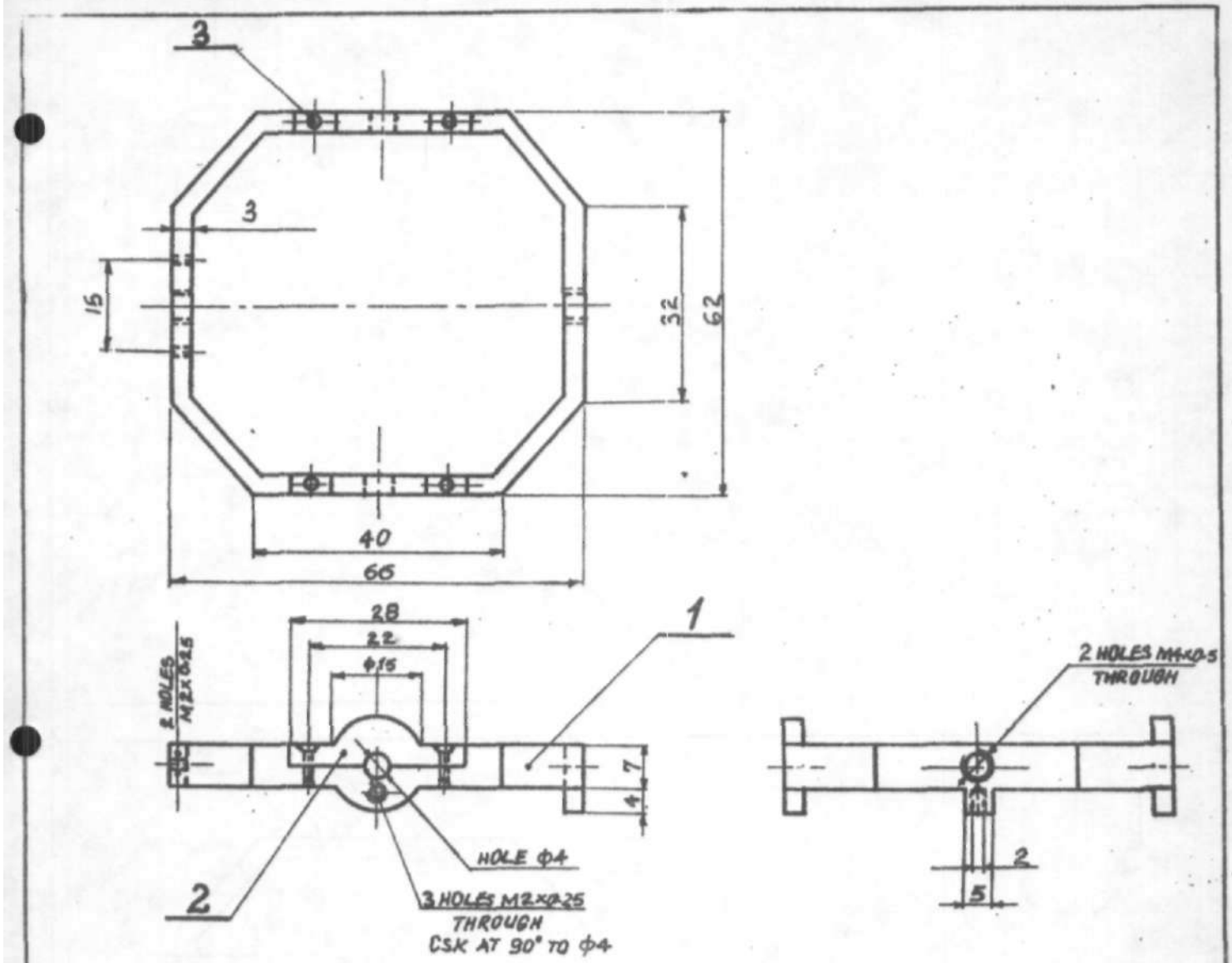


DRAWN	CHECKED	APPROVED	DESCRIPTION:	RATE GYRO DESIGN		
M.L.AUDU	K.P.Z		INERTIA RING	WEIGHT	SCALE	SHEET NO.
MATERIAL: BRASS				—	1:1	9



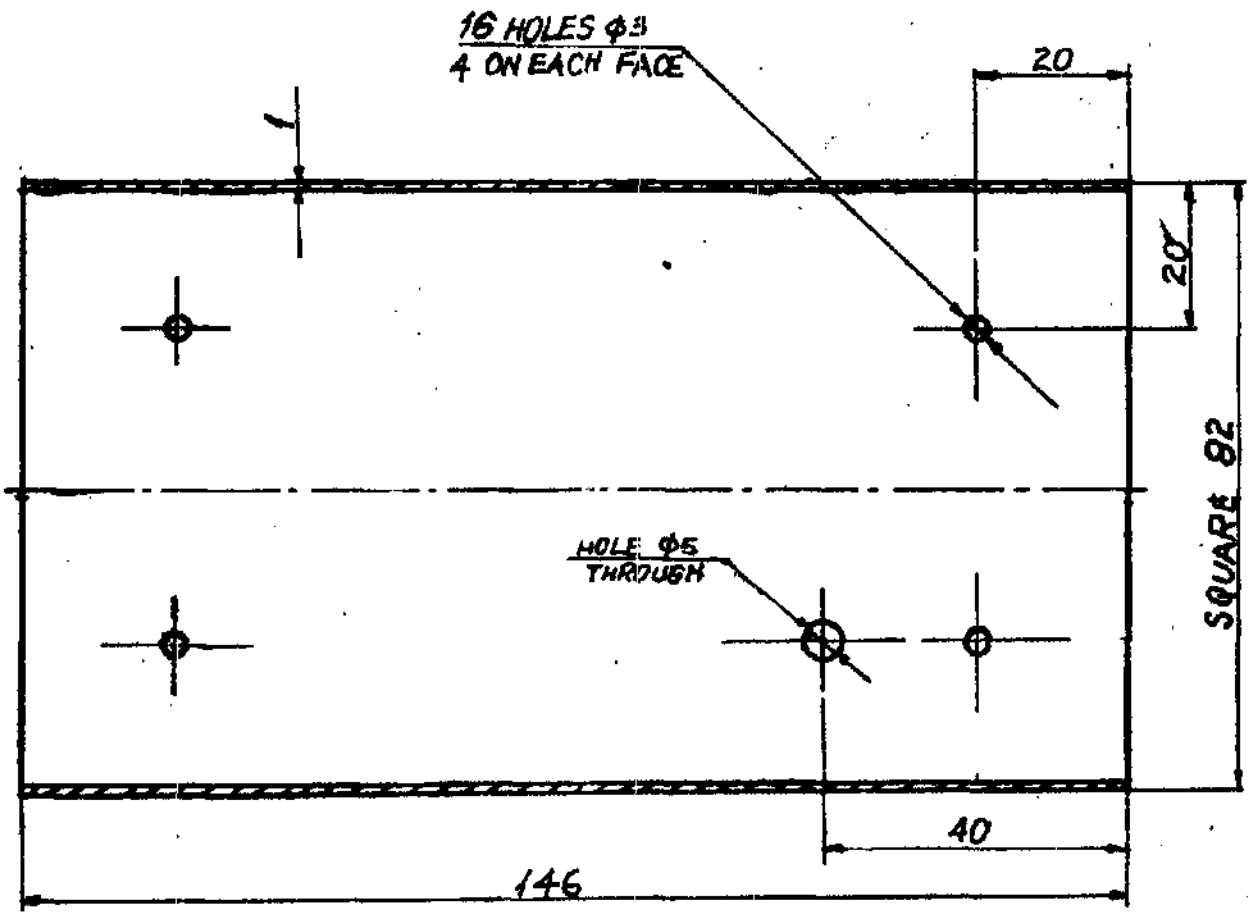
▽7

DRAWN	CHECKED	APPROVED	DESCRIPTION:	RATE GYRO DESIGN		
				WEIGHT	SCALE	SHEET NO.
M.L.AUDU	K.P.Z		MOTOR COVER	—	2:1	10
MATERIAL: ALUMINIUM ALLOY 2018 – T6						



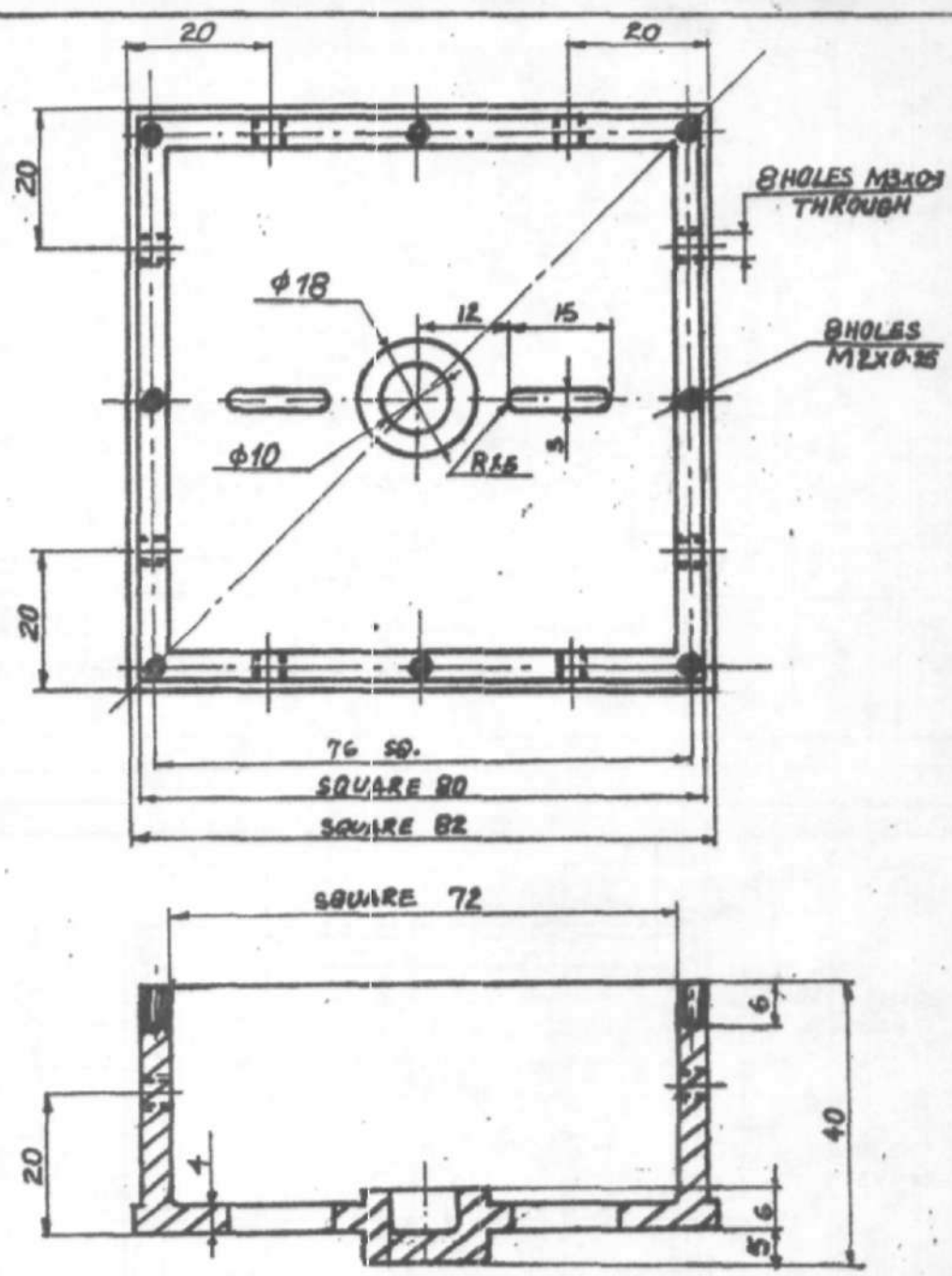
DETAIL / UNIT No.	DESCRIPTION	No. Off	MATERIAL	WEIGHT	NO. OF DRAWING OR STANDARD
3	COUNTERSUNK HEAD SCREWS	4	BRASS	—	
2	SHAFT CLAMP	1	AZ80A	—	—
1	MAIN GIMBAL FRAME	1	MAGNESIUM ALLOY AZ80A	—	—

DRAWN	CHECKED	APPROVED	DESCRIPTION:	RATE GYRO DESIGN		
M.L.AUDU	K.P.Z		GIMBAL ASSEMBLY	WEIGHT	SCALE	SHEET NO.
MATERIAL: MAGNESIUM ALLOY AZ80A				—	1:1	11



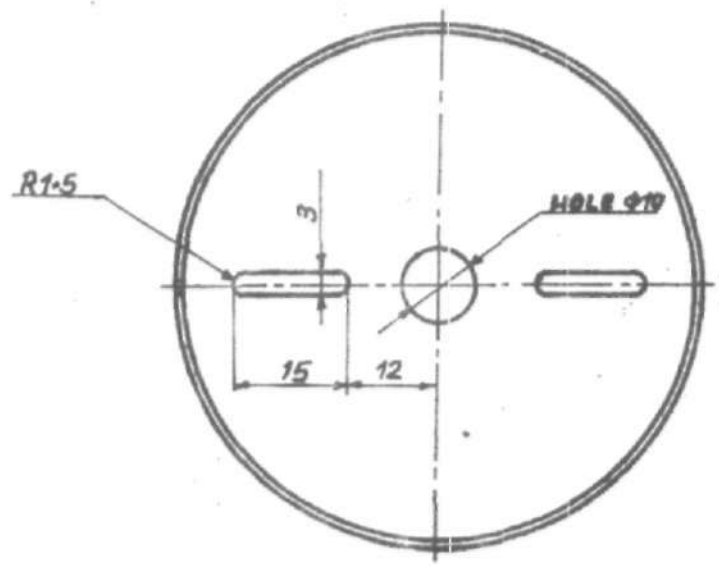
▽7

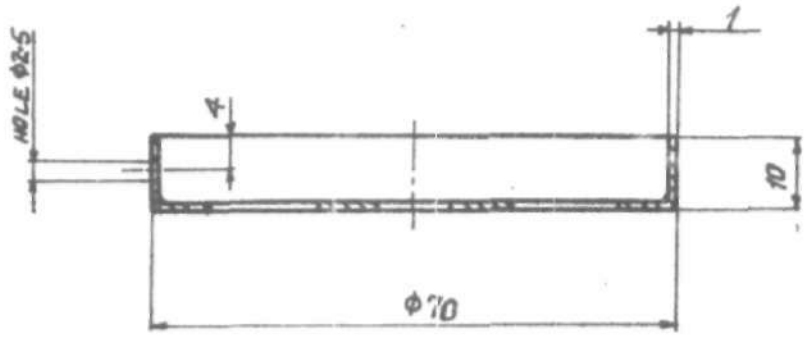
DRAWN	CHECKED	APPROVED	DESCRIPTION:	RATE GYRO DESIGN		
M.L.AUDU	K.A.Z		CASING	WEIGHT	SCALE	SHEET NO.
MATERIAL: MAGNESIUM ALLOY				–	1:1	12



UNDIMENSIONED FILLETS R1 ▽7

DRAWN	CHECKED	APPROVED	DESCRIPTION:	RATE GYRO DESIGN		
M.L. AUDU	K.P.Z		REAR COVER	WEIGHT	SCALE	SHEET NO.
MATERIAL: ALUMINIUM ALLOY 6066-0 T6				—	1:1	13

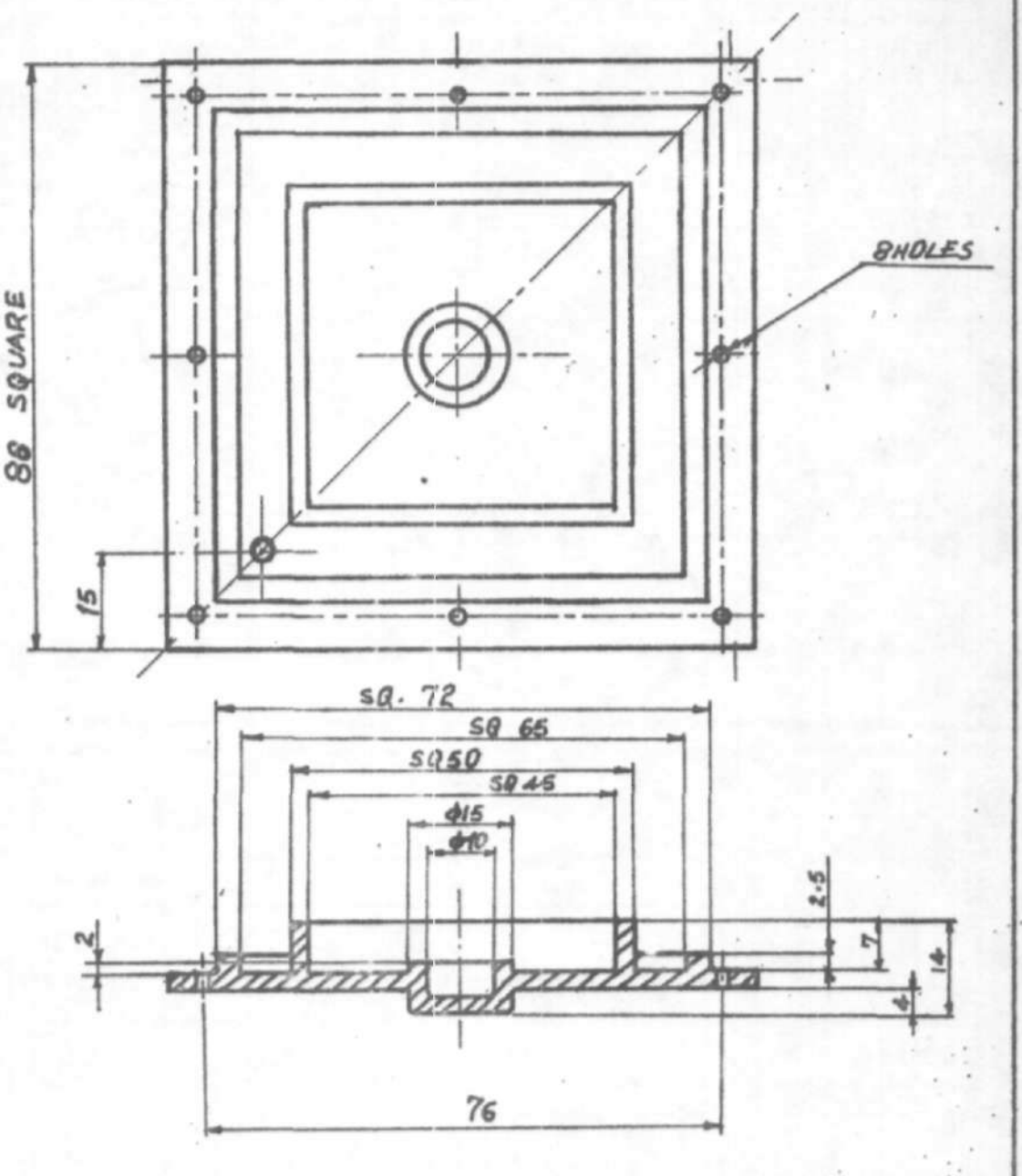




UNDIMENSIONED FILLETS R1 ▽7

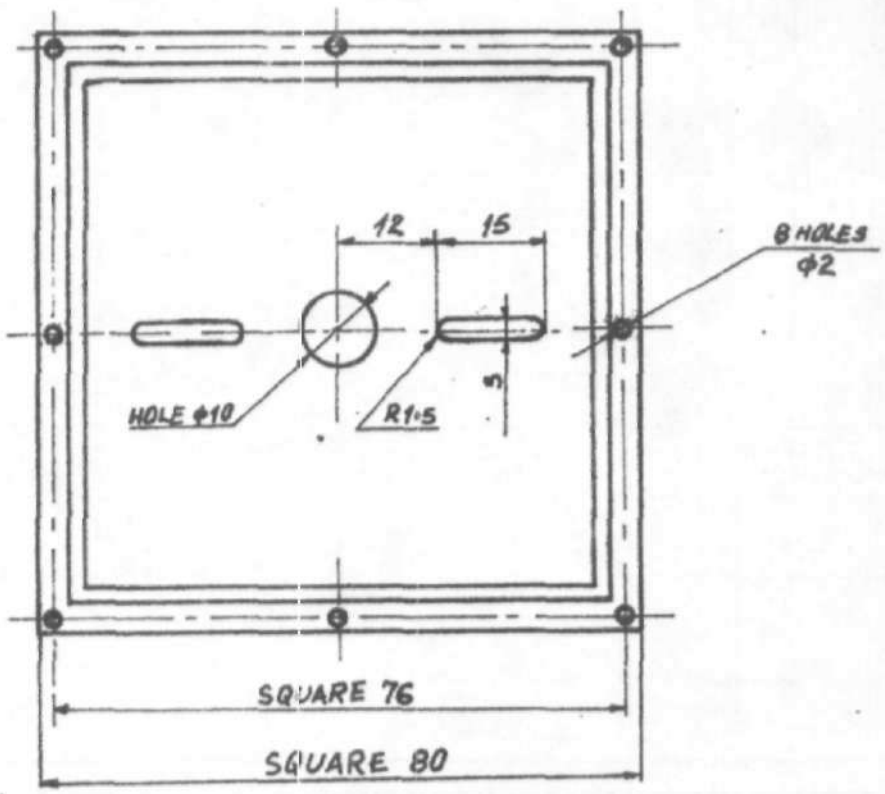
DRAWN	CHECKED	APPROVED	DESCRIPTION:	RATE GYRO DESIGN		
				WEIGHT	SCALE	SHEET No.
M.L. AUDU	K.P.Z		SPIRAL SPRING PROTECTING COVER	—	1:1	14
MATERIAL: ALUMINIUM						

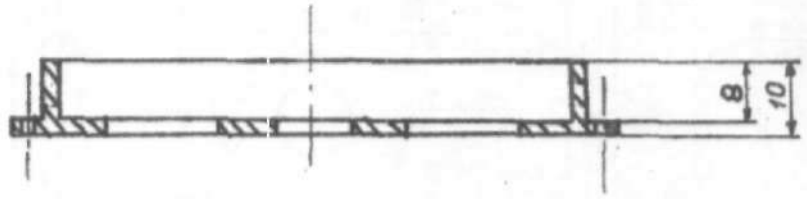
1)



UNDIMENSIONED FILLETS R1 ▽7

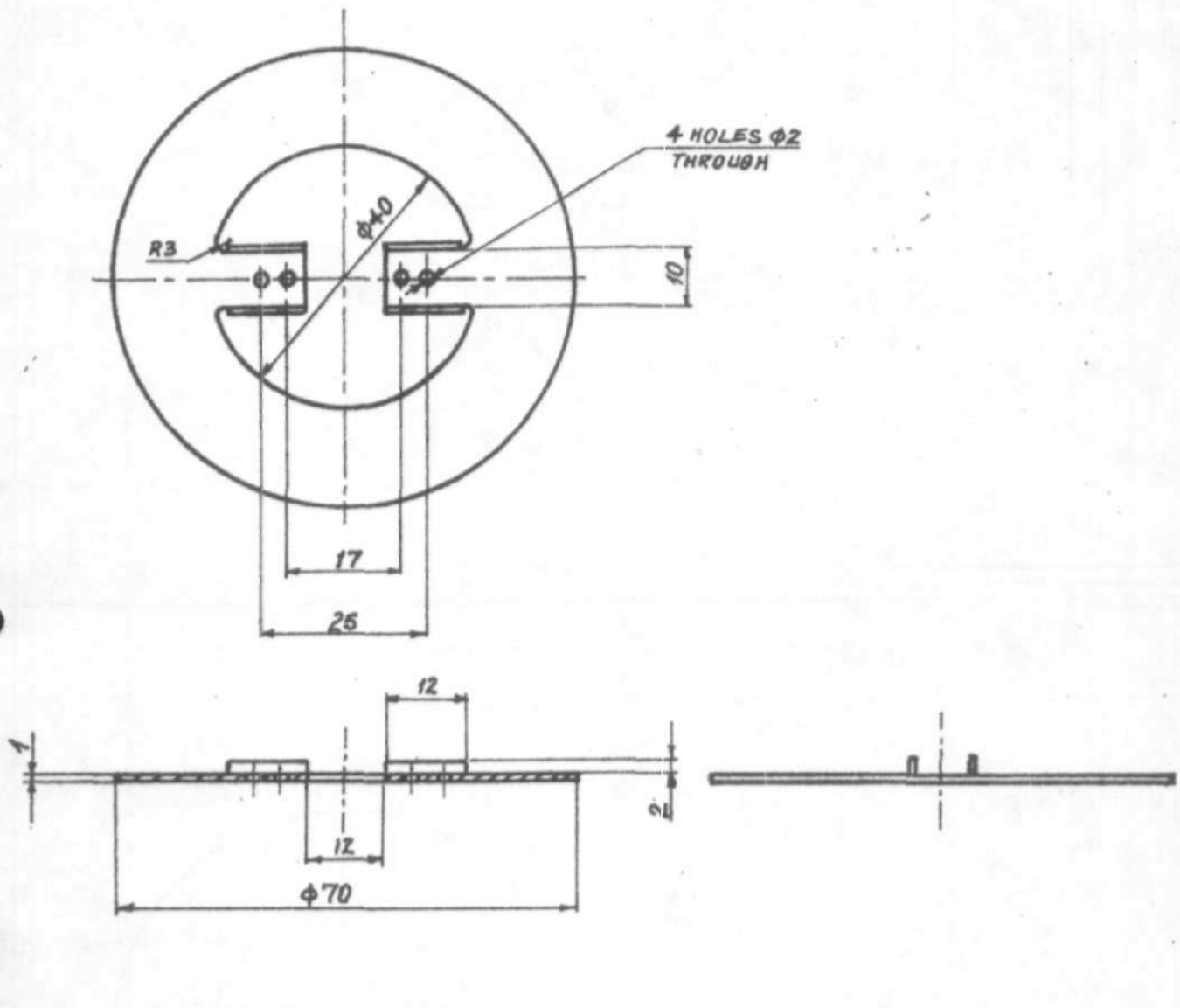
DRAWN	CHECKED	APPROVED	DESCRIPTION:	RATE GYRO DESIGN		
M.L.AUDU	K.P.Z		FRONT COVER	WEIGHT	SCALE	SHEET NO.
MATERIAL: ALUMINIUM ALLOY FORGE-B T6				—	1:1	15





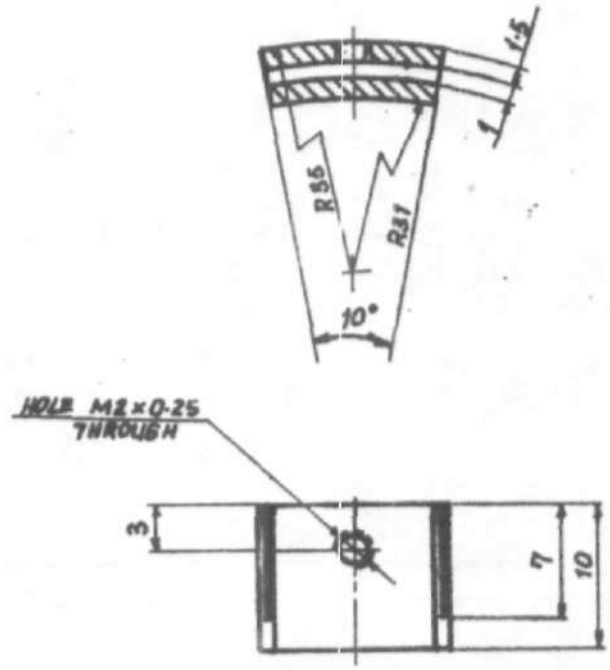
UNDIMENSIONED FILLETS R1 ▽7

DRAWN	CHECKED	APPROVED	DESCRIPTION:	RATE GYRO DESIGN		
M.L.AUDU	K.P.Z		DAMPER COVER	WEIGHT	SCALE	SHEET No.
MATERIAL: ALUMINIUM ALLOY				—	1:1	16



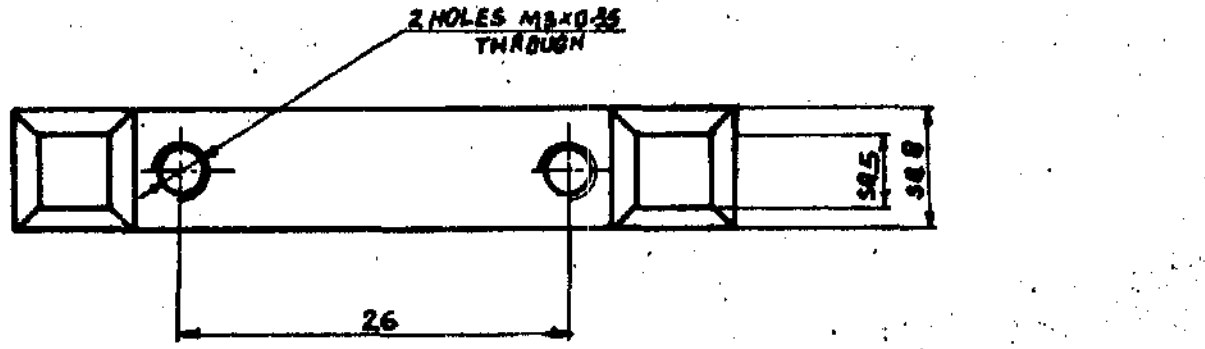
▽5

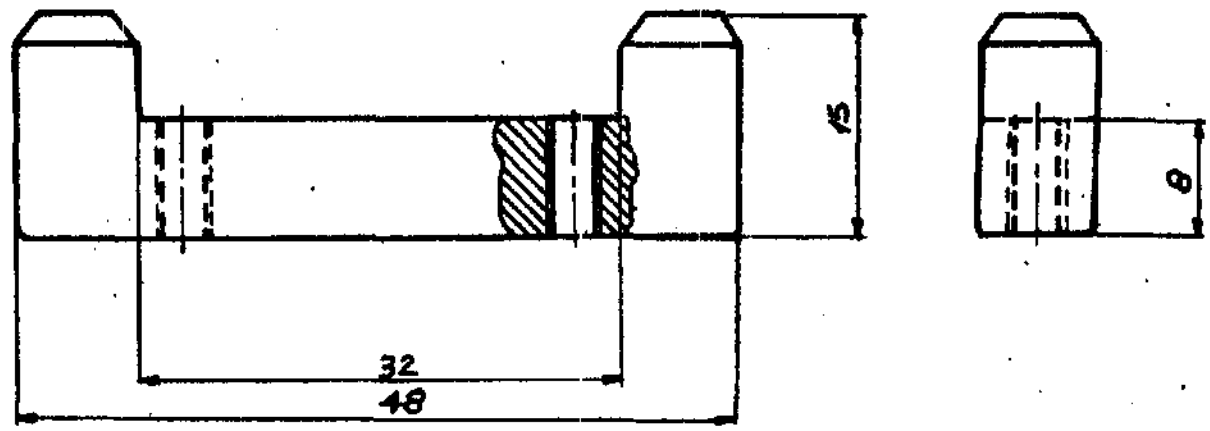
DRAWN	CHECKED	APPROVED	DESCRIPTION:	RATE GYRO DESIGN		
M.L.AUDL	K.P.Z		DAMPING DISC	WEIGHT	SCALE	SHEET NO.
MATERIAL: ALUMINIUM				—	1:1	17



▽7

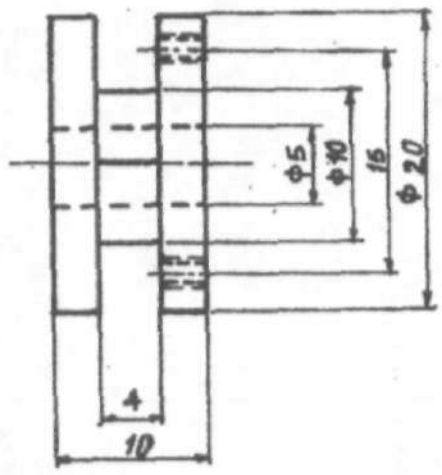
DRAWN	CHECKED	APPROVED	DESCRIPTION:	RATE GYRO DESIGN		
M.L.AUDU	K.P.Z		SPIRAL SPRING CLAMP	WEIGHT	SCALE	SHEET NO.
MATERIAL: ALUMINIUM				—	2:1	18

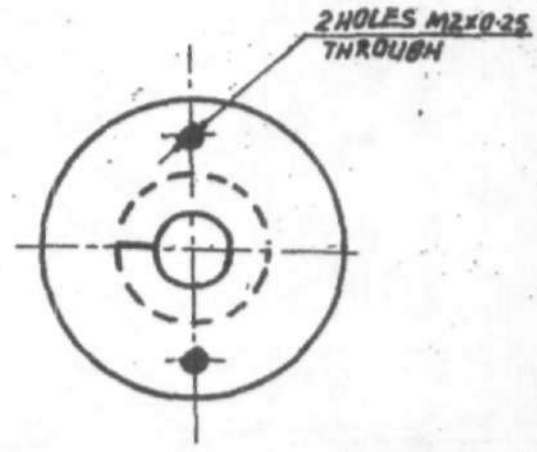




▽7

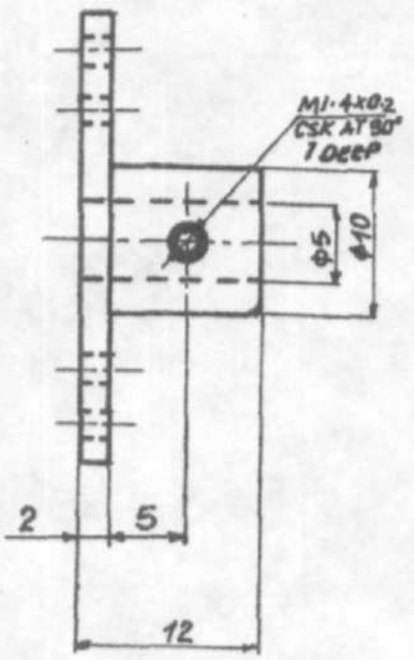
DRAWN	CHECKED	APPROVED	DESCRIPTION:	RATE GYRO DESIGN		
M.L. AUDU	K.P.Z.		PERMANENT MAGNETS	WEIGHT	SCALE	SHEET NO.
MATERIAL: 15% COBALT STEEL				—	2:1	19

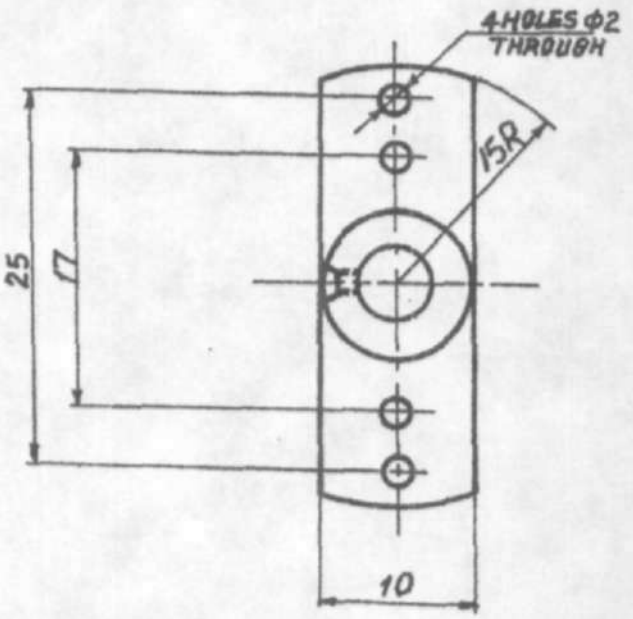




▽7

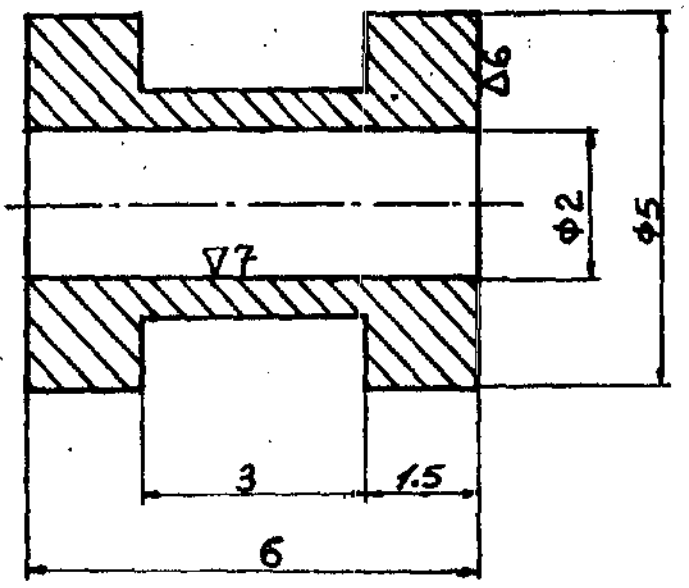
DRAWN	CHECKED	APPROVED	DESCRIPTION:	RATE GYRO DESIGN		
M.L.AUDU	K.P.R.		SPOOL OR HUB	WEIGHT	SCALE	SHEET NO.
MATERIAL: BRASS			FOR SPIRAL SPRING	—	2:1	20



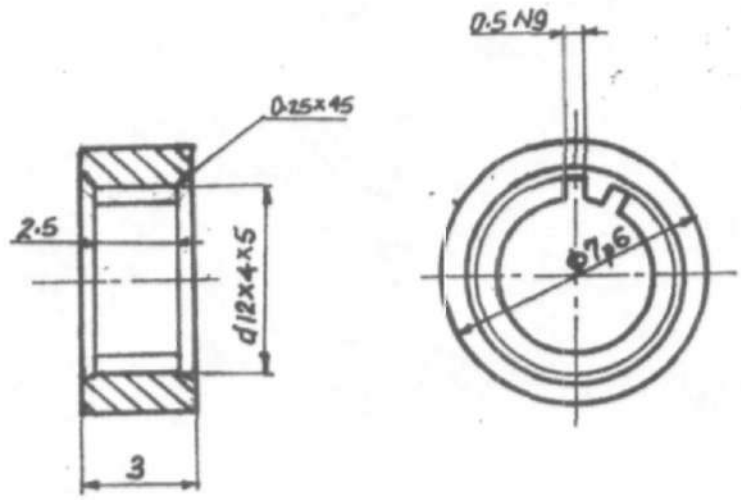


▽6

DRAWN	CHECKED	APPROVED	DESCRIPTION:	RATE GYRO DESIGN		
M.L. AUDU	K.P.Z.		DAMPING DISC HUB	WEIGHT	SCALE	SHEET No.
MATERIAL: BRASS				—	2:1	21

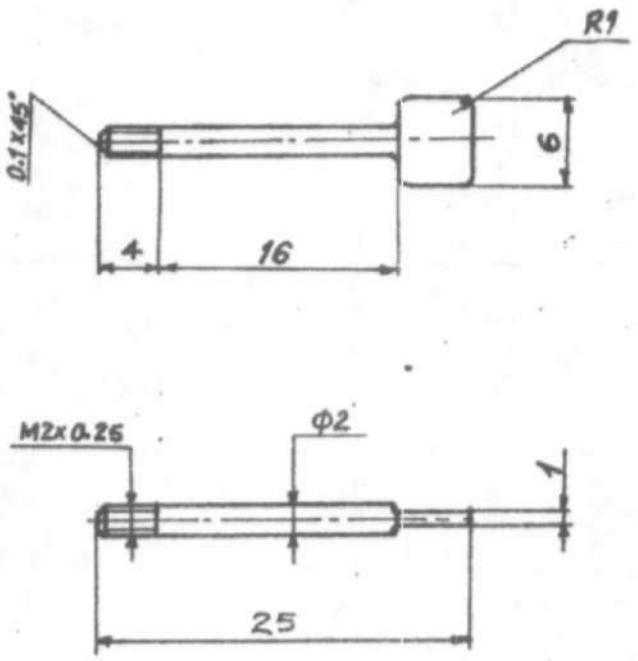


DRAWN	CHECKED	APPROVED	DESCRIPTION:	RATE GYRO DESIGN		
M.L.AUDU	K.P.2.		ROLLER	WEIGHT	SCALE	SHEET NO.
MATERIAL: ACETAL PLASTIC				—	10:1	22



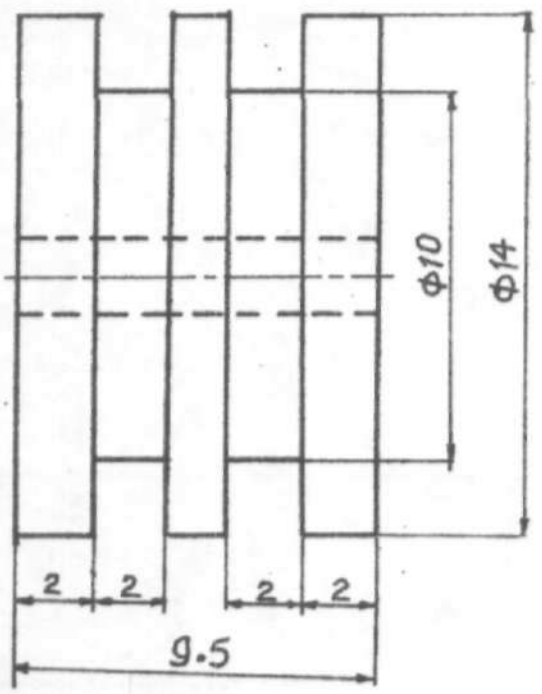
▽7

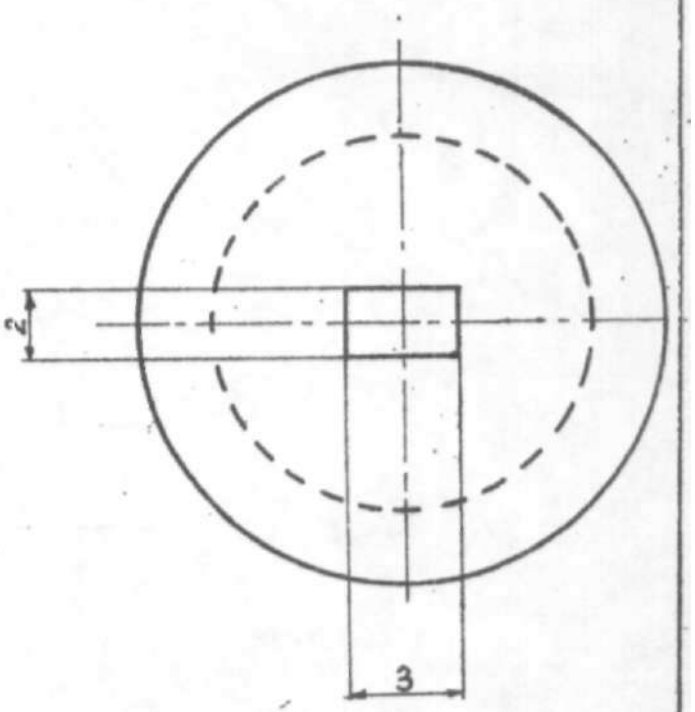
DRAWN	CHECKED	APPROVED	DESCRIPTION:	RATE GYRO DESIGN		
				WEIGHT	SCALE	SHEET NO.
M.L.AUDU	K.P.Z.		SPLINED INSERT	—	5:1	23
MATERIAL: BRONZE						



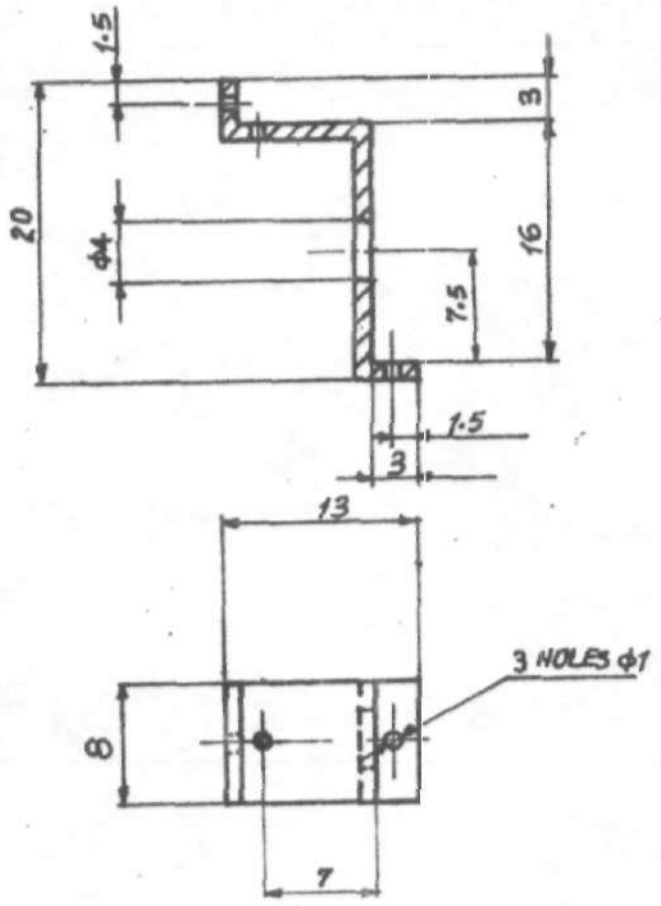
▽7

DRAWN	CHECKED	APPROVED	DESCRIPTION:	RATE GYRO DESIGN
M.L.AUDU	K.P.Z.		LIMIT STOP ATTACHED TO GIMBAL	WEIGHT: — / SCALE: 2:1 / SHEET NO. 24
MATERIAL: ALUMINIUM				



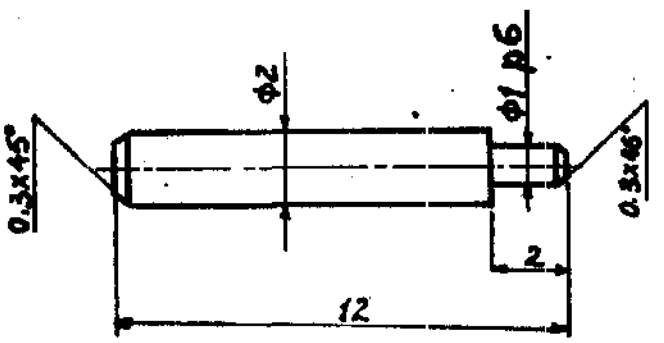


DRAWN	CHECKED	APPROVED	DESCRIPTION:	RATE GYRO DESIGN		
M. L. AUDU	K. P. Z		SPOOL FOR ADJUSTING MECHANISM	WEIGHT	SCALE	SHEET NO.
MATERIAL: ACETAL PLASTIC				–	5:1	25



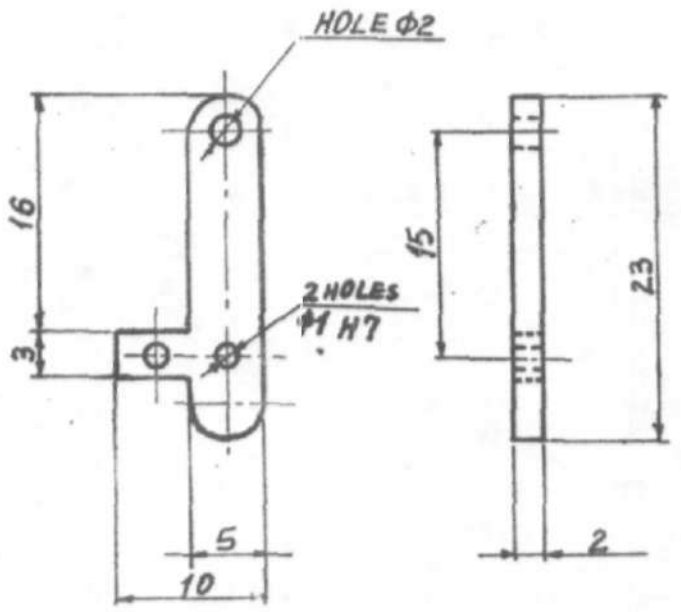
▽3

DRAWN	CHECKED	APPROVED	DESCRIPTION:	RATE GYRO DESIG
M.L.AUDU	K.P.Z.		BRACKET	WEIGHT: — / SCALE: 2:1 / SHEET NO.: 26
MATERIAL: ALUMINIUM				



▽7

DRAWN	CHECKED	APPROVED	DESCRIPTION:	RATE GYRO DESIGN		
M.L.AUDU	K.A.Z.		LIMIT STOP	WEIGHT	SCALE	SHEET NO.
MATERIAL: STEEL AISI 1020				—	5:1	27



▽5

DRAWN	CHECKED	APPROVED	DESCRIPTION:	RATE GYRO DESIGN		
M.L.AUDU	K.P.Z.		LIMIT STOP LEVERS	WEIGHT	SCALE	SHEET NO.
MATERIAL: STEEL AISI 1020				—	2:1	28